universität wien

DISSERTATION / DOCTORAL THESIS

Titel der Dissertation /Title of the Doctoral Thesis

„Non-Visual Photoreception by a G_o-type Opsin in the Annelid *Platynereis dumerilii*“

verfasst von / submitted by

Thomas Ayers

angestrebter akademischer Grad / in partial fulfilment of the requirements for the degree of

Doctor of Philosophy (PhD)

Wien, 2018 / Vienna 2018

Studienkennzahl lt. Studienblatt / degree programme code as it appears on the student record sheet:	A 794 685 490
Dissertationsgebiet lt. Studienblatt / field of study as it appears on the student record sheet:	Molecular Biology
Betreut von / Supervisor:	Univ.-Prof. Dr. Kristin Tessmar-Raible

This thesis is dedicated to my Parents, Helen and Graham Ayers

"Time flies over us, but leaves its shadow behind" – Nathaniel Hawthorne

ACKNOWLEDGEMENTS

Id firstly like to thank Kristin Tessmar-Raible for always being available to discuss work and results and for being open to new avenues of inquiry, without which I would not have been able to conduct my investigation into the annelid shadow reflex, the portion of my PhD project which I enjoyed the most. I'd additionally like to thank the members of both the Tessmar and Raible laboratories for regular helpful and constructive discussions about the work at hand, particularly, Martin, Sven and Mirta.

Most of all, I would like to thank my Father, Graham Ayers, my Mother, Helen Ayers and my Grandmother, Ruth Griffiths, for supporting me financially and emotionally during the final difficult year of my PhD and for always being there for me.

I'd like to give a special thankyou to Iga Willmann, who has been by my side during my best and worst times, and always knew just how to cheer me up and keep me strong.

I would like to express my immense gratitude to Claudia Walthers, Anja Petersen, Sandra Schleder and Kirsten Achenbach of Boehringer Ingelheim Fonds for providing me with funding, without which 2 years of this project would not have been possible.

I'd like to thank all of the friends whose company and counsel has kept me relatively sane for the duration of my PhD, especially Brian, Liam, Jamie, Rob, Falko, Matt and my brother, Dan. I'd like to finally say "Gratias tibi ago" to Martin Gühmann for his legendarily entertaining email exchanges, and give my gratitude to the many members of the species *Platynereis dumerilii*, whose diverse behaviours have allowed me to complete this work.

Non-Visual Photoreception by a G_o-type Opsin in the Annelid *Platynereis dumerilii*

Contents

ABSTRACT

Light represents an invaluable source of environmental information for life on earth, making visually-guided behaviours potent evolutionary driving forces. This evolutionary pressure has encouraged the extensive propagation and diversification of photoreceptive proteins capable of detecting light, the largest group of which is the opsins. Whilst conventional opsin research has typically focussed on those conferring image forming vision, non-ocular photoreceptors are common and widespread throughout many multicellular organisms, contributing to such functions as biological clock entrainment.

Another light dependent behaviour reliant on non-visual photoreception is the so-called shadow reflex. As a defence against predation, most complex organisms exhibit this withdrawal behaviour upon the sudden loss of ambient light. This reflex is especially apparent in sessile marine organisms within the Lophotrochozoan clade, for which a looming shadow can represent a hungry fish. Despite ample species possessing a shadow reflex, we know very little about the molecular underpinnings of this response due to a lack of genetic tools in these model organisms. However, *Platynereis dumerilii* (*P.du*), a marine annelid worm with a well-established molecular toolkit and a wide array of opsins expressed, represents the ideal model to further understand this response. *Platynereis* exhibits several behaviours which are influenced directly by non-visual photoreceptors, a circadian clock controlling daily locomotor activity, a circalunar clock enforcing monthly maturation timing and the shadow reflex. However, the specific proteins responsible for processing light information in these cases are largely unknown. Two main groups of opsins represent likely candidates for photoreception in these behaviours, ciliary opsins which are implicated in non-visual photodetection in Sabellid worms and Go-type Opsins which comprise the motion detecting eyelets in scallops.

Here, we show that Go-Opsin is required for the *Platynereis* shadow reflex, but not for entrainment of the circalunar or circadian clocks. We identify regular expression of Go-Opsin in the cirri of the worm and demonstrate that the loss of these cirri, but not the rhabdomeric cells of the eyes, impairs the shadow reflex. These results are congruous with our finding that the *P.du* shadow reflex is spectrally specific to 500nm, similar to the excitation spectrum of *pdu*-Go-Opsin1. Go-Opsin1 mutation does not completely abolish the shadow reflex however, and we put forward a case that c-Opsin2 likely compensates for its absence, thanks to favourable expression domains and excitation characteristics.

We confirm here a direct sensory function of a peripherally-expressed photoreceptor in contrast to conventional clock entrainment. Furthermore, we suggest that the crucial shadow reflex has incorporated different opsins at different points in evolutionary time.

ABSTRACT (GERMAN)

Licht ist eine der wichtigsten Quelle von Umweltinformationen für Leben auf der Erde, was die Evolution und umfassende Diversifizierung von photorezeptiven Proteinen zur Folge hat. Während sich die konventionelle Photorezeptorforschung typischerweise auf diejenigen konzentriert, die in den Augen gefunden werden, steuern nicht-visuelle Photorezeptoren gewöhnlich das Verhalten in vielen mehrzelligen Organismen. Ein solches Verhalten ist der Schattenreflex, der durch ein ausgeprägtes defensives Rückzugsverhalten als Reaktion auf den plötzlichen Verlust von Umgebungslicht zur Vermeidung von Prädation gekennzeichnet ist. Obwohl die meisten Lophotrochozoen einen Schattenreflex aufweisen, wissen wir sehr wenig über die molekularen Grundlagen dieser Reaktion; vorwiegend liegt dies an einem Mangel an verfügbaren genetischen Werkzeugen. Platynereis dumerilii, ein mit molekulargenetischen Werkzeugen gut ausgestatteter Vertreter der marinen Anneliden, weist mehrere Verhaltensweisen auf, die direkt von nicht-visuellen Photorezeptoren gesteuert werden; der eingangs erwähnte Schattenreflex und sowohl circadiane als auch circulunare Uhren. Die spezifischen Proteine, die für die Verarbeitung von Lichtinformation für diese Verhaltensweisen verantwortlich sind, sind weitgehend unbekannt, aber zwei Hauptgruppen von Photorezeptoren repräsentieren wahrscheinliche Kandidaten, Ciliar-Opsine und Go-Typ-Opsine.

Hier zeigen wir, dass Go-Opsin für den Platynereis Schattenreflex benötigt wird, aber nicht für das Einkoppeln der circulunaren oder circadianen Uhren. Wir identifizieren reguläre zelluläre Go-Opsin1-Expressionsdomänen im Cirrum des Wurms und zeigen, dass der Verlust dieser Cirri, nicht aber der Rhabdomärzellen der Augen, den Schattenreflex beeinträchtigt. Diese Ergebnisse stimmen mit unserer Beobachtung überein, dass der Platynereis-Schattenreflex für eine Wellenlänge von 500 nm spezifisch ist und dem Anregungsspektrum von pdu-Go-Opsin1 entspricht. Die Go-Opsin1-Mutation hebt den Schattenreflex jedoch nicht vollständig auf, und wir zeigen, dass c-Opsin2 wahrscheinlich, dank günstiger Expressionsdomänen und Anregungseigenschaften, dessen Abwesenheit kompensiert. Dies stellt eine seltene funktionelle Bestätigung eines spezifischen peripher exprimierten Photorezeptors dar, der den lophotrochozen Schattenreflex vermittelt und die Rolle von Platynereis als wirksames und zugängliches molekulares Modell für die nicht-visuelle Photorezeption zementiert.

INTRODUCTION

NON-VISUAL PHOTORECEPTION

Our impression of the nature of light-driven behaviours has changed frequently as we uncover more molecular evidence for the mechanistic underpinnings of biological light detection. A major leap forward was the revelation that light detection by anatomical structures other than the eyes is both widespread and in charge of many distinct and biologically relevant behaviours. Understanding ambient light level detection in the non-ocular cells of simple organisms represents a promising avenue of research to further our idea of how light detection has shaped life on earth. We know little about the functions of non-visual photoreceptive molecules other than the entrainment of the daily clock in a handful of commonly used organisms. Setting the circadian clock is just one of many relevant biological functions provided by non-visual photoreceptors. In this thesis, I functionally assess the contribution of specific photoreceptive proteins to less well known light-driven behaviours.

Non-visual Photoreceptors

Due to the availability of light on our planet, the ability to perceive the immediate surroundings via light information has been a highly potent selective force in the evolution of multicellular organisms. As such, photodetection is conventionally associated specifically with the development of the eye and its varying states of intricacy and acuity occurring across most recognised phyla. The sensory input provided by ocular image-forming vision has taken the spotlight in terms of biological research, leading us to a detailed and comprehensive understanding of this highly specialised organ (1). As largely visual creatures, acutely aware of our reliance on visual information, it's hardly surprising that humans place such an anthropocentric emphasis on the merits of the eye (2). However, sensory photoreception is by no means limited to ocular vision, and there have since been many photosensory cells and organs found outside the eyes throughout Animalia. Indeed, non-ocular photoreception has been present even more widely throughout the basal and ancestral species of Eumetazoa, where prior to the development of complex eyes, single cells capable of detecting light were both diverse and widespread (3).

Previously thought to be only present in invertebrates as little as 4 decades ago (2), non-ocular photoreceptors have relatively recently come to light as important for ambient light level perception in fish, amphibians, reptiles and even mammals. In avians and reptiles, the vestigial structure known as the pineal eye has been demonstrated to perform a photodetective function (4), whilst in fish, non-visual photoreceptors in the skin are responsible for mediating photomotor response behaviour independently of the eyes or brain (5). All non-visual photoreceptor cells were also assumed to also be non-ocular prior to the discovery of intrinsically photosensitive retinal ganglion cells (ipRGCs) in

the eyes of vertebrates (6). Similarly, photosensitive cells in the iris of vertebrates such as frogs are known to evoke the pupillary reflex, despite not contributing to image-forming vision (7). Therefore, these cells are now referred to as non-visual photoreceptors and are, by definition, “light sensitive cells which do not contribute to the perception of spatial or motion information” (2). Despite its presence throughout vertebrate species, non-visual photodetection appears with astonishing frequency and variety in invertebrates. Within the Lophotrochozoan superphylum which includes molluscs, annelids, cephalopods and brachiopods, two notable examples which demonstrate the prevalence on non-visual photoreceptive systems are bivalves and annelid worms. Mounted on stalks around the rims of bivalve shells such as the scallop, *Pecten maximus*, are arrays of tiny photodetective cell clusters which act to warn the scallop of impending danger (8). Acting similarly as burglar alarms, simple eyespots known as ocelli are present on the florid branching crowning tentacles of fan worms (9). However, considering the complexity of some of these lophotrochozoan ocellar photodetective structures which are labelled as non-ocular in nature, the line between what does and does not constitute an eye is blurred somewhat.

Basic Non-visual Photoreceptor Functions

Despite not contributing to conventional image forming vision, the physiological functions of these non-visual photoreceptors are diverse and equally, if not as immediately, as important as visual mapping of the immediate environment. Notably, non-visual photoreceptors have long been implicated in mediating phototactic behaviours, mostly in invertebrates (10). In mammals and amphibians, non-visual photoreceptors in the retina modulate the pupillary response (the autonomous reflex of pupil constriction in response to bright light), discovered after the revelation that iris size modulation is still present in blind mice (11). Despite not being suited to forming a visual representation of the immediate environment due to their dispersed and non-directional nature, non-visual photoreceptors are still able to coordinate many precise behaviours and responses.

Biological Clock Entrainment

The most well-studied and seemingly ubiquitous function of non-visual photoreceptors within life on earth is the entrainment of biological clocks. A biological clock is an internal biochemically-driven timer which runs endogenously within an organism and controls aspects of its physiology to better suit the conditions of its environment. Often, light levels such as the daily or annual oscillations of solar light are used as cues to set these clocks, a process known as entrainment. Entrainment of these clocks by non-visual photoreceptor proteins involves detecting the cyclical oscillations of ambient light levels, and enforcing physiological changes in order that an organism can operate more effectively in its environment during the current period (12). The most evident and familiar of these clocks is the circadian clock, which allows organisms to take into account the daily oscillations in solar

light to better anticipate changes in temperature, visibility and food availability levels. It is fairly ubiquitous throughout multicellular and unicellular life on earth, and is entrained by a variety of non-visual photoreceptor proteins.

Additionally, and somewhat more recently classified, the monthly oscillations in nocturnal light caused by the variable states of the moon is anticipated for in some organisms by a biological circalunar clock. This clock stimulates profound fluctuations in the physiology of organisms which have been noted since antiquity. For example, fluctuations in the yields of edible parts of gathered molluscs has long been noted to coincide with the neap and spring tides, dependent on the phases of the moon (13). Certain species of marine invertebrates, from corals to annelids, use internal cellular circalunar clocks to control their sexual maturity, so that they can coincide the release of their gametes on a certain night. These marine mating swarms are impressive feats of communal synchronicity, timed according to the dim nocturnal light provided by the moon, which marine species use to increase the chances of fertilisation of sperm and eggs released into the wide open ocean (14). One such lophotrochozoan species which uses a moonlight-entrained circalunar clock to control this mating strategy is the marine polychaete bristleworm, *Platynereis dumerilii* (*P.du*), whose visible maturation from its benthic immature form into its sexually mature epitokous form is reliant on the monthly oscillations of dim nocturnal light (15). Furthermore, this synchronised maturation occurs even when *P.du* animals are removed from their natural environment and not given subsequent lunar stimuli, demonstrating that the maturation process is enforced by an internal circalunar timer which is entrained by dim nocturnal light, rather than being caused purely by moonlight alone (14). Immature *P.du* worms also demonstrate nocturnal activity perpetuated by their internal circadian timers.

Platynereis dumerilii as a model for Non-Visual Photoreception

Whilst non-visual photoreception systems are found throughout all phyla of Animalia, an astonishing variety of photoreceptor proteins are expressed within invertebrates, particularly Lophotrochozoans. Amongst Lophotrochozoa, annelid worms stand out as relatively simplistic organisms with rather archaic body plans bristling with arrays of novel and conserved photoreceptors throughout their entire bodies (16,17). Sabellid worms, a sub-phylum of Annelidae (Figure 1), have even been described as “Nature’s Eye Factories”, referring to their evolutionary propensity to become clad in a patchwork of photosensitive structures, large and small (18). Scallops, with their mantle edge eyes, are one of many bivalve species possessing rudimentary photoreceptive spots throughout their body (19). Cephalopods, as well as possessing some of the largest visual eyes in the animal kingdom (20), have taken the incorporation of non-visual photoreceptors into their sensory apparatus to the extreme. In the longfin squid, *Doryteuthis pealeii*, non-visual photoreceptors have been found in the

fin central muscles, hair cells, arm axial ganglia and sucker peduncle nerves (21). Though the extent to which non-ocular photoreceptors control visually-guided behaviours in cephalopods is yet to be established.

One factor limits the utility of these diverse members of the lophotrochozoan clade as models for non-visual photoreceptions, and that is that most compelling Lophotrochozoan models lack up-to-date genetic tools. However, with recent developments in genetic and physiological manipulation techniques, *P.du* stands ahead of the rest as an ideal candidate to further characterise non-visual photoreceptors in the lophotrochozoan superphylum (22). The advent of accessible CRISPR-mediated mutagenesis and its optimisation for use in diverse model species is likely to accelerate the utility of other lophotrochozoan models in the near future, but until then, Platynereis eclipses its Annelid, Bivalve and Cephalopod cousins in terms of its genetic malleability.

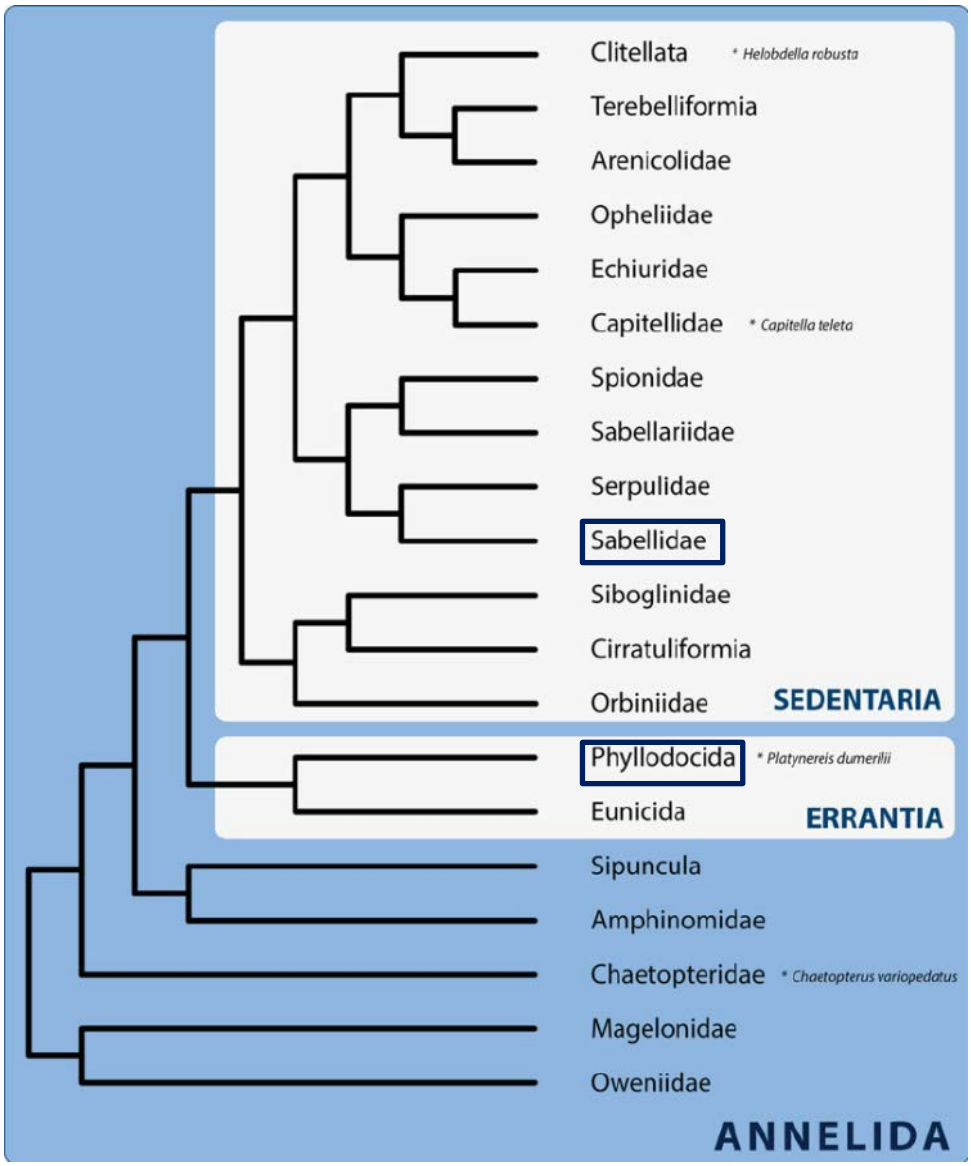

Figure 1: Phylogeny of Annelida. The respective positions of both *Platynereis dumerilii* and fan worms (Sabellidae) are highlighted within a representation of the ancestral relationships between annelid worms. Adapted from Weigert et al. 2014

With at least 10 different types of photoreceptor proteins identified within its transcriptome, *P.du* is no exception from the trend of non-visual photoreceptor-covered lophotrochozoans (23). In addition to the expansive array of photoreceptor proteins contained within it, the *Platynereis* genome is also host to a large number of intron rich sequences, a trait typically characteristic of later vertebrate genomes (24). In fact, approximately two thirds of human intronic sequences are shared by this marine annelid worm, despite the fact that the majority of these sequences were lost from nematode and insect genomes. One ramification of this is that the *Platynereis* genome likely reflects that of a general bilaterian ancestor far more closely than the genomes of more commonly used model organisms. This accumulation and retention of intron-rich sequences in the *Platynereis*

genome has been demonstrated to be a result of *P.du* having a particularly slow rate of molecular evolution, comparable in speed even to humans (24). Humans and other higher primates have some of the slowest rates of molecular evolution so far documented, 5 times slower than in mouse, sea urchins or Drosophila (25). Being similarly slowly evolving and possessing many cell types and physiological structures thought to be ancestral to all bilaterians, *Platynereis* is often referred to as a "living fossil", and this archeatypical quality suits *P.du* to the study of some of the most ancient proteins, photoreceptors (26).

Furthermore, Lophotrochozoa and in particular nereid polychaete worms possess several other aspects of physiology which are considered ancestral, such as a simple body plan which demonstrates the generalisable evolutionary advances of cephalisation and bilateral symmetry (23). *P.du* also represents a potent model system for the study of evolutionary nervous system development due to its basic compartmentalised arrangement of transcriptional domains of cells within its nervous system that are generalisable to other bilaterian lineages (27). Without question, *P.du* represents an extremely promising model organism for the further characterisation of non-visual photoreceptors.

OPSINS

Opsin Structure

Opsins are membrane-bound proteins which have evolved in animals for the purpose of photodetection. They all contain seven transmembrane domains and are members of the G-Protein Coupled Receptor (GPCR) protein superfamily. All opsins also contain a binding pocket in which a photo-activatable chromophore, often 11-cis-retinal, can be covalently bound to by a defined lysine residue. Once attached, this chromophore acts as a protonated Schiff base, and is capable of undergoing a structural change when excited by a photon of the appropriate energy level (Figure 2). This structural change, from 11-cis-retinal to all-trans-retinal in the case where retinal acts as the chromophore, induces a conformational change in the opsin protein, allowing it to transduce its signal into the cellular cytoplasm (28,29).

All opsins also possess an amino acid residue motif which allows them to bind to the alpha subunit of a guanine nucleotide-binding protein (G-protein). The conformational change originating from photoexcitation allows the G-protein to access this binding domain and form a G-protein heterotrimer on the intercellular side of the opsin. Once formed and activated by GTP-GDP exchange by the photoactivated opsin, the G-protein heterotrimer transduces the light signal further downstream (30). The downstream cellular effects of these G-proteins are extremely varied, but those bound to opsins alter the cell's polarity in order to send the light information via neuronal

signalling to the rest of the body, so that an appropriate behavioural response can be induced. Some photoreceptors hyperpolarise their host cells in response to light, like human rods and cones, generating a so-called “dark current” where the photosensory neuron is in a constant state of activation when not illuminated. This is however energetically costly for organisms in darkness and some opsins accomplish the opposing cellular effect, depolarising its host cell in response to light. This hyper- or depolarisation is attenuated by the type of G-proteins which the opsin signals through, and can vastly impact the potential functions which these photoreceptors can perform (28,30).

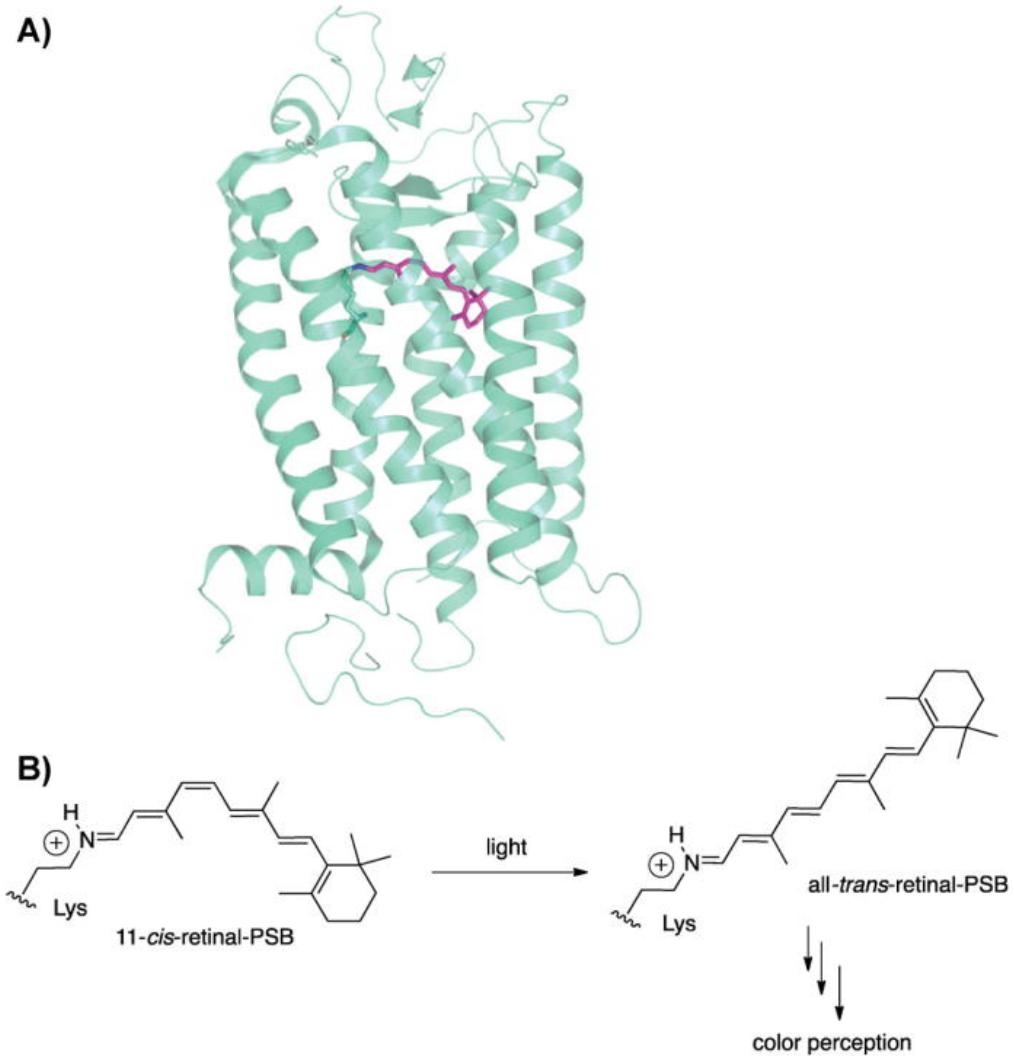

Figure 2: Schematic of Opsin Phototransduction. (**A**) The crystal structure of human rhodopsin (blue) showcasing its seven coiled transmembrane domains. The skeletal structure of retinal (pink) in the form of a protonated Schiff base is shown in its binding pocket. (**B**) Chemical structure equation demonstrating the change which the protonated Schiff base (PSB) undergoes when excited by a photon of the correct wavelength, which stimulates the bound opsin to transduce its signal onto G-proteins (Wang, Geiger and Borhan, 2013.).

Opsin Spectral Absorbance

Due to the incorporated retinal molecule accompanying opsins and the fact that this compound is inherently photoactivated most efficiently by a single photon of a specific wavelength, all opsins demonstrate a preference to become photoactivated by a specific wavelength of light, known as its maximal absorbance wavelength (29). The range of potential maximum absorption wavelengths across opsins is vast, with opsins in various organisms demonstrating photoactivation by anywhere between 380nm and 600nm light, straying even outside of what humans think of as the conventional "visible" spectrum into ultraviolet and far red light (30).

The protein environment surrounding the opsin's associated retinal (or other molecule acting as the necessary protonated Schiff base) dictates the necessary energy level of the proton capable of photoactivating the protein and inducing it to signal. This environment is attenuated by the amino acid residues adjacent to the lysine residue to which the schiff base is covalently bonded, but can also be impacted on by other parts of the opsin protein which come into contact with the associated chromophore (28)(Figure 2). This optimal absorption wavelength is a major factor in deciding the function and utility that each opsin is capable of providing to the organism and physiological location in which it is expressed.

Opsin Classification and Phylogeny

The most widespread and common light-sensitive proteins in animals are opsins (31). Because of the expansive proliferation of these photoreceptors in most life on earth, their classification and categorisation has undergone many shifts in its phylogenetic nomenclature throughout the years. Classically, at least 2 types of opsin have been recognised based on the morphological features of the cells which incorporate them and their electrophysiological response. One type of cell depolarises in response to light, and possesses increased surface area via the inclusion of microvilli known as rhabdomeres, becoming known as rhabdomeric. Another type of photoreceptor cell hyperpolarises in response to light and hosts a modified cilium, henceforth called ciliary. Classically and rather neatly, these delineations appeared to coincide with the division between vertebrate and invertebrate eye photoreceptors, leading to the assumption that vertebrates detect light using ciliary photoreceptors and invertebrates detect light using rhabdomeric photoreceptors (32).

It did not take long however before this clear and binary description of photoreceptors began to fall apart as techniques advanced and exceptions appeared. So-called vertebrate type opsins have been found in the invertebrate brain (17) and conversely invertebrate-type opsins have been shown to be expressed in the vertebrate retina (33). Opsin phylogeny is inherently complex and sprawling, due to both the high number of opsins and their tendency to appear in varying combinations in different cell types throughout Bilaterians. There is actually very little replicable correlation between an opsin's

type, the components of its phototransduction cascade and the morphology of its expressed-cell type (34), leading researchers to develop a new, very transcriptomics-heavy, approach to classifying newly discovered opsins. The most up to date transcriptomic classification of all known opsin sequences identifies 9 distinct groups of opsins present within bilaterians: Bathyopsins, canonical C-opsins, canonical R-opsins, non-canonical R-opsins, Chaopsins, Xenopsins, and three distinct groups belonging to the Tetraopsins, RGR/Retinochromes, Neuropsins and Go-Opsins (3). Of these, canonical r-Opsins, canonical c-Opsins and Tetraopsins have stood out as the most well-studied photoreceptors in animals, but the intricacies of their variations in function, expression and phototransduction are too vast to be covered fully in this thesis.

Opsins have also gone through nomenclature conventions which have attempted to group opsins based on the specific G-proteins which they transduce through. However the relationships between opsins and their associated G-proteins are fickle and can differ even between two very closely related opsins (30). For example, whilst in ciliary and rhabdomeric type opsins, the motif which dictates which G-proteins are signalled through remains relatively conserved (NKNQ for ciliary and HPKR for rhabdomeric)(17), whilst Go-Opsins seem more prone to varying this binding domain. One example demonstrates this, as two very closely related Go-Opsins in *P.du*, Go-Opsin1 and Go-Opsin2, have G-protein-binding motifs of NRK and NKK respectively, hinting that they are more capable of evolving to utilise different G-proteins depending on the task at hand (35). Due to the complex recruitment of various transduction systems and G-proteins to new sites of opsin expression, it is somewhat unsurprising that entirely novel opsins occur at non-ocular locations. Illustrating this are horseshoe crabs (*Limulus polyphemus*), a particularly ancient relative of arachnids bristling with eyes ranging in type from compound to larval to simply ocellar, which express unique extraocular photoreceptors similar to known peropsins in their tail and segmental ganglia. With 18 distinct opsins, the *Limulus polyphemus* genome contains an even larger number and range of different photoreceptors than *P.dumerilii* (36), though its utility as a photoreceptor research model is stifled by its relative lack of molecular and genetic tools.

Of these diverse opsin clades present in Bilateria and beyond, two distinct types stand out as particularly promising non-ocular photoreceptors with multiple non-visual functions in diverse species. These are the Ciliary Opsins and the Tetraopsins.

Ciliary Opsins

Ciliary Opsins are one of the largest and most well-studied groups of these prolific proteins, and canonically are responsible for visual photoreception via expression in retinal rods and cones in vertebrates (37). Ciliary opsins have also relatively recently been discovered to be deployed in diverse species for varied non-visual functions. Vertebrate ciliary opsins such as VAL-opsin in

zebrafish and pinopsins in avian and reptilian pineal organs are just a couple of examples of ciliary opsins in vertebrates with diverse theorised roles in non-visual behaviours such as clock entrainment and body colour change (4). The non-visual expression of ciliary opsins is not limited to vertebrates however, as the cerebral eyes of a protostome larvae (38) and the ciliary photoreceptor cells in the brain of the invertebrate *P.du* have been demonstrated to express ciliary-type opsins (17).

Tetraopsins

Historically, Tetraopsins, a monophyletic opsin group containing RGR/Retinochromes, Neuropsins and Go-Opsins, have been poorly understood and characterised despite being recognised as having high sequence diversity and being well-supported within their three subgroups. Originally called either Go-RGR Opsins or Group 4 Opsins (31), this diverse group of photoreceptors has recently been renamed "Tetraopsins" to avoid ambiguity amongst the growing number of distinct opsin clades known to exist within Bilateria whilst reflecting their previous title (3). Tetraopsins were identified as their own clade long after the two canonical opsin types, rhabdomeric and ciliary, were characterised. This later characterisation can be attributed to the fact that tetra-opsin expression is not typically limited to one morphologically distinguishable cell type or group of organisms (39), as was initially suspected with ciliary and rhabdomeric opsins. In fact, the most notable examples of Tetraopsin cellular expression are those colocalised with rhabdomeric opsins in the adult eyes of marine annelids (40).

Tetraopsins are inferred to be a particularly ancient class of proteins, having been present in at least the latest eumetazoan ancestor (41), and theorised to pre-date even G_t-signalling opsins (3,34). Thus, studying their evolutionary development is likely to provide us with a greater understanding of how opsin-type photoreceptors became such a flourishing group of proteins in life on earth. We are led to speculate as to whether these enigmatic and evidently conserved photoreceptors provide non-visual photoreceptive functions to animals unlike the chiefly visual functional of the better understood c- and r-opsins.

G_o-TYPE OPSINS

G_o-type Opsins throughout Bilateria

Initially named Go-type Opsins due to them signalling through downstream G_o type Go-protein subunits, at the time a seemingly characteristic trait, the first Go-Opsin was classified in the mantle edge eyes of the scallop *Pecten maximus* (42). The Photoreceptor cells (PRCs) of these mantle edge eyes were found to hyperpolarise in response to light, just as vertebrate rods and cones do (43). Go-Opsins were later also identified in both echinoderms and cephalochordates (44) and diverse lophotrochozon species other than bivalves, but importantly are found across both protostomes and

deuterostomes (3). Go-Opsins, Neuropsins and RGR/Retinochromes have been shown to be present in the last common bilaterian ancestor by confirmation that they are expressed in the simple ocellar eyes of the tardigrade *Hypsibius dujardini* (45). This places the Tetraopsins as one major group of opsins which emerged earlier than the divergence of bilaterians (3), meaning that opsins of this group were likely formative in the early evolutionary development of the multicellular eye as we know it today.

No specific Go-Opsins have been found within vertebrates, although a deuterostome Go-type opsin has been found to be expressed in the chordate vertebrate ancestor, *Amphioxus* (46). By contrast, other Tetraopsins, the Retinochromes and RGR-opsins are found in vertebrates, with a non-visual Go/RGR type opsin being expressed within the cone photoreceptor cells of human and bovine retinas (47). Go-type transmembrane opsins themselves may have been lost within vertebrates and ecdysozoans (31). However, the G_o type G-protein subunit for which Go-Opsins were first named has a high level of homology to the G_o G-protein subunit found to transduce the signal for varied opsins within mammalian neurons (42), meaning that at least the utility of Go-Opsin-like phototransduction is retained. Evidently, to further our understanding of Go-Opsins and the severely undercharacterised Tetraopsin group in general, we must embrace the use of model organisms belonging to Lophotrochozoa, where Tetraopsins are most well represented.

G_o-Opsin in *Platynereis dumerilii*

As explained previously, *P.du* represents our most effective lophotrochozoan model organism for studying opsin function. Two Go-Opsins have been identified by transcriptome sequencing in *P.du* (39), Go-Opsin1 and Go-Opsin2. Go-Opsin2 is expressed in extremely low concentrations in *P.du* and therefore localisation of its expression pattern has not been attempted. However, *pdu*-Go-Opsin1 has undergone considerable characterisation in *P.du* pertaining firstly to its expression in larvae. In contrast to the Go-Opsin discovered in the scallop which was co-expressed in ciliary-type photoreceptor cells (42), *Pdu*-Go-Opsin1 is co-expressed in the rhabdomeric cells of the developing adult eyes (39). This demonstrates a high level of mutability in the cell types which Go-Opsins can inhabit. Furthermore, Go-Opsin1 expression in larval *Platynereis* is localised in single neurons proximal to, but not within, the ciliary photoreceptor cells in the brain (17,39). Purification of *pdu*-Go-Opsin1 *in vitro* from mammalian COS-1 cells has also allowed an approximation to be made of the maximal absorbance wavelength of the Go-Opsin1 protein itself, revealing that Go-Opsin1 is most strongly photoactivated by photons with a wavelength of approximately 500nm, roughly corresponding to cyan light in the visible spectrum. Finally, it has been ascertained that the function of Go-Opsin1 in larval *Platynereis* is to facilitate phototaxis, an important behaviour to optimise algal feeding for the free-swimming larvae, via the detection of ~500nm light (39).

The function of Go-Opsin1 in larval *Platynereis* has therefore been characterised, but its function within adult worms, which do not display photokinetic tendencies, is still unknown. This breakthrough study generated a line of *P.du* animals with a deleterious mutation in the Go-Opsin1 gene using targeted mutagenesis by zinc finger nucleases (39). They kindly donated animals from this mutant line to us for this study so that we could conduct further functional characterisation of the Go-Opsin1 in *P.du*.

Pdu-G_o-Opsin1 and the Circalunar Clock

The circalunar clock in *Platynereis dumerilii* is responsible for inducing maturation into their epitokal sexually mature form, so that mass spawning can be synchronised between members of the polychaete population (15). Evidence exists that the *Platynereis* circalunar clock is entrained by dim nocturnal light which is detected independently of the adult eyes, since eye removal does not impact the animal's ability to synchronise maturation between individuals (48). As a non-ocularly expressed opsin in larvae, Go-Opsin1 has potential to operate as the entraining photoreceptor for this circalunar clock. To address this, previous literature collected the timing of maturation for both Go-Opsin1 mutant and wildtype *P.du* worms over the course of three months. Both populations were stimulated by the dim nocturnal light of a 10 watt bulb for seven days each month to simulate three successive lunar cycles (39)(Figure 3).

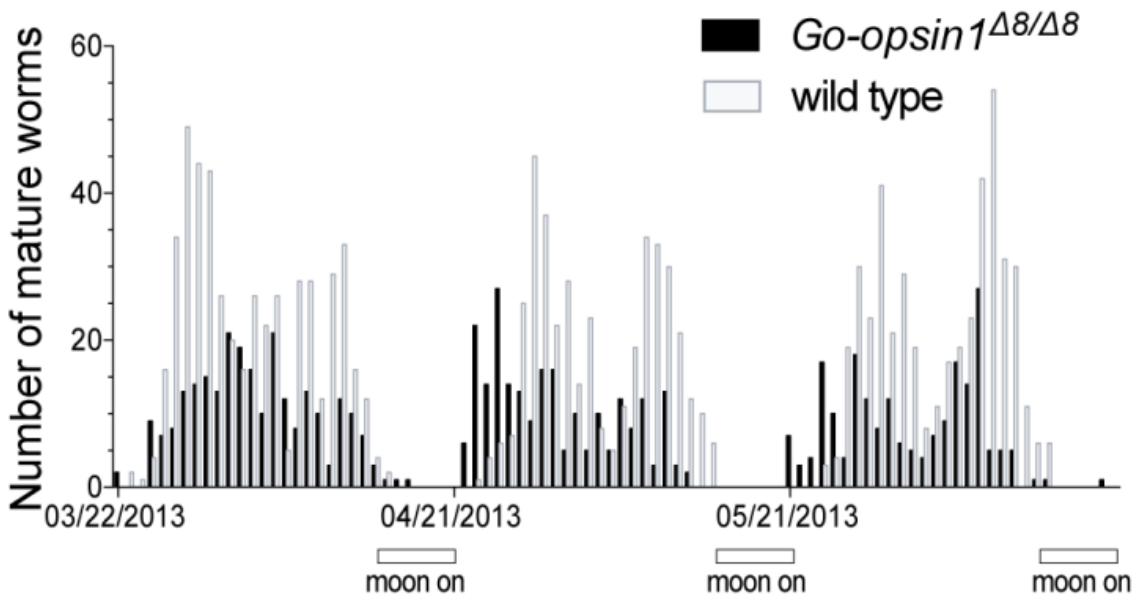

Figure 3: "Go-Opsin1 mutant *Platynereis dumerilii* display a normal circalunar maturation rhythm". Number of maturing worms per day. Full moon phases depict the nights during which a 10W light bulb was switched on. Adapted from Guhmann et al., 2015: Supplemental figure 2A.

Thereafter, a conclusion was made that Go-Opsin1 mutant animals display a normal lunar cycle of maturation, meaning that Go-Opsin1 does not modulate the circalunar clock (39). However, for

methodological reasons which we outline within our results here (Figure 10), the conclusions made from this data are questionable, and therefore deserve reanalysing. With no data available for Go-Opsin1 expression in *Platynereis* past their brief larval stage, we are unable to confirm that Go-Opsin1 expression in the brain persists into adulthood. It therefore remains ambiguous whether Go-Opsin1 is even capable of performing photoreception for entrainment of the circalunar clock.

THE SHADOW REFLEX

Evolution of the Shadow Reflex

The shadow reflex or shadow response is a general term for the autonomous defensive behaviour performed by an animal in response to the sudden diminution of ambient light levels, such as that caused by the shadow of a predator looming overhead. This has evolved as an early warning system which can allow an animal to react to a predator by the simplest photic stimulus available without having to undergo visual processing. The behaviour triggered by the shadow reflex is as varied as the animals which it is present in, but it generally appears as a defensive or withdrawal behaviour to remove the animal from immediate harm, whereafter other sensory systems can assess whether the threat is a real one. This avoidance of predation is an extremely potent evolutionary driver of behaviour and physiology.

This response is most specifically characterised in bivalves such as *Pecten maximus*, which close their shells quickly and tightly in response to sudden loss of ambient light levels (8). It is clear that sedentary or sessile animals such as bivalves benefit greatly from exhibiting a shadow reflex, as with the exception of a few free swimming examples, they are unable to effectively escape with their mobility and must rely on quick reflexes and withdrawal to save them from predation. Instances of distinct shadow reflex behaviour are most commonly apparent in marine organisms, where predators are more likely to pass between the organism and its light source (the sun). Similarly, terrestrial animals which are prone to aerial predation also demonstrate a pronounced behavioural shift in response to overhead shading. In mice, this takes the form of either freezing or escape behaviour in response to a seeing a looming dark disk. This looming response to a shaded object stimulus is theorised to be conducted by normal visual pathways in mice, since its selectivity is consistent with specific retinal pathways (49). Therefore, this behaviour does not strictly fit our definition of a shadow response which rather focusses on the light source suddenly being extinguished immediately on top of the organism itself. In *Drosophila* too, shadow stimuli prompt immediate escape behaviour (50).

It seems that the shadow response in most organisms relies on photodetection by non-visual sources, allowing even animals without complex eyes to take advantage of this reflex which grants a

significant survival benefit. The evolutionary necessity of the shadow reflex is ubiquitous throughout almost all groups of multicellular life on earth. As a testament to this, the shadow response has, in many distinct animal groups either convergently or by conservation, evolved to be triggered independently of the eyes and primary visual systems. For example, even the blind cavefish *Astyanax mexicanus* retains a distinct shadow response despite possessing completely atrophied eyes and having evolved for millions of years in the absence of sunlight (51). Echinoderms without conventional visible eyes exhibit a shadow reflex, further cementing the fact that the shadow reflex throughout animals is perpetuated by non-visual opsins. Sea urchins either retract or bristle and wave their sharp spines in the direction of shadows passing overhead to make themselves appear more formidable to potential predators (52). It is in these basic organisms, echinoderms, molluscs and other lophotrochozoan species, where study of the shadow reflex is likely to glean the most significant findings, as the simplicity of their body plans makes isolating the physiological structures responsible for conducting the shadow reflex easier to isolate and manipulate.

The Shadow Reflex in Annelids

Most notably, polychaete worms of the subclass Sedentaria, named as such because they live the majority of their lifecycle encased in immobile fixed tubes, display a very noticeable shadow reflex (Figure 1). These Fan Worms belonging to Sabellidae and Serpulidae only extend part of their bodies from their protective tubes, that being their colourful and delicate branchial crowns (18). When presented with an overhead shading stimulus, they abruptly cease their feeding and respiration and withdraw their fans into the safety of their tubes. Whether burrowing, flattened tube building or hardened vertical tube building, Polychaete worms all share this shadow-induced withdrawal reflex (53), making them tempting models for further experimentation. When feeding or ventilating partially outside of their protective tubes, *P.du*, an errantid polychaete related to the Sedentarids, is also vulnerable to predation by organisms which traverse the water column above their static tubes adhered to the benthic strata, such as fish, birds and crustaceans. *P.dumerilii* therefore also has a recognisable shadow reflex, involving sudden longitudinal shortening and the momentary cessation of movement. Despite living in considerably deeper water (up to 20m depth) than similar burrowing and tubiculous polychaetes (*N.diversicolor* and *N.pelagica*), where ambient light levels are considerably reduced, *P.du* exhibits a recognisable shadow reflex with a comparable intensity and frequency to its more shallow relatives (54). This suggests that the utility of the shadow reflex in predator evasion is retained across species in differing environments.

Platynereis larvae possess a startle response similar in physiological output to the shadow reflex exhibited by adult worms, also consisting of longitudinal contraction. Ventilation and parapodial beating is ceased immediately, likely due to the ability of some predators, copepods for example, to

detect the hydrodynamic signal generated by these ventilation currents (55). Whilst this larval startle response is shown to be triggered by mechanical vibrations of the water column as opposed to discontinuation of illumination, the physiological circuitry which enforces such a contraction could feasibly persist into adulthood on a larger scale. Whilst the molecular toolkits within Sabellids, Serpulids and molluscs are accelerating in their complexity, they do not yet come close to the wealth of established genetic tools available to *P.du* (22). Thus, we find that despite not having been considered as a behavioural model for the shadow reflex since the 1960s, with this advent of considerable genetic tools, we posit that *P.du* is poised to be the model which can tell us more about the molecular underpinnings and photoreceptors responsible for mediating the shadow reflex.

In vertebrates such as *Xenopus laevis* and *Astyanax mexicana* (51), a general characteristic of the shadow response is a prominence during early development which then decreases in adulthood. It is therefore first relevant to establish that adult *Platynereis* do have a persistent and reproducible shadow response.

AIM OF THIS THESIS

This thesis concentrates on a molecular and behavioural characterisation of *pdu*-Go-Opsin1 and will explore how peripheral expression of this photoreceptor contributes to its function. Possession of a robust shadow reflex is an evolutionary necessity throughout almost all life on earth. However, until now, the molecular understanding of this response has been trammelled by the lack of genetic tools available in representative model organisms. The findings of this thesis further our understanding of one potential evolutionary origin of the shadow response. We also explore how this ubiquitous reflex has influenced expression localisation of peripherally expressed photoreceptors.

In the course of this thesis, I addressed the following questions:

- What is the wavelength specificity of the shadow reflex in *Platynereis dumerilii*?
- Does Go-Opsin1 mediate the shadow reflex in *Platynereis dumerilii*?
- Where is Go-Opsin1 expressed in adult *Platynereis dumerilii*?
- Are the adult eyes of *Platynereis dumerilii* required for shadow reflex activation?
- How can specific expression domains of Go-Opsin1 contribute to its function as a shadow detection system?
- Does *pdu*-Go-Opsin1 contribute to entrainment of the circalunar or circadian clock in *Platynereis dumerilii*?
- Which other photoreceptors could be responsible for shadow detection?
- How can we further our understanding of the neuronal mechanisms underlying light reflexive behaviours in *Platynereis dumerilii*?

In this thesis, I follow a line of enquiry stemming from a general functional assessment of the biological significance of Go-Opsin1 and, more broadly, peripheral photoreceptor systems in adult *P.du*. This took on three major lines of investigation. Firstly, I established a paradigm under which the innate shadow reflex of *P.du* can be assessed quantitatively and with moderate throughput. I utilised this assay in conjunction with several molecular and surgical techniques to ascertain the physiological domains and photoreceptive proteins which conduct this crucial survival response. Secondly, as expressed previously, extra-ocular photoreceptors are typically associated with the entrainment of biological oscillators, the most prevalent of which are the circadian and circalunar clocks known to be present within *P.du.* For this reason, we approached our investigation of Go-Opsin1 with the intention of either proving or disproving the involvement of Go-Opsin1 in the setting of these clocks by assessing the phenotypes of wildtype and Go-Opsin1 mutant animals under established maturation-based and locomotor activity assays. Having addressed both the phototactic input of Go-Opsin1 and the behavioural output thereof, a full understanding of the Go-Opsin1-driven shadow reflex should therefore take into account the neuronal mechanism connecting the two. With this in mind, I finally sought to establish imaging tools to accelerate and aid in the future study of peripheral photoreceptor systems in *P.du*.

RESULTS

G_O-OPSIN1 AND THE SHADOW REFLEX

DISCLAIMER: The results within the following section have been previously published (35):

Ayers.T, Tsukamoto. H, Gühmann. M, Veedin-Rajan. VB, Tessmar-Raible. K, A Go-Type Opsin mediates the shadow reflex in the annelid *Platynereis dumerilii*, 2018, BMC Biology, 16:41 https://doi.org/10.1186/s12915-018-0505-8

Received: 21 November 2017. Accepted: 12 March 2018. Published: 18 April 2018

Please refer to the Author Contributions section of the above publication for any clarifications.

Design of the Shadow Reflex Paradigm

Optimisation was necessary to ensure reproducible and quantifiable stimulation of the shadow reflex. Unlike analysis of *Platynereis* locomotor activity, which can be accurately and robustly quantified using automated tracking software (14), no tracking software was available to detect the sudden contractions associated with the shadow reflex. We therefore set out to design an assay which could be quantified manually with medium throughput and high replicability.

We first modified existing hardware (14) to record worm behaviour using an infrared camera and its associated infrared light source in a light-shielded enclosure. Remotely operated monochromatic LED arrays inside the enclosure then simulated the sudden loss of ambient light levels associated with a passing shadow. Unlike previous behavioural monitoring methodologies, shadow reflex quantification relies upon individual animals being separated from each other so that social interaction or potential chemical signalling cannot influence group defensive behaviours. An enclosure of concave wells was devised to achieve this, which has now been adopted for further behavioural analyses in our laboratory. Following extensive optimisation, and in congruence with previously explored literature, we concluded that desensitisation to the shadow stimulus occurs in *Platynereis* when presented with stimuli less than one minute apart or when subjected to ~15 or more instances of abrupt darkness in less than 20 minutes. Therefore, our assay contains a 60 second refractory period between each “shadow” and only 12 stimuli per trial (Figure 4).

The shadow reflex occurs in Nereid worms regardless of whether they currently inhabit their home tube, since even a tubeless swimming animal will cease its characteristic serpentine swimming motion and straighten up upon light diminution. However, under infrared light recording, the observer’s ability to reliably and reproducibly detect that a robust reflex has taken place is greatest when the animal was previously stationary and aligned in its home tube. Therefore, to ensure tube formation, all animals were allowed to inhabit their individual wells for two days prior to the shadow

reflex assay. Furthermore, the observer's ability to detect whether a shadow reflex has taken place in a given worm is greatly improved if the worm was initially partially stretched out of its tube undergoing foraging behaviour. To encourage this, worms were both kept without food prior to the assay and, upon assay commencement, treated with spinach conditioned water to encourage food searching behaviour. We also found that in order to minimise the overlap between different monochromatic spectra, 500-590nm LED arrays (~$1x10^{12}$ photons/cm^2/s) had to be ran at a roughly 10-fold lower intensity than those of shorter wavelengths (~$3x10^{13}$ photons/cm^2/s)(Figure 4).

Once fully optimised, the shadow reflex assay was able to generate quantitative, reproducible data at a sufficient throughput (36 worms per trial) to adequately address the research question of whether Go-Opsin1 plays a role in photoreception for the *P.du* shadow reflex. Further visualisation of this assay and its quantification is available in video format in (35) and at https://osf.io/f3bq5/

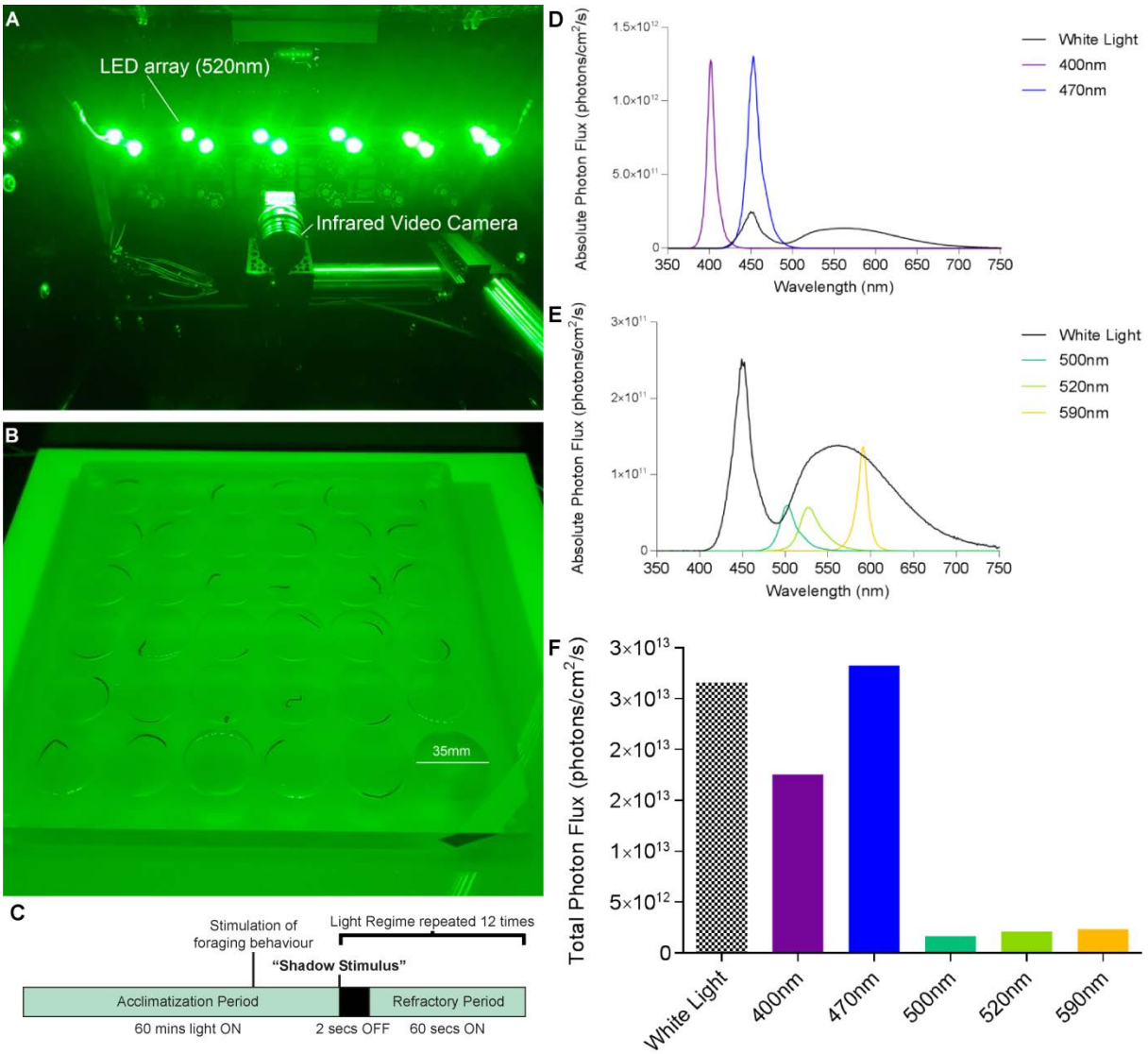

Figure 4: Optimised Conditions and Protocol of Shadow Reflex Assay for adult *Platynereis dumerilii*. Images of the assay chamber illuminated by inbuilt 520nm light depicting the overhanging light and camera array (**A**) and the concave well plate containing 35 acclimatised *P.du* worms (**B**). (**C**) Light regime schematic for assaying the shadow reflex in *P.du*. Constant monochromatic light establishes an acclimatisation period and the addition of spinach-conditioned seawater prompts foraging behaviour 15 minutes prior to the first shadow stimulus. One trial consists of 12 shadow stimuli, each starting with 2 seconds of sudden disillumination with 60 seconds of normal monochromatic light in between. Irradiance spectra (photon flux) of white light, 400-470nm (**D**) and 500-590nm (**E**) monochromatic light stimuli subjected to the animals in each shadow reflex assay. (**F**) shows the total summated photon flux of all monochromatic and white light sources used in the assay.

Wavelength Specificity of the *Platynereis dumerilii* Shadow Reflex

Initially, we set out to simply test our assay by mapping the spectral response curve of the *Platynereis* shadow reflex under different wavelengths of light, much like had been conducted in *Pecten maximus* (8). Overall, we observe that the shadow response success rate is inherently variable between individuals. From this cross section of 5 varied monochromatic light sources, we observe a

distinctive response curve showing a wavelength dependence in the *P.du* shadow reflex. Whilst effectively non-existent under 400 and 590nm light, the shadow response builds in efficacy through 470 and 520nm to its zenith at 500nm, where its success rate is statistically similar to white light. Our results here suggest that it is the 500nm component of white light which is chiefly responsible for triggering the *Platynereis* shadow reflex (Figure 5).

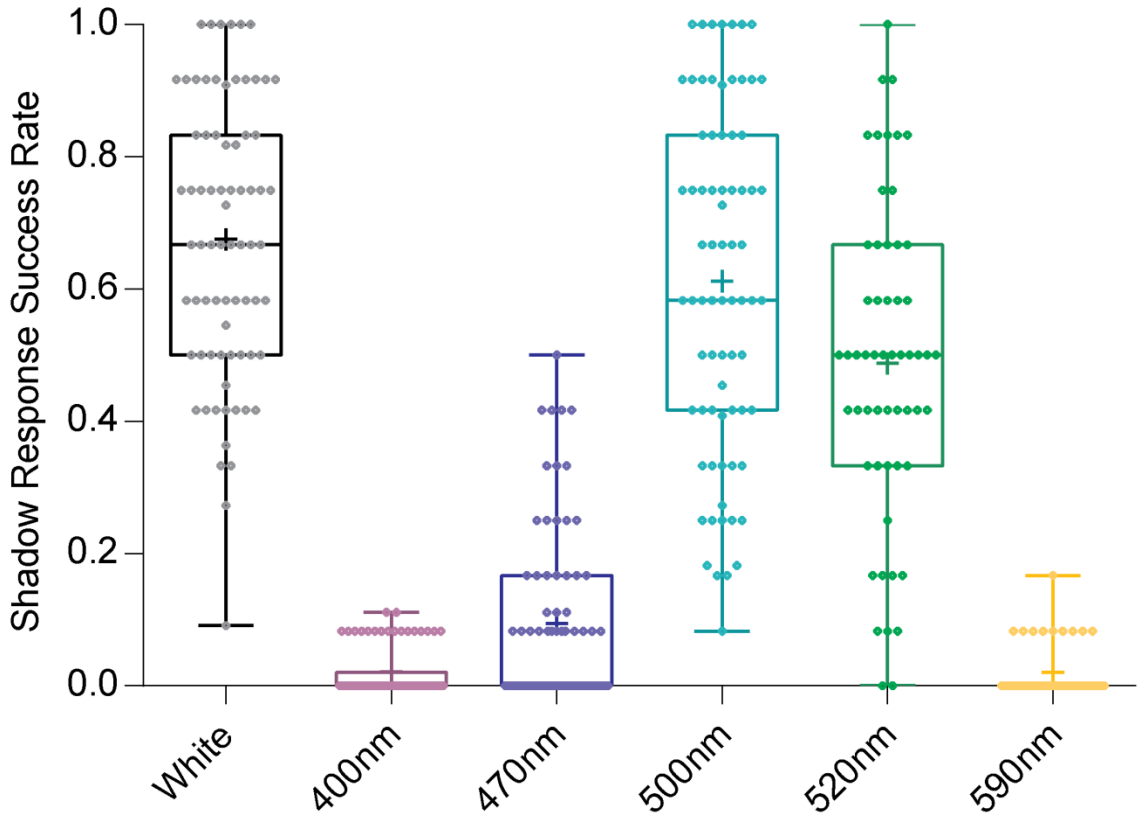

Figure 5: Wavelength dependence of the wild type *Platynereis dumerilii* shadow response. Success rates of the shadow reflex in wild type worms under 6 chromatically distinct light sources, white light (n=74), 400nm (n=74), 470nm (n=74), 500nm (n=74), 520nm (n=56) and 590nm (n=44). Whiskers represent range, Means are marked by a cross and all individual scores are denoted with diamonds.

Go-Opsin1 Mutant Animals have an impaired Shadow Reflex

As before (Figure 5) we see a distinct sensitivity curve of all animals to specific wavelengths, with 400 and 470nm light conditions producing negligible responses which rise through 520nm to a success rate comparable with white light at 500nm. This is preserved in all genotypes. Most notably, we find that Go-Opsin1 homozygous mutant animals produce significantly lower shadow response success rates in our assay than their wild type siblings under white light ($p<0.0003$), 500nm ($p<0.0001$) and 520nm ($p<0.0036$) conditions (Figure 6). This importantly implicates Go-Opsin1 in the photodetection

process necessary for eliciting effective shadow reflex responses in adult *P.du*. Consistently, under wavelengths which elicit a measurable response we see that the mean values of success rate scores for heterozygous animals fall directly between those of their homozygous and wild type brethren, hinting at a possible dosage dependence of the Go-Opsin1 protein. More specifically, we see a significant difference in response rates between heterozygous and homozygous mutant sibling animals under 500 and 520nm wavelengths.

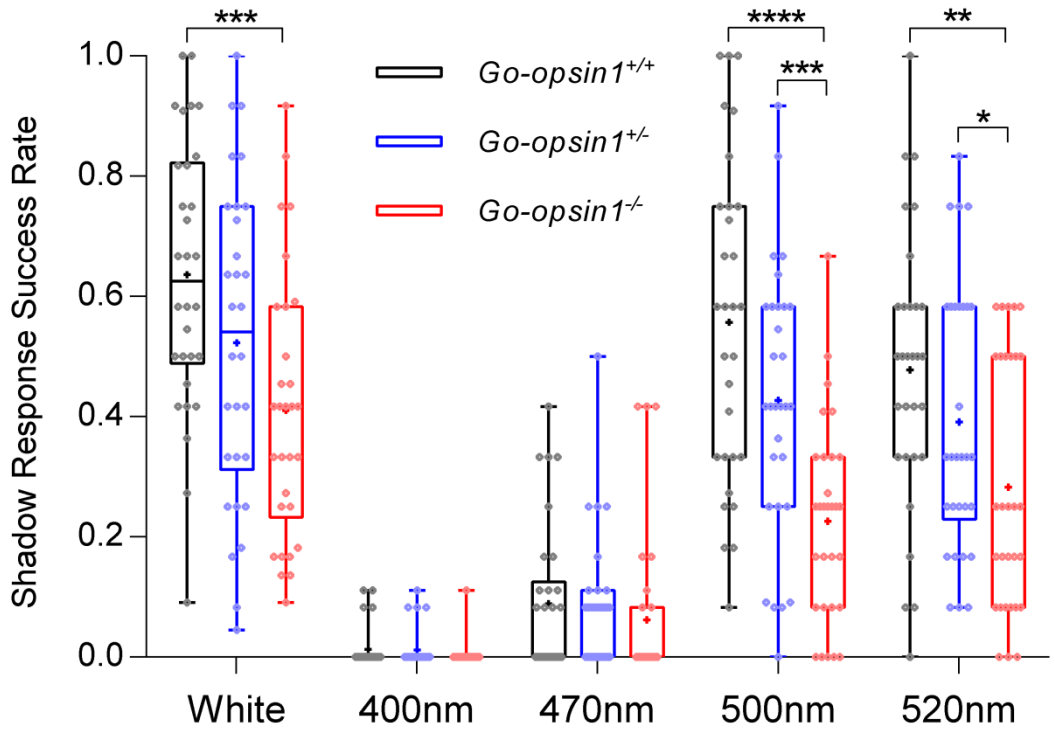

Figure 6: Go-Opsin1-dependent responses to shadow stimuli under a range of wavelengths. Success rates of shadow reflex responses of Go-Opsin1+/+ (black, n=30), Go-Opsin1+/- (blue, n=30) and Go-Opsin1-/- (red, n=30) sibling *Platynereis dumerilii* worms under white, 400nm, 470nm, 500nm and 520nm light conditions. Whiskers represent range of scores, means are marked with a cross and individual scores are presented as diamonds). Significant differences between genotypes are marked with asterisks (*; p<0.05, ** p<0.01, ***; p<0.001, ****; p<0.0001).

Go-Opsin1 Expression in Adult *Platynereis dumerilii*

We firstly noted that the Go-Opsin1 expression domains found in *P.du* larvae (39) are preserved into adulthood, as we observe dense cellular expression in the developing photoreceptor cells around the adult eyes and sparse neuronal expression in the dorsal brain proximal to the medially located ciliary photoreceptor cells. Following this, we classified novel expression domains of Go-Opsin1 in adult *P.du,* both in the peristomal (anterior) and anal (posterior) cirri. These long peripheral tentacle-like

structures extend from the worm at both ends and contain single cellular Go-Opsin1 expression from base to tip, the regularity and alignment of these cells suggesting some kind of sensory function (Figure 7).

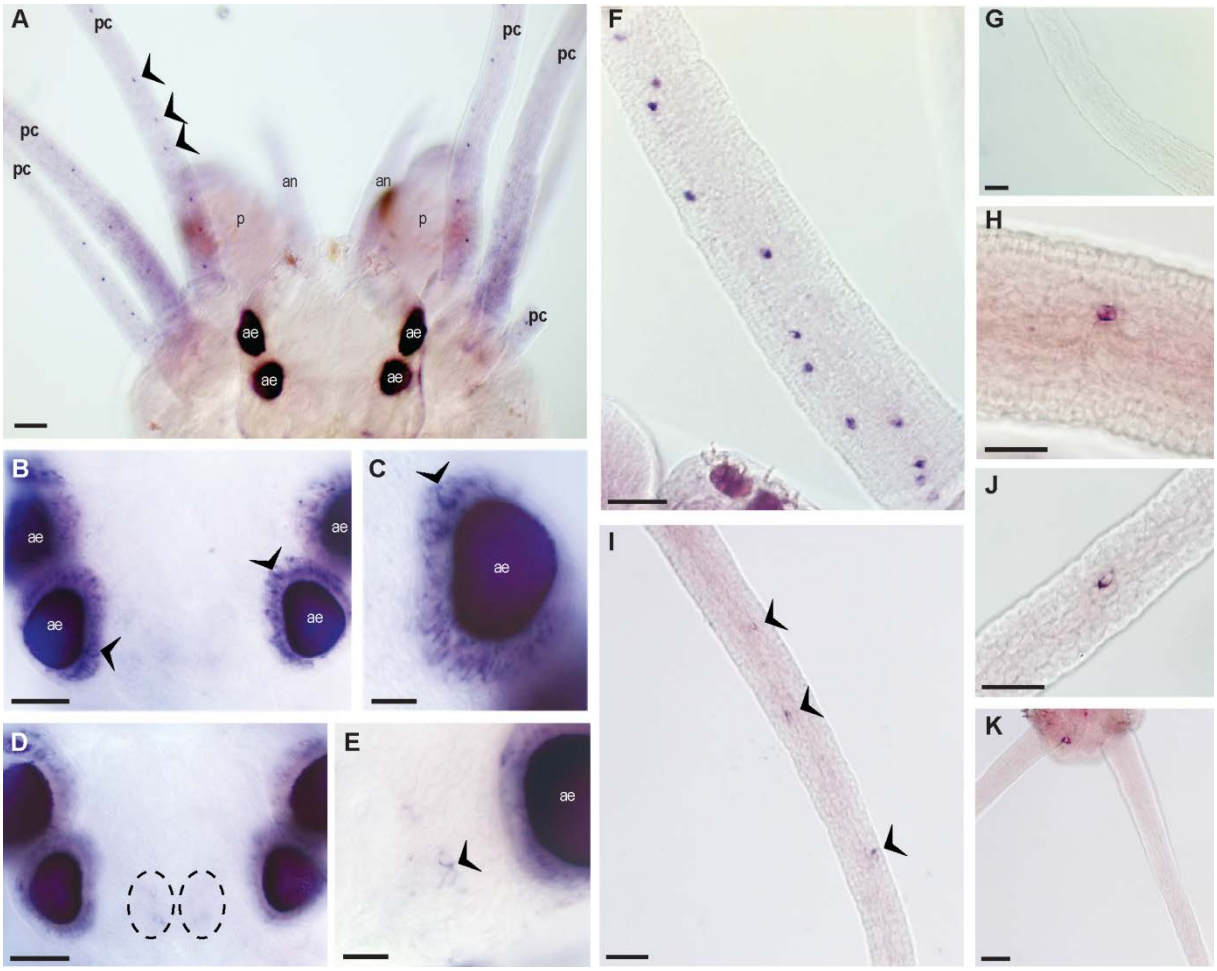

Figure 7: Go-Opsin1 expression domains in adult *Platynereis dumerilii* head and peripheral structures. Light microscope (Differential Interference Contrast) images of immature *Platynereis dumerilii* body parts stained by Whole Mount *In Situ* Hybridisation to show Go-Opsin1 mRNA expression (purple), highlighted by black chevrons in the cases of individual defined cells. (**A**) Entire prostomium containing the adult eyes (ae) and attached peripheral structures, the palps (p), antennae (an) and peristomal cirri (pc), dotted by regular staccato Go-Opsin1-positive cells. Ocular (**B,C**) and dorsal neuronal (**D,E**)(black circles) Go-Opsin1 expression are highlighted in the adult *P.du* head at 20x (B,D) and 40x (C,E) magnification. Isolated Go-Opsin1-expressing cells in the Peristomal (**F,H**) and Anal (**I,J**) cirri with sense probe-bound negative control peristomal (**G**) and anal (**K**) cirri are displayed at 40x (F,I) and 63x (G,H,J,K) magnification. All specimens are viewed dorsally and aligned with their anterior direction towards the top of the figure. Scale Bars represent 20µm in subfigures C, E F, G H and J and 50µm in subfigures A, B, D, I and K.

Cirri Removal impairs the *Platynereis dumerilii* Shadow Reflex

Considering that the shadow reflex in *P.du* is reliant upon Go-Opsin1 and these worms express Go-Opsin in their cirri, we decided to conduct the shadow assay on worms after surgically removing their cirral appendages to assess whether or not this abolishes the shadow reflex. We were able to successfully surgically remove all 10 cirri, 8 peristomal and 2 anal, give the cut animals two days to recover, and compare them to uncut animals in the shadow reflex assay. We found that cirri removal results in a significant decrease in the efficacy of the shadow reflex under all light conditions which are capable of stimulating measurable shadow responses, white light ($p=0.023$), 500nm ($p=0.0467$) and 520nm ($p=0.0227$)(Figure 7). Paired with our previous observations, this represents compelling evidence that sensory neurons expressing Go-Opsin1 in the cirri are integral to shadow reflex photoreception in *P.du*. However, surgical cirri removal does not completely eradicate the worms' abilities to react to shadows, raising questions as to what extent other physiological structures are also able to compensate for a lack of cirri in stimulating shadow responses.

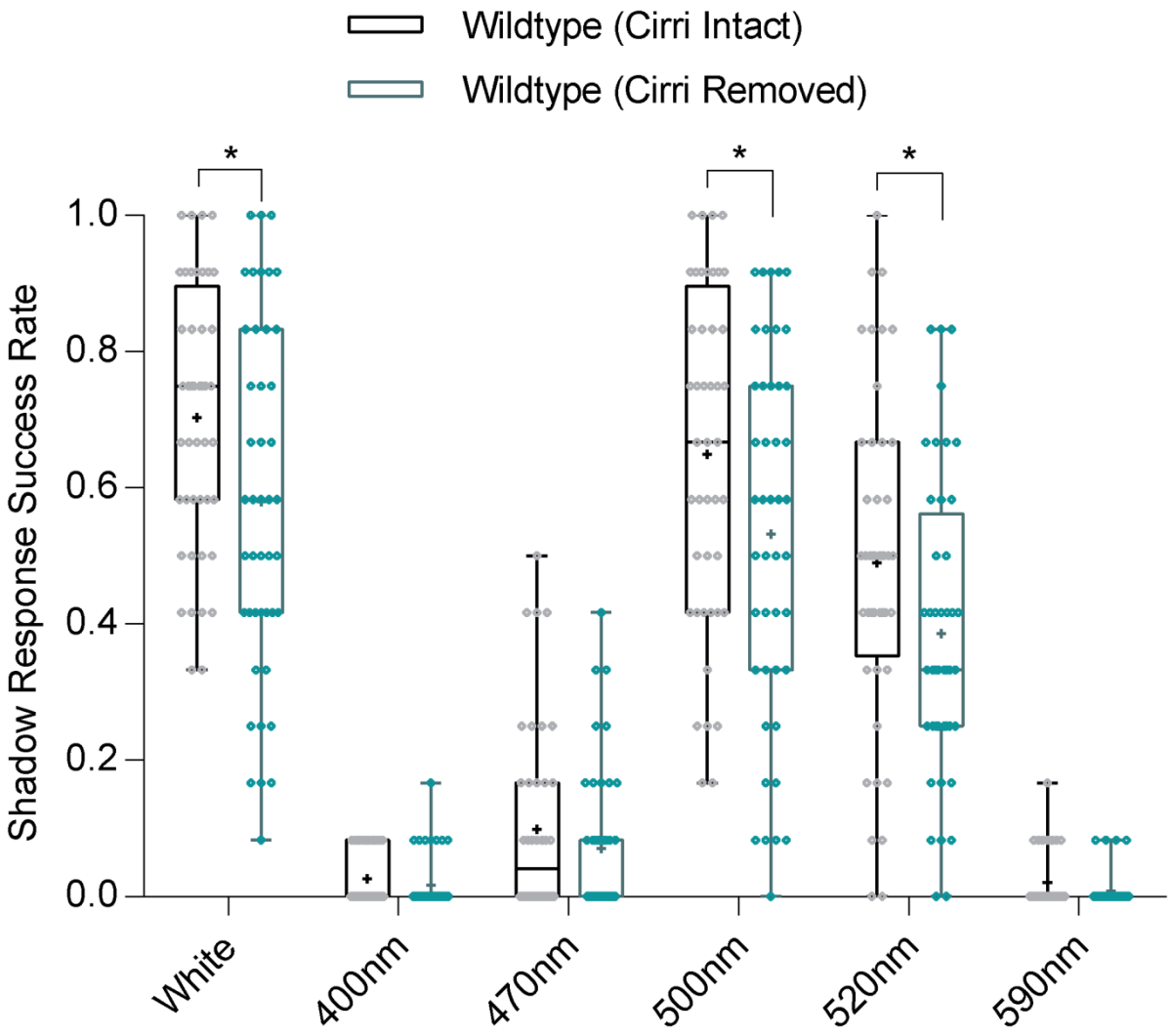

Figure 8: Necessity of the Cirri in the adult *Platynereis dumerilii* shadow response. Shadow reflex success rates of intact wildtype worms (black, n=44) and sibling wildtype worms with surgically excised cirri (teal, n=44) under white light and 5 monochromatic light conditions. Significant differences between groups are marked with asterisks (*; $p<0.05$). Range of scores is displayed as whiskers, means are shown as crosses and individual scores are diamonds.

The *Platynereis* Shadow Reflex is conducted independently of the *r-Opsin1*-positive cells of the Adult Eyes

To assess whether the adult eyes of the worm play an appreciable role in conducting the shadow reflex, we used a previously established technique (56) to specifically chemically ablate the r-Opsin1-positive cells in the eyes of a transgenic *P.du* line containing an *r-opsin1::eGFP-F2A-ntr* cassette. When exposed to metronidazole, the cells expressing this nitroreductase cassette are selectively induced to undergo apoptosis. The full ablation of the image-forming r-Opsin1-positive cells in the transgenic metronidazole-treated animals was confirmed by observing a loss of GFP fluorescence in the adult eyes. It took 5 days of continuous metronidazole treatment to entirely ablate these cells

and extinguish their inherent GFP fluorescence, after which the assay was conducted following a short (2 day) recovery period. We ascertained no significant differences between any two experimental groups under any light conditions (Figure 9), and therefore conclude that ablation of the rhabdomeric cells of the adult eyes does not impact *Platynereis*' ability to react to shadows. This lack of significant differences between groups was calculated by assessing whether or not the difference between medians surpassed 95% confidence intervals according to the Hodges-Lehmann non-parametric estimator.

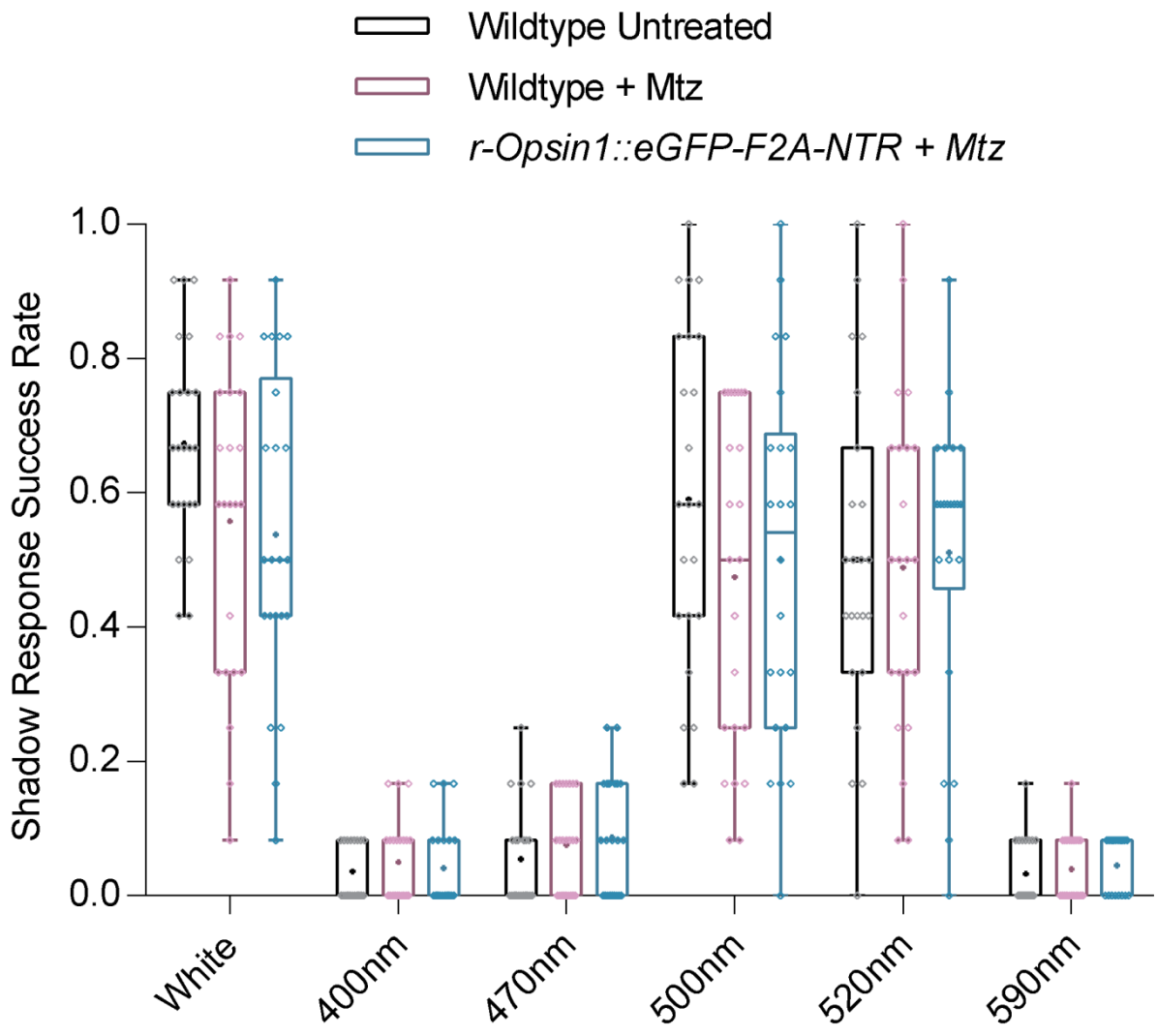

Figure 9: Effect of adult eye cell-specific ablation on the adult *Platynereis dumerilii* shadow response. Shadow reflex success rate scores of untreated wildtype immature *P.du* animals (black, n=23), and control wildtypes (violet, n=23) and *r-opsin1:egfp-f2a-ntr* transgenic animals (teal, n=22) both treated with 12mM metronidazole under white light and 5 different monochromatic light conditions. Range of scores is displayed as whiskers, means are shown as crosses and individual scores are diamonds. No significant differences were observed between any groups.

G_O-OPSIN1 AND BIOLOGICAL CLOCK ENTRAINMENT

Re-analysis of available data brings into question the Circalunar Maturation Timing of Go-Opsin1 Mutant *Platynereis*

Previous evidence concluded that Go-Opsin1 homozygous mutant *P.du* display have a normal monthly maturation rhythm on a population level. Several aspects of this data draw this conclusion into question. Here, I reanalysed the available data from Guhmann et al to assess whether Go-Opsin1 mutant animal display any abnormality in their monthly maturation rhythm (39). We show the same mutant and wildtype maturation curves before (Figure 3) and after (Figure 10A) reanalysis, the main differences being threefold. Firstly, the initial data displays 3 consecutive months depicting 3 separate lunar cycles, whereas our data representation displays all data grouped into a single "lunar month". Secondly, whilst the initial figure (Figure 3) shows raw numbers of animals for each genotype, the reanalysed figure (Figure 10A) shows the proportion of maturing animals per day normalised to the total of animals assayed per genotype (Wildtype n=1345, Go-Opsin1-/- n=682). Finally, we conducted statistical testing consisting of a Mann-Whitney U test of both distributions, finding that there is in fact a significant difference between the distributions of Go-Opsin1-/- and wildtype animals in this three month collection window ($p<0.0001$)(Figure 10A), counter to the conclusion made in previous literature (39)(Figure 3).

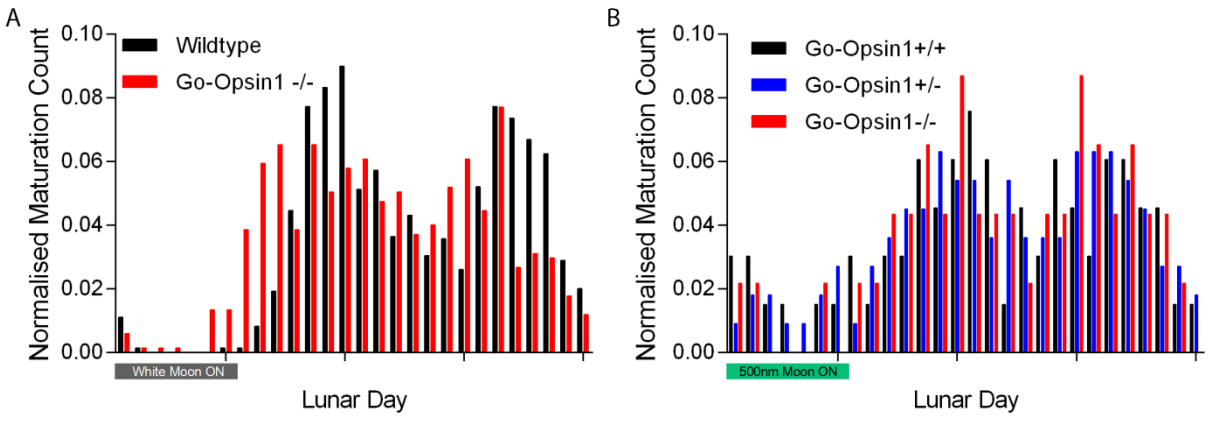

Figure 10: Comparison of Go-Opsin1-dependent Circalunar Maturation profiles of mature *Platynereis dumerilii* obtained with two differing experimental setups. The maturation count of how many animals undergo maturation on each lunar day of several lunar months under regular dim nocturnal light pulses is normalised to the total number of animals per genotype. (**A**) Re-analysed graph of data published in (Gühmann et al, 2015) comparing non-sibling animals treated with a dim nocturnal white light stimulus over the course of 3 months. (**B**) Maturation profiles of heterozygous incross sibling animals treated with a moonlight-intensity 500nm monochromatic circalunar stimulus over the course of 12 months.

Go-Opsin1 mutant *Platynereis dumerilii* do not exhibit a significant deviation in their Circalunar Maturation Timing

The significant difference between distributions of maturation timing between Go-Opsin1-/- animals and generic wildtype animals (Figure 10A) can be explained by a number of factors outlined in our discussion. However, it still warrants further investigation into Go-Opsin1 as a mediator of the *Platynereis* circalunar clock. We therefore set about redesigning the methodology of this Go-Opsin1-dependent maturation analysis to be more stringent in 4 major ways. Firstly, Go-Opsin1-/- (n=46), Go-Opsin1+/- (n=111), and Go-Opsin1+/+ (n=66) sibling animals were compared directly to avoid strain differences in maturation timing, a known phenomenon (14). Secondly, we subjected animals to purely 500nm light stimuli (Go-Opsin1's optimal activation wavelength), both lunar and solar, to avoid the potentially compensatory effects from other photoreceptors if white light were used. Furthermore, we used defined and regulated intensities of both lunar and solar stimuli comparable to known light levels present in nature at a maximum of $3.3x10^{11}$ photons/cm^2/s for simulated sunlight and $2.5x10^{10}$ photons/cm^2/s for simulated moonlight (Figure 11). Finally, to account for potential annual seasonal effects, maturation data was collected over the course of a full consecutive 12 months, rather than 3. The data yielded was also normalised and processed identically to the above re-analysis (Figure 10). According to statistical tests, we detected no significant differences between Go-Opsin1+/+ and -/- (p=0.7113), Go-Opsin1+/+ and +/- (p=0.7465), and Go-Opsin1+/- and -/- (p=0.9028).

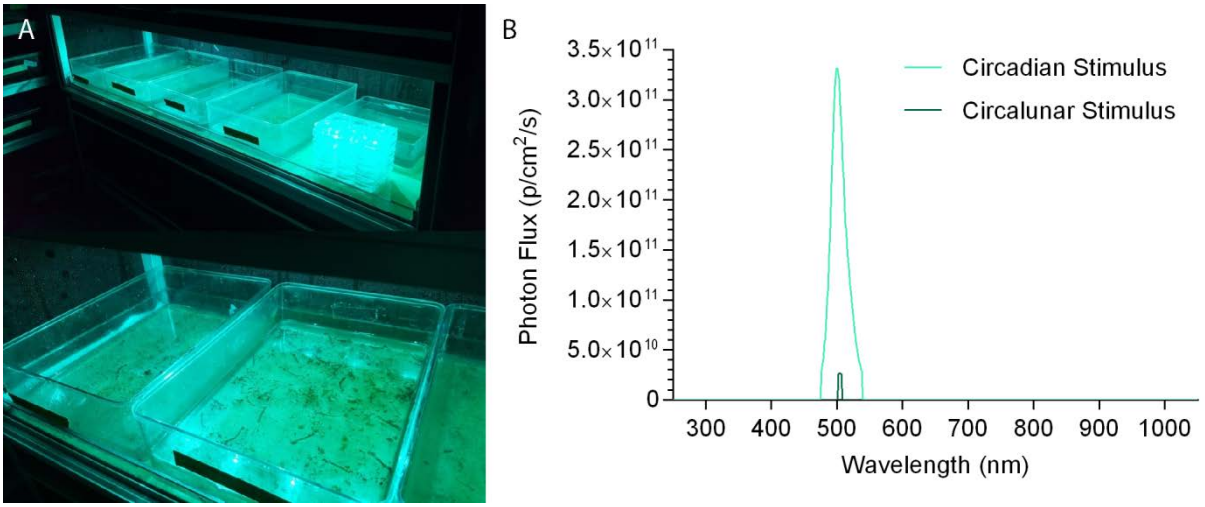

Figure 11: Controlled lighting conditions for Go-Opsin1-dependent circalunar maturation pattern monitoring. (**A**) Light-tight shelf containing separated colonies of adult *Platynereis dumerilii* of varying Go-Opsin1 genotypes. 500nm daylight monochromatic light source can be seen switched on. (**B**) Intensity in Photon Flux (photons/cm^2/s) of both circadian and circalunar 500nm monochromatic light sources used in this circalunar analysis.

Re-entrainment of the *Platynereis* Circadian Clock is not affected by the loss of Go-Opsin1

We tested whether *P.du* circadian clock re-entrainment by a phase shifted light regime is affected in Go-Opsin1 mutant animals. Our light regime subjected each worm to a full control day of ordinary 16 hours of white light and 8 hours darkness (LD) to quantify normal nocturnal locomotor activity under standard conditions (Figure 12C). Following this, the light regime was inverted (DL)(or in other words shifted by 12 hours) using monochromatic light. Where the presumptive dark period would fall if the phase shift had not occurred is designated the subjective night, now occurring in the middle of the monochromatic DL day. This inversion light regime is summarised below (Figure 12A). Nocturnal locomotor activity which occurs in this subjective night period represents an inability to immediately adjust the animal's circadian clock to the new monochromatic light regime. Higher normalised locomotor activity per hour during the subjective night period implies dysfunctional circadian clock entrainment. We found no significant difference ($p=0.0957$, Mann-Whitney U test) between the subjective night activity levels of Wildtype ($n=44$) and Go-Opsin1-/- ($n=44$) animals whose light regime had been inverted by 470nm light (Figure 12B). These animals were however not siblings, the homozygous mutant animals being directly donated from the laboratory of Gasper Jekely (39) whilst all wildtype animals were of the PIN strain bred within the Tessmar-Raible laboratory.

We also observed that whilst the total nocturnal activity over the course of each standard LD 8 hour dark period is comparable between Wildtype and Go-Opsin-/- animals, the profile of their average activity traces differs greatly between genotypes (Figure 12C). The Wildtype strain behaves distinctively biphasic, peaking twice throughout the night, whereas the Go-Opsin1-/- strain displays only a single nocturnal peak in the latter half of the dark period, despite the fact that both animals react to the immediate onset of darkness.

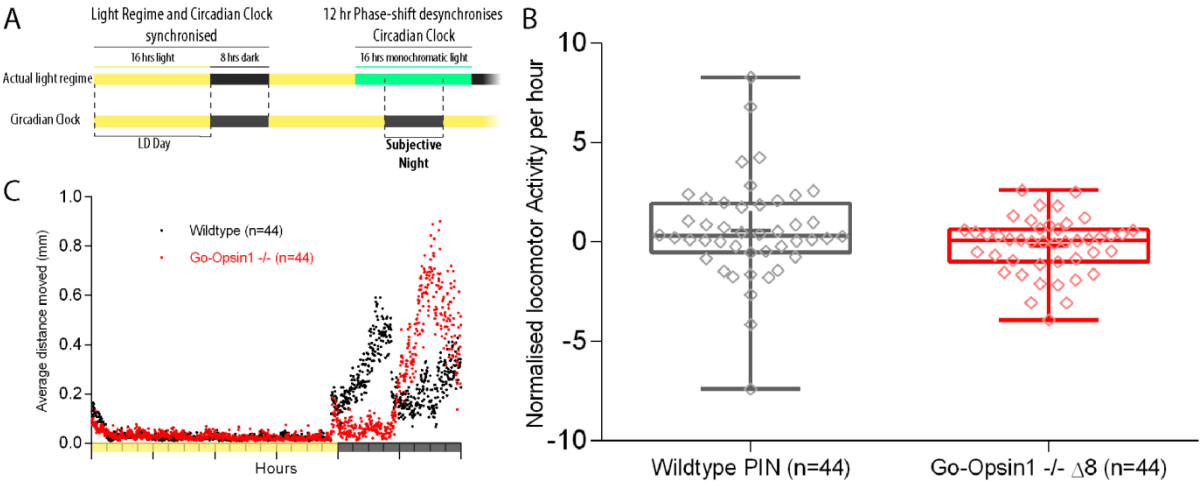

Figure 12: Go-Opsin1-dependent comparison of circadian clock re-entrainment by a 12-hour phase-shift with 470nm monochromatic light. (**A**) Schematic of the monochromatic 12-hour phase-shift light regime used to prompt re-entrainment of the *Platynereis dumerilii* circadian clock. An initial normal light dark day-night cycle is recorded and average activity levels during the ensuing Subjective Night are normalised by average LD Day activity levels. (**B**) 12-hour phase-shifted 470nm-induced subjective night locomotor activity levels (average distance moved per hour during 8 hour subjective night period in millimetres) normalised to baseline daytime activity levels (average distance moved per hour during 16-hour normal LD light period in millimetres) for both Wild type (PIN strain)(grey) and homozygous Go-Opsin1 -/- (Δ8 mutation)(red) non-sibling adult *Platynereis dumerilii*. Means are shown by a cross, individual scores are diamonds and whiskers indicate range. (**C**) Averaged locomotor activity traces (mm) of Wild type (PIN strain)(black) and Go-Opsin1 -/- (Δ8 mutation) (red)adult *Platynereis dumerilii* over a normal 24 hour Light-Dark (16h Light (yellow):8h Dark (grey)) cycle.

This experiment was repeated comparing sibling animals, and similarly, found no significant difference in normalised subjective night activity resulting from a 470nm light regime inversion between Go-Opsin1+/+ (n=7), Go-Opsin1+/- (n=9) and Go-Opsin1-/- (n=7) genotypes (Figure 13A). Finally, we repeated the inversion with 500nm monochromatic light instead of 470nm light and similarly found no significant difference between the normalised subjective night activity levels of Go-Opsin1+/+ (n=26), Go-Opsin1+/- (n=10) and Go-Opsin1-/- (n=11) sibling animals (Figure 13B).

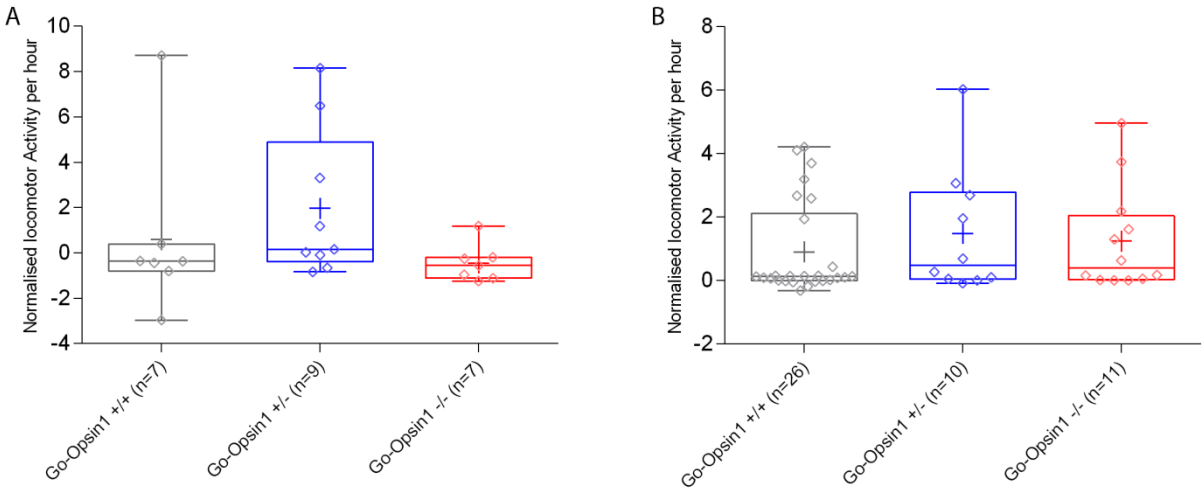

Figure 13: Go-Opsin1-dependent sibling comparison of circadian clock re-entrainment by a 12-hour phase-shift with 470nm and 500nm monochromatic light. Subjective night locomotor activity levels (average distance moved per hour during 8-hour subjective night period in millimetres) induced by 470nm (**A**) and 500nm (**B**) 12-hour phase-shifts normalised to baseline daytime activity levels (average distance moved per hour during 16 hour normal LD light period in millimetres) for sibling Go-Opsin1 +/+ (grey), Go-Opsin1 +/- (blue) and Go-Opsin1 -/- (red) adult *Platynereis dumerilii* all obtained from a heterozygous Go-Opsin1+/- incross. Means are shown by a cross, individual scores are diamonds and whiskers indicate range.

C-OPSIN2 AS A COMPENSATORY SHADOW REFLEX PHOTORECEPTOR

Phylogenetic Analysis of *Pdu*-c-Opsin2

We conducted a phylogenetic analysis of *P.du* Ciliary Opsin 2 (*pdu*-c-Opsin2) to illustrate its degree of similarity to 20 other ciliary opsin sequences and 24 diverse opsin sequences from a wide variety of species across Animalia. From this dataset (35), we found that both *pdu*-c-Opsins clusters most readily with Ciliary Opsin subtypes within arthropods (*Daphnia pulex and Anopheles gambiae*). Subsequently, we find that *pdu*-c-Opsins are more closely related to other Ciliary-type Opsins within chordates than to rhabdomeric Opsins even within our subset of fellow Lophotrochozoan species (Figure 14).

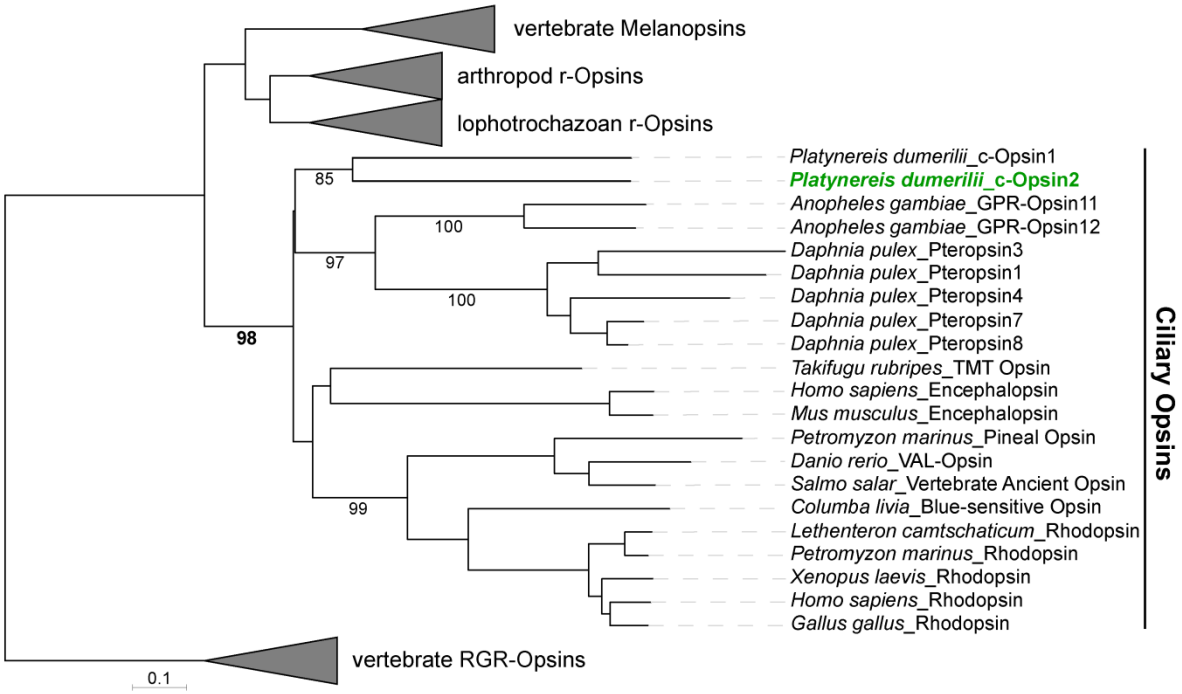

Figure 14: Phylogenetic tree placing *Platynereis dumerilii* c-Opsin2 (green) firmly amongst various other metazoan ciliary opsins. Bootstrap values (displayed as percentages of 1000) of less than 50 are omitted. Figure is derived from Figure 4 of Ayers et al., 2018 and all protein sequences used are available in the supplementary figures thereof.

c-Opsin2 is expressed in the adult *Platynereis dumerilii* brain

We detected the presence of *pdu*-c-Opsin2 in the adult *P.du* brain using immunostaining of whole adult *P.du* heads, where c-Opsin2 is localised by red fluorescence. Co-staining with an anti-Acetylated Alpha Tubulin (a protein expressed in the axonal shafts of neurons) antibody outlines the underlying neuronal architecture in green, revealing that only two distinct and symmetrical cells express c-Opsin2, located in the brain medial to the posterior adult eyes (ae) in the same plane as the Neuropil (n). We find that these cells are less consistently found in the corresponding positions medial to the anterior adult eyes. Magnification of one of these cells demonstrates that expression is localised to the cell membrane of a single cell whose nucleus is stained blue with DAPI solution, as would be expected of a membrane bound GPCR. Secondarily, we observe a lack of c-Opsin2 antibody binding in the cells of the adult eyes themselves (Figure 15).

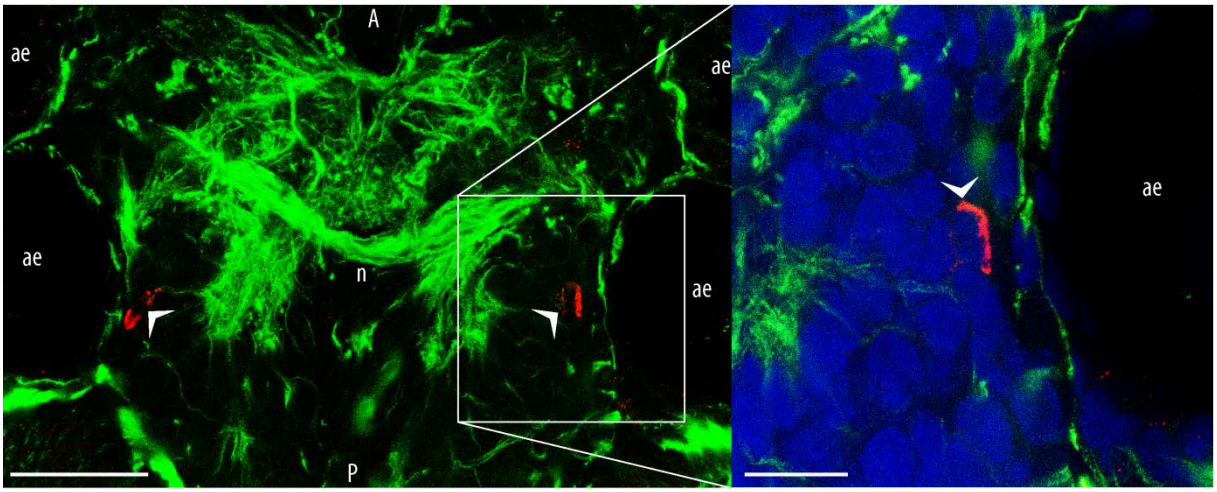

Figure 15: Three-channel confocal microscopy image of *pdu*-c-Opsin2 expression (red) in single cells (white chevrons) within the adult *Platynereis dumerilii* brain. Representative image displays acetylated tubulin (green) highlighting the neuronal architecture of the *P.du* brain between the adult eyes (ae) aligned anterior (A)-posterior (P) in a plane with the massive congregation of neuronal processes known as the neuropile (n). Magnified image centres on one c-Opsin2-positive cell and additionally shows DAPI fluorescence (blue), highlighting individual nuclei. Scale bars represent 50µm in the whole prostomium image (left) and 20µm in the magnified single adult eye image (right).

Development of TALEN pairs for the generation of c-Opsin2 mutant *Platynereis dumerilii*

The sequence flanked by each genotyping primer, represents the entire coding sequence of exon 1 of *pdu-c-opsin2*. To induce targeted mutations in the first exon of *pdu-c-opsin2*, we designed two TALEN pairs (15-18bp in length) which would selectively bind to repeat variable diresidue (RVD) sequences flanking a spacer region containing a unique or rare restriction enzyme cutting site (Figure 16). TALEN-induced mutagenesis of this cutting site disrupts restriction digestion, allowing us to screen for mutations using a general PCR and gel electrophoresis-based protocol. TALEN mRNA of both pairs of c-Opsin2-targeting TALEN pairs was then injected into *P.du* zygotes, which were then genotyped.

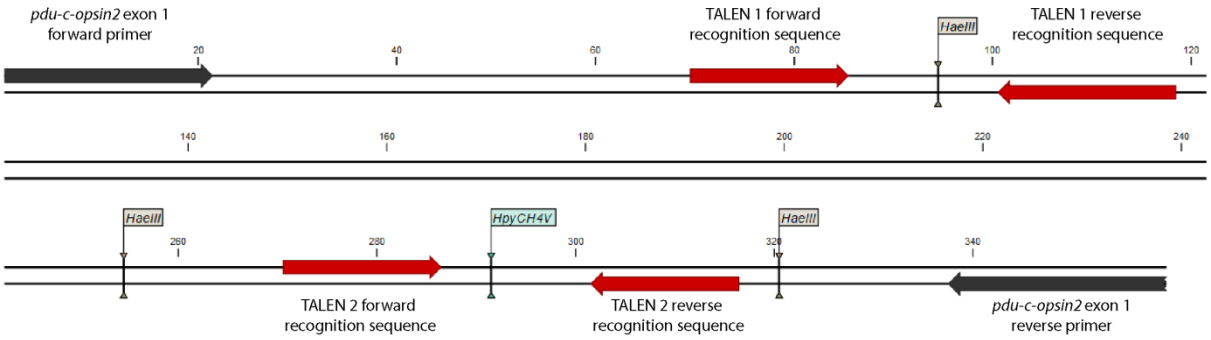

Figure 16: Schematic of TALEN binding domains (red) within Exon 1 of *pdu-c-opsin2*. Genotyping primers encapsulating entire exon are denoted with black arrows. Cutting sites for HaeIII and HpyCH4V restriction enzymes are marked in grey and blue respectively. Numbers of nucleotides within the exon are noted above each strand. Precise nucleotide sequences of both c-Opsin2 exon 1 primer sequences and all TALEN RVD sequences are available in Materials and Methods.

To assess the efficacy of each TALEN pair, we extracted gDNA from injected and uninjected larvae, amplified the c-Opsin2 coding sequence by PCR and subjected the resultant DNA amplicon to restriction digest. Mutation at the site flanked by TALEN pair 1 is differentiated by HpyCH4V restriction digest, and yields an uncut band at 360bp if successful. For TALEN pair 2, HaeIII digestion was used and successful mutation will display a 254bp band (Figure 16). The DNA from animals not injected with TALEN mRNA (d and e) is digested completely by both HpyCH4V and HaeIII, lacking these uncut bands and displaying cut bands at 291bp and 160bp respectively. We find that TALEN pair 1 fairly consistently disrupts the HpyCH4V recognition site in injected larvae (a,b and c), whereas TALEN pair 2 is less effective at disrupting the HaeIII cutting site, where only one injected larva (a) displays a 254bp uncut band more detectable than the uninjected controls (Figure 17). Further genotyping of an additional 20 larvae (not shown) injected with both TALEN pairs indicated that successful mutation occurred at the TALEN pair 1 target locus (HpyCH4V-cut) with ~70% efficiency and at the TALEN pair 2 target locus (HaeIII-cut) with ~10% efficiency.

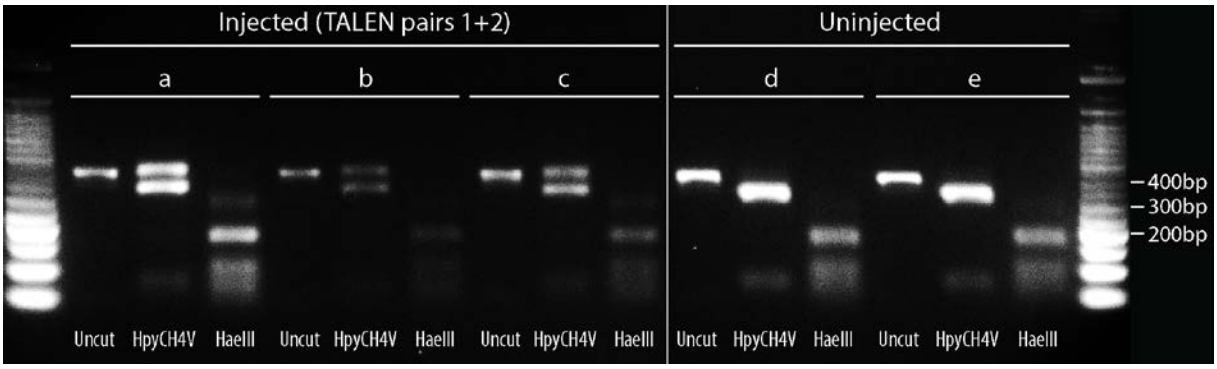

Figure 17: Agarose Gel Electrophoresis image demonstrating functional viability of two separate TALEN pairs on exon 1 of the *pdu-c-opsin2* gene. Bands ofc-Opsin2 exon 1 DNA obtained by PCR of gDNA from 5 *P.du* larvae, 3 injected with c-Opsin2 TALEN mRNA (a-c) and two uninjected (d-e). Each set of larval DNA is displayed in an uncut lane, a lane cut with HpyCH4V (testing TALEN pair 1 viability) and a lane cut with HaeIII (testing TALEN pair 2 viability). Cutting occurs according to the schematic shown in the previous figure. Band sizes are confirmed by a standard 50bp ladder. Blank lanes between larvae c and d were omitted.

NEURONAL IMAGING IN *PLATYNEREIS DUMERILII*

Endogenous Transient Fluorescence in *Platynereis dumerilii* interferes with GFP Fluorescence detection

To gain a greater understanding of non-visual photoreceptors and how they influence behaviours through neuronal activity modulation, studies in *P.du* will inevitably have to embrace methods for detecting and quantifying this activity. At present, fluorescence imaging of genetically encoded calcium indicators (GECIs)(57) represents the state of the art for neuronal activity monitoring. The most advanced of these GECI's (GCAMP) infer neuronal depolarisation, and the associated intracellular calcium increase, by increasing the fluorescence level of a GFP molecule conjugated to an associated Calmodulin domain. This technique requires the user to monitor differential green fluorescence and compare it to stable background fluorescence. Within wild type *P.du* however, we have found and documented a phenomenon which complicates this particular task (Figure 18). Upon excitation specifically with 488nm light, neurons in the head and eyes of wildtype adult *P.du* emit bright transient flashes of ~509nm fluorescence, remarkably similar to the fluorescence spikes elicited by a GECI such as GCaMP in the presence of neuronal activity. What triggers this phenomenon is not clear, as the flashing is seemingly random, but no longer occurs in deceased worms. This endogenous transient GFP-like fluorescence is quantifiable and detectable over background autofluorescence, and the profile of its fluorescence over time appears comparable to depolarisation spikes in studies of neuronal activity imaged indirectly by GECIs (Figure 18D). We found this phenomenon occurring reliably in multiple individuals (n=20) from every wild type strain we have available to us (PIN, VIO, FL2, Naples). For clarity, a full video of this phenomenon from the

individual in Figure 18 is available on the Open Science Framework online repository at https://osf.io/sp48e/

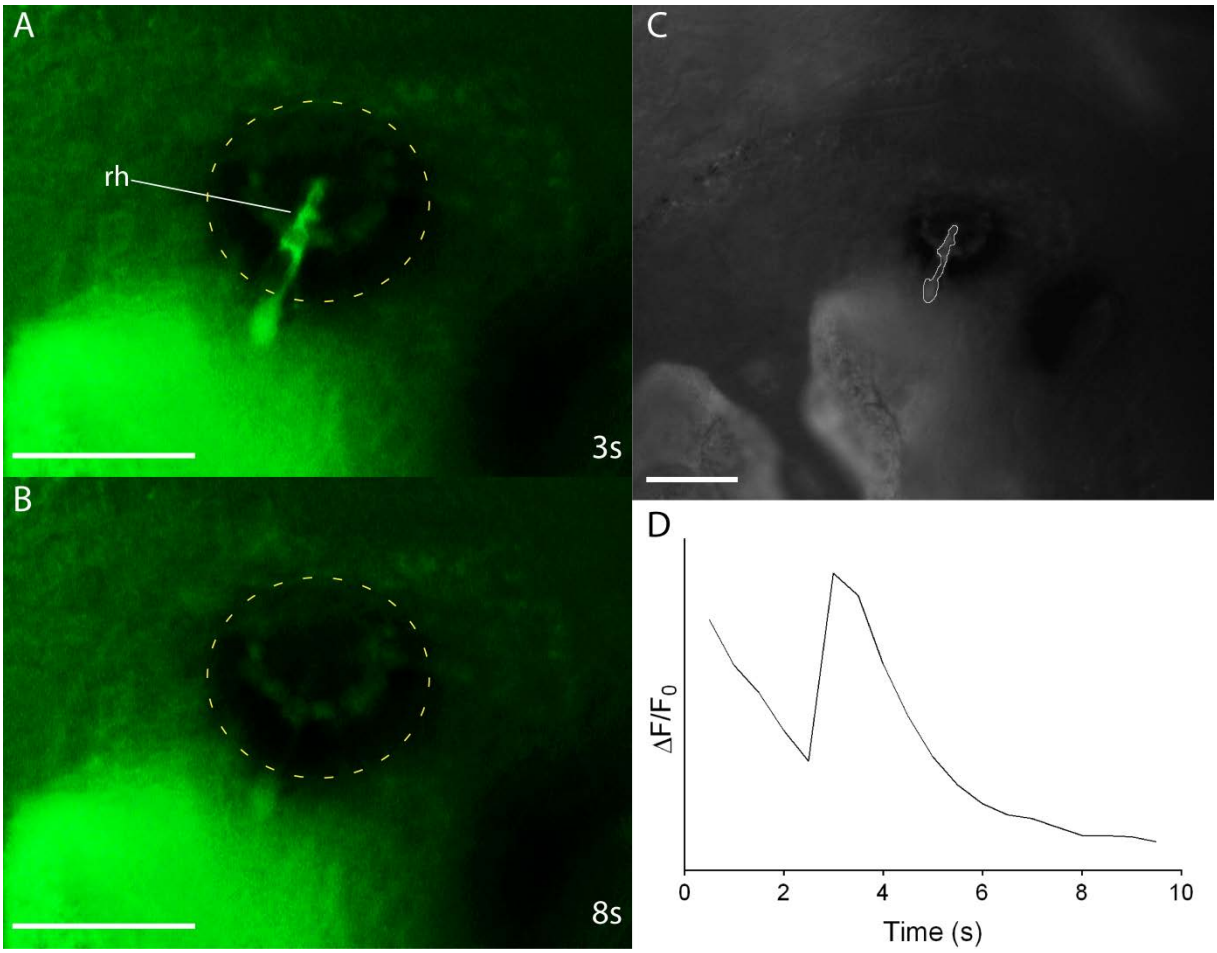

Figure 18: Endogenous Transient GFP-like Fluorescence observable in distinct neuronal domains within Wild Type adult *P.du* eyes and brain. (**A-C**) Single channel light microscope images of the dorsal view of an adult *Platynereis dumerilii* head centred on one posterior adult eye (yellow circle) under standard EGFP light filter settings (488nm excitation/509nm emission) (Scale bars = 50µm). Still images from a time course recorded at a rate of 2 frames per second at 3 (**A**) and 8 (**B**) seconds after recording onset demonstrate the differential fluorescence of the rhabdomere (rh) and cell body of a single photoreceptor cell. (**C**) outlines the boundaries of this distinct cell to define a region of interest (RoI)(white) for fluorescence quantification by image analysis software. (**D**) plots the trace of the differential fluorescence intensity of the RoI across the entire nine second time course normalised to background fluorescence.

Discussion

IMPLICATIONS OF GO-OPSIN AS A SHADOW REFLEX PHOTORECEPTOR

The role of Go-Opsin1 in *P.du* larvae has already been demonstrated to be the perception of cyan light (~500nm) to facilitate phototaxis (39). However, we saw that adult *P.du* are not phototactic, and in fact display scotokinetic behaviours (14), where locomotor activity generally occurs nocturnally in darkness. Therefore, the Go-Opsin1 expression in diverse domains in adult *Platynereis* (Figure 7) likely has a different photodetective purpose. This is indeed the case, and in the process of proving this, we established several other interesting findings concerning the shadow reflex and peripheral photoreception in adult *Platynereis* worms.

Our assay reveals that the shadow reflex is heavily dependent on the 500nm component of light (Figure 6). Evolutionarily, this makes complete sense, as cyan light is the region of the visible electromagnetic spectrum which has the highest penetration in the water column (58), allowing the shadow reflex to remain a robust survival mechanism even down to 10m below sea level, the maximum depth of the zone where *P.du* are known to habitually reside (59). As a demonstration of the extent of this wavelength specificity, 500nm monochromatic light shadow reflex success rates match those of white light (Figure 5), despite the fact that our 500nm light stimulus has approximately one tenth of the intensity of both 470 and 400nm conditions (Figure 4). This lower initial irradiance of our 500nm condition decreases the photic contrast between our light (ON) and dark (OFF) stimuli, and yet still we see a similar response rate to that in bright white light, dramatically cementing our finding of strict wavelength specificity. This discrepancy between the total photon fluxes was a necessity in order to ensure chromatic separation between each condition and avoid overlapping of their monochromatic light sources. Due to the naturally heightened sensitivity of human rhodopsin to green and yellow wavelengths (60), commercial LEDs of wavelengths from ~500-600nm do not need to be as bright or precise as their <500nm counterparts in order to be seen and appreciated by consumers. For this reason, 500, 520 and 590nm commercial LEDs, such as the ones used to create the behavioural chamber for this assay, are built with less stringent precision and their entire spectral profile is approximately twice as wide as 400 and 470nm lighting (Figure 4). To avoid overlap of light wavelengths between monochromatic conditions, these imprecise wavelengths were reduced in intensity.

Whilst not always significantly different, the means of Go-Opsin1 heterozygotes consistently lie between their homozygous and wildtype siblings under every light condition which elicits a shadow response, leading us to conclude that there is dosage dependence on Go-Opsin1 protein levels for the reliable conduction of the shadow response (Figure 6). This protein level dependence of the

behavioural response mirrors the Go-Opsin1 dosage dependence in Platynereis larvae concerning their phototactic capability to cyan light (39), further increasing our confidence in our results.

Despite the remarkable regenerative capacity of *Platynereis* and annelids in general, following the surgical removal of their cirri and after 4 days of recovery time (2 days recovery and 2 days tube formation in the shadow assay wells)(Figure 8), we demonstrated that the cirri had not yet even begun to grow back (35). Concerning this, one would expect the cirri of *Platynereis* to be a major user of the worm's regenerative capacity, due to the fact that they are semi-expendable extremities which are often nipped and broken and bitten off by predators and rival worms in lieu of losing more integral body parts.

The frequent unavoidable loss of portions of the cirri due to their vulnerable physiological location has inherently encouraged them to become expendable in nature. As suggested by Cronin et al (2), this expendability is one evolutionary explanation for why shadow reflex photoreceptor systems in annelids have become so decentralised and yet remained simple, with single photoreceptor cells being dispersed evenly across the cirri or radioles, instead of investing in more complex directional eyes which would naturally have higher visual acuity. The cost to reflex efficiency and biological energy reserves from losing a single peripheral photoreceptor cell, rather than an entire complex eye, is much less if many others can compensate until regrowth occurs. Concerning this, and to further clarify how such decentralised photoreceptive structures can consistently elicit a full body reflex, an interesting next step for experiments on the necessity of single cirri for the conduction of the shadow response would be the surgical grafting of wild type cirri onto Go-Opsin1 mutant animals, a technique theoretically possible in annelids (61). If such grafting experiments could be optimised, our knowledge of these peripheral photoreceptors could be furthered by an analysis of how many cirri are required to rescue the phenotype of decreased shadow response success rate which we observe here in surgically cirri-less *P.du* (Figure 8) or Go-Opsin1-deficient animals (Figure 6).

Generally speaking, the tendency for shadow photoreceptors to be expressed in the peripheral regions of lophotrochozoan species aids in their function, be they Sedentarid radiolar ocelli (18,62,63), bivalve mantle edge eyes (9), or nereid cirral PRCs (35). Photodetective domains placed around the edge of an animal or on their distal extremities are inherently more likely to catch "sight" of a passing shadow than domains in the head or central body, and so we see shadow photodetectors placed on ever more branching and extended structures to increase their utility (Figure 7).

We observed that metronidazole treatment appeared to have a general negative effect on all animals due to its inherent toxicity and the necessity of metronidazole being administered dissolved in 0.2% DMSO to make it soluble and cell membrane permeable (56). This results in an increased variability of success scores, though not significantly so, in the animals which have undergone metronidazole treatment. Our inclusion of wildtype mtz-treated animals dismisses the possibility that metronidazole treatment alone can reduce the efficacy of the shadow reflex as no significant difference in shadow reflex success rates is detected between the treated and untreated groups (Figure 9). Our data suggests that the r-Opsin1-positive cells of the eyes which provide visual information to *P.du* do not contribute to shadow detection. This finding is consistent with the implication that other polychaete worms, namely the upright tube-dwelling umbrella worms (Sabellidae) do not utilise their adult eyes in predator detection, although in their case this is likely because their eyes are permanently occluded within their opaque tubes (18). Whilst *Platynereis* silken tubes are transparent, their ability to detect potentially hostile shadows without relying on their fixed adult eyes is likely still a considerable survival advantage. It was noted almost 50 years ago that removing the eyes of *P.du* worms does not completely abolish the shadow reflex (54). Upon removing the animals prostomium by decerebration, which *Platynereis* are quite capable of fully regenerating from (23), it was noted that headless animals exhibited a maintained shadow reflex (54). This previous literature attributed the source of non-visual photoreception to theorised photoreceptors within the trunk, since they were not yet aware of the Go-Opsin1 photoreceptors present in the cirri (35). The manner in which they "decerebrated" the animals effectively cut out the adult eyes without damaging the cirri, since it involved surgically making "incisions in the prostomium in front of the anterior eyes, behind the posterior eyes and along the side, lifting the flap of epidermis and picking out the encapsulated ganglion with forceps" (64,65). Therefore, these previous findings are congruous with our experiments, as we too demonstrate that non-ocular photoreceptors are the source of photoreception for this reflex. There has since been evidence that photoreceptors do indeed exist in the trunk of *Platynereis* (66), though these are rhabdomeric type opsins and as per the findings of this thesis (Figure 9) do not contribute to the shadow reflex either. This lack of involvement of the rhabdomeric cells of the adult eyes in the *P.du* shadow reflex is especially interesting considering that we find strong Go-Opsin1 expression persisting in the adult eyes during this developmental phase (Figure 7).

In the described results, each shadow stimulus for each individual worm was analysed manually by eye, making quantification a labour-intensive and time-consuming process. The speed and replicability of this quantification step would have benefited from a degree of automation similar in principle to the tracking software used in the established computerised locomotor activity assay (14)(Figures 12 and 13). In principle, this software could have operated by observing the constantly

recorded length of the worms, “length of animal” being a variable which had already been demonstrated to be trackable in previous iterations of the locomotor tracking software (67). With this, a more objective quantification of shadow reflex success could have been determined by assessing whether the worm length suddenly decreases by more than a certain threshold upon light disillumination. We are however confident in the empiricism of the current data produced by the shadow reflex assay, due to the behavioural grader being made both blind to the genotypes of the observed animals and to the randomly introduced wavelength conditions under which they were being tested. All shadow reflex success rate behavioural scoring was conducted by one person. This avoided any potential differences between behavioural analysers in terms of what they subjectively consider constitutes a robust shadow reflex. Ideally, this subjectivity could have been reduced further by the double-checking of each video by a second behavioural analyser to reach a consensus, although this would have required appreciably more manpower. Admittedly, these issues could have been avoided entirely by the inclusion of computerised tracking software to binarily decide on shadow reflex success rates. Sufficiently high throughput was crucial to the adequate quantification of this shadow reflex, as both our optimisation and historical sources with similar nereid worms found that the variation in shadow response success rates within and between individual populations was extremely high (Figure 5)(53). For this reason, our assay had to be constructed to gather large enough numbers of biological replicates (36 per trial) to overcome the natural variability of the shadow response success rate and make appropriate conclusions.

Concerning the random ordering of light conditions presented to each cohort of worms, this served a dual function. Firstly to ensure that grading by the behavioural analyser was conducted blindly without expectation of wavelength dependent behaviour levels, and secondly to avoid any potential chance that the worms may be learning to anticipate our conditions and respond accordingly. According to literature (53), the sensitivity to shadows of two related polychaete worms, *Nereis pelagica* and *Nereis diversicolor*, “is not influenced by previous experience”, despite the fact that *N.diversicolor* has a fully burrowing lifestyle and so has no prior experience of shadows. We therefore felt it would not introduce experimental bias for individual worms to be presented with multiple different consecutive light conditions. We further decreased the chance that worms could be induced to react differently to one wavelength by the previous presentation of another by enforcing a 60 minute acclimatisation period prior to each different conditions’ shadow stimuli (Figure 4).

Our shadow stimuli were not strictly enforced by what is conventionally considered a shadow, but rather by the sudden switching off of the behavioural chamber’s light emitting diode arrays. Whilst this difference may seem inconsequential, a true shadow stimulus defined by of an object moving between the light source and the organism could have different biological connotations than simply

abrupt darkness. It is possible that a shadow passing over an organism from one side to another, occluding photoreceptors in sequence rather than simultaneously, is one crucial component of light information which allows organisms to identify shadows. The fact that we observe a robust and reproducible shadow response success rate under white light and 500nm conditions is an indication that despite us not presenting a moving shadow front, we still sufficiently elicit a reliable shadow reflex. Additionally, this light cessation as an imitation of a true shadow is the same as previous shadow reflex assay protocols in vertebrates and crustaceans (68) and *P.du* itself (69).

However, due to the regular and spread out nature of the Go-Opsin1-expressing cirral photoreceptor cells in adult *P.du* (Figure 7) and their implication in the shadow reflex (Figure 8), one might expect a true moving shadow to elicit an even greater response. Hypothetically, Go-Opsin1 expression could be spaced specifically to detect the sequential disillumination of each cell along a single cirri caused by a shadow front moving down its length. In this case, if we were to adjust our assay to use a true shadow with an object eclipsing a light source, it is possible that we could obtain higher shadow reflex success rates with less variability between animals. Moving shadow front stimuli have been constructed before with mechanical shutter systems (8). However, we avoided such mechanical shutter systems in this assay to avoid any potential vibrations which would occur when blocking the light source, favouring instead a purely electronic shutoff.

Even under white light, very few worms had a 100% shadow reflex success rate (Figure 5). This may be due to the fact that in nature, the *P.du* shadow reflex is triggered by more than simply photic stimulation, and relies on a combination of photic, mechanosensory and chemosensory cues. This is demonstrated in the closely related *Nereis pelagica*, a burrowing relative of *P.du* (53), where it has been concluded that the Nereid worm doesn't recognise a predatory presence by a simple disillumination stimulus as some other polychaetes such as Sabellids may do, but rather as a combination of various coincident stimuli. For this reason, in our assay we took measure to isolate worms from any potential tactile vibrations and separated the worms so that no secreted chemical signals could interfere with our assessment of the purely light-induced shadow reflex. Startle reflex activation by purely chemical signalling is well-characterised in the polychaete *Nereis virens* (70). Olfactory signalling with chemosensory markers of anxiety between individuals has been shown to hypersensitise the startle reflex in humans (71) and so we avoided the potential influence of this signalling between worms in our assay. Further to this, the shadow reflex of a nereid worm in its natural environment can be thought of as in a more or less constant state of partial activation, due to the abundance of non-threatening light, chemical and mechanical signals, causing this reflex to be especially prone to desensitisation (53,69).

By its nature, the *P.du* shadow reflex is energetically costly to the organism, not just because the rapid contraction of muscles requires energy, but because time spent retracted within the tube is time not spent foraging and feeding. Whilst evolutionarily, this energy cost is compensated by the benefit of predator evasion, in practise an organism would rather avoid having its shadow reflex triggered by a false alarm. These false alarms are caused by a sudden loss of illumination not by a looming predator, but by the presence of constant non-threatening shadows of seagrass or other vegetation which routinely grows between typical *Nereid* habitats and the sources of light in typical polychaete habitats (72). Therefore, the shadow reflex has a generally low threshold for becoming desensitised. For this reason, the design of my shadow reflex paradigm has been specifically tailored towards avoiding overstimulation and desensitisation. Congruous with classical literature (53), we found that the *P.du* shadow reflex requires a refractory period of 60 seconds between each shadow stimulus to avoid habituation and a rapid drop in shadow reflex response rate, where they react only rarely to newly presented stimuli (Figure 4).

There have been suggestions that a combination of shadow stimuli and chemoreception of predator-based signals is required in *N.virens* for shadow reflex initiation, thus preventing false signalling (70). Overall, literature seems to suggest that shadow detection acts as a complimentary trigger of the withdrawal reflex compared to the ubiquitously useful chemosensory detection of a predator, as chemosensation can take place at night. This is backed up by the fact that *Platynereis* is most active at night (14) and chemosensory predator detection has therefore been described as the annelid's primary withdrawal stimulus in lieu of sufficient illumination (70). Whilst *Platynereis* does possess an abundance of chemosensory apparatus in the form of its antennae, and to a lesser extent the palps and nuchal organs (73), these are not a requirement for shadow reflex activation as here we reliably and reproducibly stimulate the shadow reflex in *P.du* with light alone. Our protocol goes to considerable lengths to omit any chemical or mechanical accompaniment to the shadow stimuli. This suggests that whilst in nature the response trigger is likely a complex of many sensory inputs, a pathway exists which links directly from cirral and Go-Opsin1-facilitated photodetection to a stimulation of shadow reflex behaviour.

This work confirms that Go-Opsin1 acts as a shadow reflex photoreceptor in *P.du*, but the extent to which this finding can be generalised to similar and even more highly evolved species is still debatable. Superficially, based on previous observations (74), the defensive withdrawal behaviours of various species of polychaetes, whether tube-forming (*P.dumerilii*) or burrowing (*N. diversicolor*), remain largely similar despite differing lifestyles. Attributed to the fact that these behavioural patterns retain their utility to any creature subject to predation from above, this would suggest that we are likely able to generalise our findings on the shadow reflex at least to other members of

Nereidae and perhaps to other polychaetes. This observation of the shadow reflex occurring regardless of whether the worm has a tube to withdraw into is visible here in our assays, as we were also able to consistently detect the distinctive shadow reflex of freely swimming *P.du*. When not anchored in their home tube and undergoing the serpentine swimming motion characteristic of other pelagic annelid species (75), shadow stimuli caused our worms to undergo rapid straightening and longitudinal shortening. The mechanism for enforcing the startle response in larval *P.du* is outwardly comparable to the shadow reflex we have noted here in adults, involving a contraction of the longitudinal muscles which shortens overall body length (76). In *P.du* larvae, the mechanically-triggered startle response also stimulates a raising of the parapodia. Whilst this serves to make the young free-swimming animals spiky and therefore less appetising, in the adults this would likely allow the adults to grip the interior of their tubes and withdraw more effectively. In conclusion, in adult worms, this polycystin-mediated startle response (76) could facilitate the behaviour we see in response to sudden shadows, albeit triggered by photo-, rather than mechanoreceptors, and on a larger scale with more segments being affected. To explore this concept further, one would likely begin by assessing whether the adult shadow response is also mediated by the polycystin-expressing collar neurons as has been demonstrated in *P.du* larvae (76).

Considering that the swimming motion of marine polychaetes is primarily induced by rhythmic longitudinal contractions (75), it is clear mechanically how longitudinal contraction and parapodial extension in adult worms could suddenly render these worms abruptly motionless if indeed this biological induction of the startle reflex is continued in adulthood. Whilst this shadow reflex-induced state of catatonia in adult *Platynereis* may seem counterproductive as it involuntarily stops animals from swimming away, it does mean that animals suddenly descend in the water column. Diving in the water column at the first sign of danger is a classical escape behaviour conserved through many marine species, be they invertebrates such as Cnidarians (77) or vertebrates such as zebrafish (78). This behaviour is particularly apparent in larvae and very young animals (and in our case immature *Platynereis* caught outside of their tubes), as they have a limited swimming ability and so sudden depth increase represents the most effective escape behaviour. By indiscriminately causing longitudinal contractions of the body, I hypothesise that the *Platynereis* shadow reflex is able to decrease the chances of predation regardless whether animals are inside their tubes (resulting in withdrawal) or not (resulting in depth increase) with a single reflexive behaviour of minimal complexity.

However, even within the family of Annelidae, distinct differences in the detection of shadows and the triggering of the shadow response bring into question the extent of applicability of our findings. Several of our findings here, in the context of recent literature, imply that adult *P.du* cirral

photoreceptor spots (Figure 7) and the superficially similar ocelli located on the branching radioles of Serpulid and Sabellid (both of the Sedentarid family) worms (62,63) are derived from quite drastically different evolutionary origins, despite the phylogenetic proximity of these annelid species (79). Though they range drastically in complexity, the radiolar ocelli share the same function the cirral photoreceptor cells we localise here, the detection of threatening shadows and activation of an appropriate withdrawal reflex (9,18).

Our first piece of evidence that these photoreceptive structures are not derived from the same evolutionary beginnings is that the colourful branching radiolar tentacles of Serpulid and Sabellid worms are a highly specialised derivative of the palps in other polychaetes. Developmental analysis of the innervation of these branchial crowns which give umbrella worms their name has revealed that they develop from the dorsal lip of the worm where Errantids (such as *Platynereis*) grow palpae, rather than cirri (80). In response to this, we briefly investigated whether Go-Opsin1-expressing photoreceptive cells, or indeed any kind of ocellar structures were present in the palps of *P.du*, finding no visible evidence of either. Secondly, radiolar ocelli are conventionally associated with some kind of underlying or screening pigment which shields the photoreceptor cells from certain directions and wavelengths to increase the specificity and directionality of the eyes (18). The incorporation of pigment cells and directionality marks a fundamental step in the evolution of complex eyes, as it is the precursor to the development of more complex light capturing structures such as the lens or the retina (81). However, these Go-Opsin1-expressing cells in *Platynereis* are even more basic than the previously theorised basal level of eye development (2). They described the most simple functional mollusc eye as having at the very least a photoreceptor cell with membrane stacking (for additional surface area) and importantly an underlying screening pigment. This screening pigment is not present in *Platynereis* cirral photoreceptive spots but is widespread in the radiolar ocelli of Sabellids, adding to the striated and floral appearances of their colourful fans (18). This lack of pigmentation is not strictly unique to *Platynereis* cirral photoreceptor cells however, as the tube feet of sea urchins contain eyes which are associated with neither screening nor underlying pigments (82). In the sea urchins case, directionality of the sensory response is thought to be instigated by the growth of the opaque calcite skeleton around the photoreceptor cells, leaving them as pinholes. It is likely that the function of threat assessment through loss of light detection need not be unidirectional, and following the principle of parsimony in evolution, simple photoreceptor spots without screening pigments are sufficient for shadow detection. Perhaps non-directional photoreceptor cells such as those we find in *Platynereis* cirri are better suited for such a job, as they are not reliant upon a stimulus occurring within their visual arc.

The final difference between nereid cirral photoreceptors and fan worm radiolar ocelli which cements their separate evolutionary origins is their utilisation of different photoreceptors to conduct phototransduction. In the Sabellid *Acromegalomma interrupta* (18,63) and the Serpulid *Spirobranchus corniculatus* (62), a ciliary-type opsin is the photosensitive component within the radiolar ocelli, in contrast to the Go-type opsin expressed in Errantid cirri (35).

The use of ciliary opsins for shadow detection in these Sedentarid species was ascertained by sequencing the transcriptome of the eyespot-like structures perched on the end of the radiolar tentacles, revealing the abundant expression of a ciliary opsin homolog in these modified structures. Whilst this is highly indicative of c-Opsin's role in radiolar photoreception, the expression of ciliary opsin does not explicitly prove its involvement in the shadow reflex. In order to definitively prove that c-Opsin is the operative photoreceptor in these cells, further experiments would likely require targeted mutation of the Sedentarid c-Opsin gene to see whether loss-of-function results in a lapse in shadow reflex behaviour. Additionally, the transcriptome of Sabellid radiolar eyes reveals the expression of a Go-type Opsin, albeit in significantly lower amounts than the transcripts of the ciliary-type opsin (62,63). Even in trace amounts, a Go-Opsin in the radiolar eyes could evoke a shadow response, due to the principle of signal amplification by membrane bound phototransductive proteins. This principle ensures that a neuronally relevant signal can be generated from just a handful of photoreceptor subunits, thanks to the manner by which GPCRs transduce and propagate their signal in an amplifying manner through G-protein subunits (83). Even without further characterisations we still find these transcriptomic studies to be compelling evidence that Sedentarid radiolar ocelli use a c-Opsin as their photosensitive protein (62,63), leading us to conclude that Sedentarid and Errantid peripheral photoreceptor cells have different evolutionary origins. Despite it seeming unlikely that Sabellid and Errantid peripheral eyespots could well have evolved from distinct origins in two species so closely related, there are biological precedents for this happening. For example, the separate evolution of eyes and eyespots, converging on a single simple design has been noted previously between closely-related species within Cnidaria, whose simplistic photosensitive eyespots are also implicated to have evolved separately due to differing morphological and photoprotein expression differences (84). This prolific and apparent independent development of non-cephalic eye-like structures in two closely related annelid species demonstrates that previous researchers were correct in thinking of annelids as "eye factories" (18).

Concerning this protein-based dissimilarity between cirral and radiolar peripheral photoreceptor systems, the type of opsins responsible for a particular function is generally a poor indicator of the evolutionary origin of the physiological structure in question, due to the tendency of opsins to be recruited to novel sites thanks to their ease of incorporation. This "genetic promiscuity" in the

photoreceptor and structures used by different photoreceptive structures is a concept which hampers efforts throughout many model systems to ascertain the true origins of eyes and eye-like structures (31,81). For example, looking purely at the utilisation of opsin subtypes, one might imagine that the Go-Opsin1-based cirral PRCs in *Platynereis* are more closely related to the Go-Opsin-laden mantle edge eyes which photodetect shadows in bivalves (4,42) than to the radiolar ocelli of their annelid cousins. However, we find this similarity to be a likely result of the post-hoc recruitment of functionally suitable photoreceptors, Go-type Opsins, and are not implying that the *P.du* cirral PRCs (Figure 7) and *Pecten* mantle edge eyes (9,42) are developmentally homologous.

Despite their obscure anatomical locations, Sedentarid radiolar ocelli are likely to be derivatives of some kind of primitive eye plan, insofar as they arose using the basal genetic template for basic eyes, due to their expression of fundamental early ocular development genes such as *pax6, eya* and s*ix4* (18,62,63). To assess whether *P.du* cirral photoreceptors share these similar proto-eyes origins, or arose sporadically incorporating available photoreceptors for novel functions, a transcriptomic assessment of isolated *P.du* cirral photoreceptor cells should focus on the presence or absence of these ocular master control genes.

Concerning the relative simplicity of these cirral shadow-detecting PRCs in Platynereis compared to other decentralised photodetection systems such as Sedentarid tentacular eyes or ocelli, this by no means indicates that *Platynereis* cirral PRCs are less well evolved or less suited to their shadow-detecting function. The evolutionary pressure for increasing the complexity of eyes was driven sequentially, by requirement for successive visually-guided behaviours. In this manner, increases in organ complexity are dictated by the sequential acquisition of specific tasks (9). For example, as mentioned previously, the inclusion of screening or basal pigments into a general eye design was prompted by a need to gain directional information for visually-guided behaviour. For this reason, since simple pigmentless photoreceptive spots are both effective and sufficient for shadow detection alone, as we demonstrate here (Figures 6 and 8), *Platynereis* has had no need to increase their complexity. One could view the cirral photoreceptor spots in *P.du* as the basal level of simplicity for photodetective systems evolved for a single task. Regardless of the evolutionary path taken by different annelid species, the fact that decentralised single photoreceptive spots on tentacular extremities have become the predominant method of predator detection in many lophotrochozoan species represents convergence upon the most robust, flexible and energetically efficient physiological method of triggering the shadow reflex (62).

This begs the question, if simple adirectional photoreceptive spots are sufficient to robustly trigger a shadow reflex, then what has prompted Sedentarid polychaetes to evolve increasingly complex and decorative radiolar eyes (18)? It is possible that the loss of the use of Sedentarids cephalic eyes and

chemosensory organs, due to occlusion within the opaque and sealed tube, has prompted their increased reliance on their radioles for predator detection. With this in mind, perhaps the shadow reflex in *P.du* is only robust in nature thanks to the contribution of mechano- or chemosensory detection systems in conjunction with photodetection. Perhaps Sabellids and Serpulids have also developed a more sensitive and foolproof shadow detection system because they stand to lose more from damaging a radiole than *Platynereis* do from losing a cirri, as radioles are the sole source of food gathering in Sedentarids (85), whereas in *Platynereis* a lost cirri is an inconvenience at worst. These questions are yet to be explored fully, but the data presented here (35) should facilitate more complex experimentation of annelid shadow photodetection in the future.

CILIARY OPSIN AS A POTENTIAL COMPENSATORY SHADOW REFLEX PHOTORECEPTOR

One detail in the results of our shadow reflex assay has a major implication for our understanding of shadow photodetection in *P.du*. Whilst decreased shadow response success rates in cirri-less and Go-Opsin1 mutant animals prove that both cirri and Go-Opsin1 contribute to the shadow reflex, their removal does not abolish the shadow reflex completely (Figures 6 and 8). This suggests that some measures are present which contribute for their absence. Seeing as the shadow reflex is a behaviour which is so crucial to survival, it is no surprise that redundancy has evolved to ensure its robust function. Taken alone, the finding that total cirri removal does not lead to total shadow reflex failure would indicate that the Go-Opsin1 expression domains in the dorsal *P.du* brain (Figure 7) are likely to be compensating for the loss of the cirral photoreceptors. This would be a reasonable explanation considering that we also rule out the contribution of the Go-Opsin1 in the r-Opsin1-positive cells of the adult eyes (Figure 7). However, seeing as shadow reflex success rates are not reduced to zero even upon the full deleterious mutation of Go-Opsin1 (39), we find that a far more likely explanation is that the shadow reflex is mostly conducted by Go-Opsin1 in the cirral photoreceptor cells, but a second unidentified photoreceptor is compensating for its loss in a different part of the body.

Another photoreceptor protein would inherently have subtly different excitation characteristics, and so would likely be detecting shadows in a different portion of the total wavelength spectrum which we see that the shadow reflex is active within (~470-520nm)(Figure 5). Congruent with this hypothesis, the removal of Go-Opsin1 reduces the mean shadow response success rate more under 500nm light than under white light (Figure 6). Whilst Go-Opsin1 conducts the shadow reflex triggered by the ~500nm spectrum, a secondary photoreceptor is more able to compensate for Go-Opsin1 loss when the entire visible spectrum is provided (ie. under white light conditions). To further explore this idea, one could repeat the investigation of Go-Opsin1 dependency of the shadow reflex (Figure 6), but under more wavelength conditions of between 10 and 20nm apart. With this information, one could see if the drop in shadow reflex success rate is greater under some wavelengths than others

and perhaps from this implicate a subsection of the spectrum where the secondary compensatory photoreceptor is most photoactive. This information could be instrumental in deciphering the identity of this secondary shadow photoreceptor. Literary evidence alone however can provide us with a potential candidate for the compensatory shadow reflex photoreceptor in *P.du*.

As concluded in the previous section of this discussion, we find that the cirral photoreceptive spots discovered in *Platynereis* (Figure 7) and the radiolar ocelli common to their annelid cousins, Serpulid and Sabellid worms (62,63) are likely to have come about via separate evolutionary origins. Importantly, the type of opsin implicated in photodetection in Sedentarid radiolar ocelli is an invertebrate ciliary opsin. Since it has been established that both Go and Ciliary Opsins can act as these "burglar alarm" shadow detectors, we posit that a *Platynereis* ciliary Opsin could act as the photoreceptor which compensates for the loss of Go-Opsin1 in our shadow reflex assay (Figure 6). Here, we present several arguments supporting its candidacy.

Transcriptomic data has identified two distinct ciliary type opsins expressed in the adult *P.du* head (16). The first, initially identified as one of the few ciliary type opsins expressed within the invertebrate brain (17), is hereafter referred to as *Pdu*-c-Opsin1. Recent mutational analyses indicate that the presence of a lysine (K) residue at position 94 of *pdu*-c-Opsin1 causes this proteins' maximal photoexcitation wavelength to stray into the ultraviolet spectrum, at around 383nm (86). Considering that our data (Figure 5) indicates that the shadow reflex is not stimulated at all by light of 400nm or less, c-Opsin1 can be discounted as a shadow reflex modulator in this species. Indeed, recent data suggests that *Pdu*-c-Opsin1 contributes instead to UV avoidance behaviour and depth calibration in larvae (87). The second ciliary-type opsin expressed in adult *P.du, pdu*-c-Opsin2, has been demonstrated with *in vitro* studies to have a maximal absorption wavelength at 490nm (35). The *P.du* shadow reflex is also strongly attenuated to this region of the visible spectrum, with a maximum of around 500nm (Figure 5), meaning that the excitation characteristics of *pdu*-c-Opsin2 would be well suited to conducting this response as a redundant compensatory photoreception system to Go-Opsin1 (Figure 6).

The ciliary opsin in fan worm radioles has been shown to be phylogenetically similar to the two ciliary opsins present in *P.du*, as confirmed by several independent phylogenetic studies (62) including our own (Figure 14). In fact, the ciliary type opsin expressed abundantly in Sabellid radiolar eyes is most closely related to the two known *Platynereis* ciliary opsins compared to ciliary opsins in other species (18). This phylogenetic proximity would suggest a shared origin, and is indicative of the ciliary opsins in *P.du* having at least at one time shared a similar function to the ciliary opsin in Sedentarid radioles.

Importantly, our phylogenetic classification (Figure 14) confirms that our *pdu*-c-Opsin2 coding sequence can indeed be counted amongst known functional ciliary opsin proteins, and that further genetic manipulation can be conducted in *P.du* using this confirmed sequence. This classification remedies a previous issue with nomenclature concerning the two known Ciliary Opsins in *P.du*. In literature utilising both *pdu*-c-Opsin1 and 2 sequences to phylogenetically place new invertebrate ciliary opsins discovered by transcriptome, their identities are switched. Namely, the nomenclature of *pdu*-c-Opsins -1 and -2 are referred to as *pdu*-InvC-type Opsin-2 and -1 respectively when compared to Serpulid (62) and Sabellid (18) Ciliary Opsins. Our phylogenetic comparison has allowed us to clear up this confusion for posterity and future analyses of both *Pdu-c-opsin-1* and *-2*.

Our data (Figure 14) indicates that *pdu*-c-Opsin2 lies in relatively close phylogenetic proximity to other ciliary-type opsins in vertebrates such as encephalopsins and rhodopsins, in comparison to rhabdomeric opsins within other lophotrochozoan species which diverged much earlier. This demonstrates the strength of conservation of ciliary type proteins which are retained in all three advanced taxa, lophotrochozoans, chordates and arthropods (Daphnia and Anopheles). Our tree demonstrates that the similarity between *pdu*-c-Opsin2 and other c-Opsins in these three diverse clades exceeds that between *pdu*-c-Opsin2 and other Opsin proteins even within more closely related Lophotrochozoan species, reinforcing our established knowledge that the diversification of opsins preceded the divergence of metazoans into chordate and ecdysozoan lineages (88). Clearly the continuing evolutionary utility of ciliary opsins as both visual and non-visual photoreceptors is a factor which contributes to their prolonged conservation throughout Animalia. The shadow reflex could feasibly represent such an overarching and ubiquitously useful function relevant to diverse groups of Metazoans, explaining the retention of this opsin subgroup.

The known arthropod opsins most similar to *pdu*-c-Opsin2 are *Dpu*-Pteropsins and *Aga*-GPR-Opsins (Figure 14). Pteropsin was first classified in the honey bee, noted then for its similarity to *pdu*-c-Opsin, and in the honeybee is also expressed non-visually in the protocerebrum (89), similar to the neuronal c-Opsin2 expression we see here (Figure 15). Pteropsins, despite being present throughout broad swathes of Arthropoda, are absent from Dropsophilid fly genomes, and so have remained elusive and undercharacterised, due to the relative monopoly that Drosophila holds as an insect model organism. This further illustrates our need to consider non-canonical organisms such as *Apis mellifera* or indeed *Platynereis* to gain a complete understanding of Opsins and their diverse functions. *Platynereis* represents an ideal model to further study ciliary opsin functional evolution throughout life on earth due to its slow rate of molecular evolution coupled with its archaetypical body plan and general experimental amenability (23,24). *P.dumerilii* perhaps even represents a more convenient model than Sedentarid worms to assess these invertebrate ciliary opsins' roles in shadow

detection due in part to the pre-established quantitative assay (Figure 4) and the aforementioned genetic experimental malleability.

We know that *pdu*-Go-Opsin1 is not closely related to either of the *P.du* c-Opsins, as previous transcriptomic and phylogenetic comparisons indicate that they fall out far from one another within their respective Tetraopsin and c-Opsin groups (18,31). From this, we can infer that any potential overlap in function between Go-Opsin1 and c-Opsin2, potentially in shadow photodetection, is due to recruitment of one or both proteins to the site of shadow detection rather than them both evolving side by side to meet this behavioural demand.

Of note is the finding that ciliary photoreceptors are ideally suited to detecting shadows and therefore conducting the shadow reflex, due to the fact that the ciliary cells classically harbouring c-opsins hyperpolarise in response to light as a result of the $G_{\alpha o}$ G-protein subunits which they signal through (90). In practise this means that a resting potential of the sensory neuron is maintained in the presence of light and depolarisation occurs immediately under a sudden shadow, thereby increasing their capability of swiftly and robustly relaying shadow information. The Go-Opsin-expressing mantle edge eyes of scallops (43) and presumably the Go-Opsin expressing cells are similarly suited to shadow detection due to their propensity to hyperpolarise in response to light. Due to the fact that ciliary photoreceptors initially evolved for vision and did so by hyperpolarising in response to light (91), it could be that their initial function involved sensation of the absence rather than the presence of light, despite their various confirmed uses in direct light detection in a wide variety of organisms (88). Perhaps the ground state of sensory photoreception in life on earth was that originally attenuated to see shadows, rather than light, as forming images out of light information requires relatively complex central processing of many photoreceptive inputs within a field of view, but as we show here (Figure 8), single isolated cells can provide a distinct survival advantage when they are designed to detect no more than simple disillumination (Figure 7).

To further implicate *pdu*-c-Opsin2 in mediating the shadow reflex, an initial experiment could concentrate on finding out whether the c-Opsin2-positive neurons we show in the *P.du* brain (Figure 15) depolarise or hyperpolarise in response to light. Similarly, one could explore whether the Go-Opsin1-expressing cirral PRCs in *Platynereis* (Figure 7) also hyperpolarise in response to light, giving us a further indication of whether shadow detection systems in general are built upon this same principle of “dark current” photoreception (92). These analyses would be most effectively accomplished by imaging these neurons with a fluorescent neuronal activity marker, a possibility explored later in this thesis.

Knowing that ablation of the r-Opsin1-positive cells of the adult eyes does not impact the viability of the shadow reflex, we attempted to localise the expression of *pdu*-c-Opsin2 in the head to confirm that this ciliary opsin is expressed outside of the eyes, a necessity if it is to contribute to the shadow reflex. Due to the extremely low levels of mRNA transcripts of ciliary opsin-2 found *in situ* within adult *Platynereis* tissues, we were unable to conduct WMISH to visualise the expression pattern of c-Opsin2 in adult *Platynereis* as we did for Go-Opsin1 (Figure 7). These low *pdu*-ciliary opsin transcript levels are not present in sufficient concentrations to be detectable by the largely qualitative WMISH technique, but they have evidently been detected in *P.du* head transcriptomes by the more sensitive quantitative technique of RNA-sequencing (16). Therefore, we conducted antibody-based immunostaining instead to localise cephalic c-Opsin2 expression. Expression of *pdu*-c-Opsin2 can be observed in single isolated cells medial to the posterior adult eyes in the same focal plane as the Neuropil, a distinctive annelid neuronal structure demarcated by a convergence of many axonal processes from either brain hemisphere at the midline of the prostomium (93). These single c-Opsin2 cells (Figure 15) appear to be in the same approximate region of the brain where we show that Go-Opsin1 transcripts are expressed (Figure 7). This would have to be confirmed using colocalisation techniques, but if found to be true would have profound consequences for the case that c-Opsin2 is capable of acting as a secondary shadow reflex photoreceptor in lieu of Go-Opsin1 whereby single neurons within the brain are capable of triggering the response by either disillumination of Go-Opsin or c-Opsin2 as necessary.

c-Opsin2's non-ocular expression pattern further highlights its candidacy as a potential shadow reflex photoreceptor, though this is hardly surprising seeing at the insect-type eyes of *Platynereis* are known to be dominated by rhabdomeric opsins (17). Thanks to our studies involving single Go-Opsin1 expressing cells in the cirri (Figure 7), we know that single photoreceptive neurons such as those seen here (Figure 15) are capable of triggering the shadow reflex. To put together a more convincing case for c-Opsin2 being a compensatory shadow reflex photodetector, other than functional studies, c-Opsin2 expression should be re-examined in the worm's peripheral structures, the palps and cirri. Regrettably, due to time constraints and the delicate nature of these extremities, we were unable to image c-Opsin2 antibody staining in intact cirri. One caveat of this immunohistochemical localisation of *pdu*-c-Opsin2 expression (Figure 15) is that the anti-c-Opsin2 antibody used is yet to have its specificity confirmed, opening these results up to critical doubt. However, the symmetry and positioning congruent with expected literature of these apparent c-Opsin2-positive cells suggests that these images do likely represent true c-Opsin2 expression. In terms of subsequent studies in this line of inquiry, a confirmation of the specificity of this c-Opsin2 antibody is of high priority to confirm our findings.

In contrast, c-Opsin1 is expressed in cells in the annelid brain characterised by buttressed ramifications of their cell membranes, known as ciliary Photoreceptor Cells (cPRCs)(17) located more dorsomedially than the c-Opsin2-positive cells observed here. These cPRCs are thought to be responsible for circadian clock entrainment due to their transcriptomic profiles which demonstrate known clock control genes oscillating with a 24 hour rhythm (14). For this reason and excitation characteristics outlined above, *pdu*-c-Opsin1 is not implicated in shadow reflex modulation. Likewise, transcripts of *pdu*-Go-Opsin2 are present in far too low concentrations to be detected using WMISH, and in this case an anti-Go-Opsin2 antibody was unable to be raised in time to assay its expression. The fact that Go-Opsin2 appears to have evolved as a duplication of the Go-Opsin1 gene (39) makes it a potential compensatory shadow reflex photoreceptor worthy of further investigation, but the characteristics of c-Opsin2 make it a far more convincing candidate which has therefore been prioritised in this study.

Overall, we find that c-Opsin2 is well placed physiologically and chemically to influence the shadow reflex in *P.du* and would be a suitable candidate for further study. However, in order to functionally implicate c-Opsin2 in this modulatory role, a knockout study demonstrating the dampening effect of a deleterious *pdu-c-Opsin2* mutation on the shadow reflex must take place. We therefore sought to generate a c-Opsin2 mutant *P.du* line using Transcriptional Activator-like Effector Nucleases (TALENs). Our work yielded two usable pairs of TALENs which, in preliminary studies on *Platynereis* embryos, produced mutation rates of ~70% for TALEN pair 1 and ~10% for TALEN pair 2 (Figure 17). This high level of variability is expected, as the successful mutation rates for this established technique in *P.du* range widely between 20 and 75% (94). TALEN pair 2's mutational efficiency is difficult to judge adequately due to there being incompletely digested bands in the relevent uninjected controls. This may be a result of low cutting efficiency of HaeIII, but regardless, the mutagenic reliability of TALEN pair 2 is poor and not guaranteed. Nonetheless, we have demonstrated that at least TALEN pair 1 is sufficiently effective at generating targeted mutations in exon 1 of *pdu-c-opsin2*, allowing further mutagenic analyses to take place using this TALEN pair in future. If conclusions are made with the resultant c-opsin2 mutant *Platynereis* line concerning the protein's involvement in shadow reflex behaviour, measures should then be taken to confirm this phenotype in an independently generated mutant line, due to the inherent risk of generating off-target effects using TALEN-induced mutagenesis alone (95).

Subsequently, selective breeding could then generate a Go-Opsin1/c-Opsin2 double mutant line to find out whether this successfully abolishes the shadow reflex in *P.du,* or whether there is yet another photoreceptor capable of shadow photodetection which has evolved to perpetuate this clearly conserved and crucial reflex.

THE HUNT FOR THE CIRCALUNAR CLOCK PHOTORECEPTOR GOES ON

Considering that upon reanalysis, the maturation timing between Go-Opsin1-/- and Wildtype animals (Figure 10) found in data pulled from previous literature (39) was found to differ significantly, the case for Go-Opsin1 as a modulator of the annelid circalunar clock was looking hopeful. However, our data (Figures 10-13) reveals that the loss of Go-Opsin1 impacts neither circalunar nor circadian clock entrainment in *P.du*, urging us to look elsewhere for the elusive circalunar clock photoreceptor.

The significant difference in this data reanalysis (Figure 10) is somewhat unsurprising, considering the visible forward phase shifting of Go-Opsin1-/- animal maturation events during the 2nd and 3rd lunar month (Figure 3) which becomes more apparent upon normalisation (Figure 10). Once appropriately controlled for through the use of sibling animals obtained by heterozygous incrossing of two Go-Opsin+/- heterozygous worms, we no longer see a significant difference in the circalunar maturation profiles of Go-Opsin1 mutant animals. We can therefore attribute this initial difference to innate differences in the monthly maturation profiles of each strain of *P.du* used, the highly inbred homozygous mutants (Go-Opsin1 Δ8) and the more heterogeneous population of laboratory wildtypes. Even within different wildtype populations within the same laboratory, standard circalunar maturation curves can look drastically different (14), in much the same way that distinctly localised populations of *Clunio marinus* have strain-differentiable circatidal hatching timing (96).

Our circalunar light regime incorporated a single wavelength known to be the maximal activation wavelength for *pdu*-Go-Opsin1 (39) in an attempt to avoid the potential compensation for the loss of Go-Opsin1 by another photoreceptor which may also feed photic information into the circalunar clock (Figure 11). More importantly however, the light intensity at the point of the animal subject for both lunar and solar light stimuli was precisely monitored and kept constant (Figure 11). Knowing that extremely low intensity light sources are capable of entraining the circalunar clock, having an accurately calibrated lunar stimulus similar to natural lunar light was especially important, as opposed to simply using a 10W bulb. Our calibrations ensured that our sunlight stimulus matched those of previous studies, with a maximal intensity at 500nm of approximately $3x10^{11}$ (14), and a total moonlight stimulus intensity approximately $1x10^{3}$ dimmer than that (97). These various aspects demonstrate that whilst the correct conclusion was made previously (39)(Figure 3), that Go-Opsin1 mutation has no impact on circalunar maturation timing, this conclusion was made rather by accident than through rigorous experimentation.

Further reinforcing the importance of accounting for strain differences within chronobiological studies are the findings expressed by our circadian phase shifting data. In much the same way as strain-differentiable phenotypes in lunar maturation timing are visible and can interfere with appropriate analyses, it has been observed that distinct strains of *P.du*, even within the same

laboratory, can have vastly different nocturnal activity patterns. For example, previous literature notes that a wild type strain cultured within the Tessmar-Raible Lab appears to display nocturnal locomotor activity spikes with two peaks (14). In a similar way, wild type Drosophila develop a biphasic daily activity pattern in captivity (98), leading to the revelation that Drosophila take on a much more crepuscular (dawn and dusk) daily behaviour pattern when in the natural environment rather than under artificial laboratory conditions (99). We see this biphasic nocturnal activity recapitulated in our wild type strain (PIN) (Figure 12C), the identical strain to that used in Zantke et al, 2013 (14). By contrast, the Go-Opsin1 homozygous mutant strain with a unique strain background (kindly donated by the laboratory of Gaspar Jekely) lacks this biphasic profile, despite both subsets of animals moving comparable total distances amounts over the course of the 8-hour LD night. For this reason, in our results, we always quantified the average distance moved per hour during the entire 8 hour dark period, and where possible conducted sibling comparisons.

Despite a quoted maximal excitation wavelength of 498nm, *pdu*-Go-Opsin1 is not photoactivated solely by this single narrow wavelength band. In fact, Go-Opsin1 was demonstrated *in vitro* to undergo robust absorption all the way between 450 and 550nm (39). For this reason, and due to limitations of availability of 500nm lighting components, we deemed the use of 470nm lighting sufficient to test the contribution of Go-Opsin1 to the *P.du* circadian clock, and later on confirmed our findings with a more appropriate 500nm LED array. In both circadian and circalunar analyses, similar n-numbers between groups were prioritised in all experiments. However, due to the random nature of genotypes occurring as offspring of heterozygous incrosses, our experiments comparing sibling animals inherently contain values of n tending towards Mendelian ratios (ie. 25% Homozygous, 50% Heterozygous and 25% wild type). This inequality in n-numbers was exacerbated by the need to compare locomotor activity of worms of similar developmental stage and size. In practise, this inadvertently selected for low numbers of Go-Opsin1 homozygous individuals in comparison to other genotypes, most notably in Figure 13. Speculatively, this lack of viable Go-Opsin1-/- animals could be the result of a growth delay compared to their wildtype siblings. This growth delay could be the result of a reduced ability to feed effectively as larvae, considering that Go-Opsin1-/- *Platynereis* larvae are known to have deficiencies in phototaxis (39), which itself is a behaviour necessary for foraging during this formative developmental stage.

Overall, the take-home message of these chronobiological analyses, whether circadian or circalunar, is to never underestimate the contributions of even minor strain differences to rhythmic phenomena when examined on a population level. The use of siblings is paramount when examining phenotypical behaviours which can be attenuated by the minor polymorphisms present between laboratory strains (14,96)(Figures 12 and 13).

CONSIDERATIONS FOR FURTHER NEURONAL IMAGING IN ADULT *PLATYNEREIS DUMERILII*

Neuronal activity imaging via calcium indicators such as GCaMP is well established in larval *P.du* due to the ability to inject growing zygotes with GCaMP6s mRNA, yielding up to 20 days of GCaMP6s expression strong enough to image differential neuronal activity (100). To study many behaviours unique to adult annelids, such as intraspecies aggression, the maturation process, the cirral-triggered shadow reflex and biological clock-based behavioural readouts, GCaMP expression must be tailored to persist into adulthood. Stable transgenesis of fluorescent protein-expressing constructs has been previously optimised in *P.du* (66), but a considerable challenge in establishing neuronal activity visualisation in a novel model organism is optimisation of the fluorescence imaging itself. To this end, we sought to characterise the conditions necessary to successfully image and quantify variable eGFP, and by extension GCaMP6s, fluorescence in the adult *P.du* brain.

In pursuit of this, we documented a puzzling phenomenon present in wildtype animals of this species which impacts on the convenience and usability of green fluorescent calcium sensors in *P.du* (Figure 18). This endogenous and transient fluorescence occurring in wavelengths nearly identical to eGFP would interfere with attempts to measure transgenically-expressed GCaMP6s by stopping there from being a stable background autofluorescence which can be subtracted from a varying measured fluorescence. It is therefore in our interest that this enigmatic flashing fluorescence is classified for three major reasons. Firstly, to ascertain the evolutionary origin and purpose of this neuronal flashing to understand what impact it has on annelid physiology. Secondly, to attempt to isolate the source of this flashing fluorescence, likely a protein, as it may represent a novel activatable fluorescent protein with further utility and applications in research in the future. Thirdly, so that measures can be taken to cancel out or circumvent this fluorescence in order to effectively establish neuronal activity imaging in adult *P.du*.

These cellular, spontaneous fluorescence producing reactions are part of greater phenomenon demonstrated in life on earth named bioluminescence. The most well-studied of these bioluminescent reactants is luciferase, originally isolated from fireflies and glow worms, which emits light upon catalysing the oxidation of a co-expressed luciferin (101), but many other light emitting biochemical reactions have been classified since in diverse phyla.

Conventionally, *Platynereis* and other nereid worms have not been noted to produce bioluminescence or notable autofluorescence beyond that deriving from their cuticle, a trait shared with all animals possessing a chitinous carapace (102). However, several other annelid species are actively bioluminescent in a variety of wavelengths and utilising a variety of different photoproteins (103). Oligochaetes such as the earthworm *Diplocardia* and the scaleworm *Harmothoe lunulata* have long been noted to produce bioluminescence at 510nm, though strangely this shared emission

wavelength is the result of convergent evolution, due to the fact that these oligochaetes use distinct biochemical reactions to achieve fluorescence. *Diplocardia* produces a conventional luciferase (104) but *Harmothoe* utilises a unique photoprotein named Polynoidin which does not act via the classical luciferin-luciferase-style reaction (105).

This diversity of bioluminescent photoproteins is perpetuated in three polychaete worms, *Tomopteris*, *Chaeopterus* and *Odontosyllis*, fellow members of the subclass Errantia which also contains *Platynereis*. Both the tubeworm *Chaetopterus variopedatus* (106) and the pelagic worm *Tomopterus* (107) gain bioluminescence through similar non-luciferase photoproteins and yet emit fluorescence at 440-455nm. As a further demonstration of the sheer variety of fluorescent systems which already exist in Annelidae, the fireworm *Odontosyllis phosphorea* uses a luciferase oxidation reaction to generate 505nm light (107). Either way, we can add Nereid worms to the ever-growing list of annelids which in some capacity exhibit bioluminescence. Considering that bioluminescence is suspected to have already evolved separately 3 times in annelids alone (108), the photoprotein and its associated mechanism for causing transient fluorescence in *P.du* could well be new to science and warrant further classification.

More recently, advancements in transcriptomics have allowed great leaps in identifying the photoproteins responsible for bioluminescence in previously obscure annelid models. For example, the Japanese Fireworm *Odontosyllis umdecimdonta*, which also emits bioluminescence in the ~505nm spectrum similar to the fluorescence documented here, have recently been shown to express their own type of luciferase, quite distinct from luciferase**s** expressed by other bioluminescent species (108). This syllid luciferase sequence in *O.undecimdonta* has high sequence similarity to another luciferase gene in *O.enopla*, reinforcing our understanding that a unique family of luciferases exists in polychaetes which has evolved separately other luciferases (109). This could mean that a luciferase-type protein in *Platynereis* could exist, but has so far gone unnoticed in countless genomic and transcriptomic screens due to its non-homology to previously characterised luciferases. Stating at the time that "Platynereis is non-bioluminescent", it was initially a source of confusion that the *P.du* transcriptome contains two sequences with high similarity to the bioluminescent coumarin CoA luciferase found in *Hermodice carunculata* (110). However, despite not being visibly bioluminescent in glowing mating swarms as *Odontosyllis* worms are, we clarify here that certain aspects of *P.du* physiology are capable of generating bioluminescence under specific conditions (Figure 18).

The evolutionary utility of this endogenous fluorescence in *Platynereis* is not immediately clear, since it is likely far too dim to be used a signalling display to other members of its species, as is the case in Syllid worms, which are attracted to 500nm light when in their mature pelagic form, demonstrated

by their tendency to swim towards a flashlight held at the surface of the water (109). This apparent uselessness of fluorescence is mirrored in another polychaete *Chaetopterus*, whose bioluminescently marked and patterned tube appears redundant, being itself buried under the seafloor stratum for its entire existence and therefore not visible (106).

Clearly we must expand our understanding of what physiological need has stimulated the prolific evolution of diverse bioluminescent features in annelids. Without further studies, we can therefore only tentatively conclude that this spontaneously fluorescent substance in the neurons of *P.du* is likely to be either a close proximity signalling mechanism between worms for use in extremely low light conditions or a leftover remnant of a fluorescent protein initially expressed in its fully bioluminescent syllid (110) or errantid cousins (103).

Should further investigation into *P.du* neuronal bioluminescence be conducted, a classification of the protein itself should be the initial line of inquiry. Despite the multitude of potential photoproteins which could be producing these endogenous spontaneous fluorescence spikes, several qualities of similar photoproteins could allow effective isolation of the protein.

It is noted that the Luciferin-Luciferase reaction in *O.umdecimdonta* does not require cofactors to function, and when extracted with biochemical means maintains its fluorescence outside of the cellular environment (108). If the fluorescence-producing substance in *P.du* shares this quality, one possible method for identifying our source of bioluminescence could involve isolating it by fractionation or HPLC and identifying the native protein by detecting its visible fluorescence alone. Furthermore, if a likely photoprotein sequence is identified based on homology to known polychaete luciferases and its size can be ascertained, this technique can be assisted by size-exclusion chromatography. On top of this, the fact that all previous annelid bioluminescent sources have been reliant on the presence of O_2, regardless of whether they are luciferases or not, (103) could also bring us closer to isolating the affecting protein in *Platynereis* by biochemical protein separation techniques. To this end, bioluminescent proteins have previously been identified by the treatment of available protein fractions with hydrogen peroxide, oxidising any fluorescent substrates and producing bright indicative fluorescence.

Whilst it appears likely that the source of endogenous fluorescence we document (Figure 18) is expressed most strongly in the rhabdomeric cells of the adult eyes, further studies should categorically confirm this, by screening for the absence of this observed phenomenon in r-Opsin1-ablated animals, which we have already utilised in this thesis (Figure 9). Operating on this assumption that the observed enigmatic bioluminescence is enriched in the r-Opsin1-positive cells, we analysed available cell type-specific trancriptomic data (111) and found that none of the

coumarin CoA Luciferase-like sequences (110) in *Platynereis* are enriched in *P.du* heads or rhabdomeric photoreceptor cells. A cursory investigation also reveals no evidence of any gene sequences expressed in the head or eyes of wild type *P.*du worms that resemble or are homologous to GFP or other common fluorophores.

Regardless of the source and evolutionary purpose of this enigmatic transient green fluorescence in *P.du*, in order to establish transgenic imaging throughout the entire lifecycle of the worm, a solution must be found to circumvent this obstacle. One promising solution is the use of a different colour of fluorophore to highlight calcium spikes in active neurons, namely RCaMP, the red version of GCaMP. Whilst the dynamic fluorescent range (the difference in protein fluorescence intensity between calcium-bound and –unbound states) of current GCaMP variants exceed those of comparable RCaMP variants, Red fluorescence has inherent benefits over green fluorescence in biological applications which may be relevant here. These include the ability to co-image with cyan fluorophores, lower general phototoxicity if excited for prolonged periods and greater tissue penetration depth of 550-600nm excitation lasers (112). However, RFP based neuronal activity detection proteins would suffer the potential drawback of not being compatible with two-photon excitation microscopy, due to the rarity of long wavelength single photon emission sources (57). Whilst red autofluorescence is strong and ubiquitous in the adult *Platynereis* head, due to the propensity of its chitinous cuticle to scatter light (102), this autofluorescence is at least consistent, and so can be subtracted from any imaging effort as background using confocal techniques. This cannot be done with green fluorescence as the variable fluorescent background intensity (Figure 18) would interfere with any objective measure to quantify the fluorescence from a calcium indicator.

Overall, this spontaneous transient GFP-like fluorescence has the potential to provide both further complications and great leaps forward in the utility of *P.du* as a future neuroscientific model organism. Only further characterisation and research of this phenomenon will decide which of these possibilities is realised first.

CONCLUSIONS

We showcase here the presence of regular photoreceptive domains in the cirri of adult *Platynereis dumerilii*, and furthermore demonstrate that these photoreceptive domains express a Go-type opsin which is responsible for detecting sudden shadows and activating the defensive shadow reflex. To supplement these findings, we note that the rhabdomeric cells of the adult eyes and trunk do not contribute to the shadow reflex in *Platynereis dumerilii*. Furthermore, we confirm that Go-Opsin1 entrains neither the circalunar, nor circadian clock in *Platynereis dumerilii*, and these data act as a compelling reminder to always compare direct siblings in analyses of chronobiological behaviours. Due to redundancy in the *P.du* shadow response, we deduced that some other photoreceptor must

be capable of compensating for Go-Opsin1 and we subsequently documented several characteristics of c-Opsin2 which make it the most promising candidate for a compensatory shadow reflex photoreceptor. Finally, we documented and quantified an enigmatic transient fluorescent phenomenon in *P.du* with profound implications for this annelid's utility as a neuroscientific model, and provided speculations and advice for how this should be tackled in the future.

Materials and Methods

PLATYNEREIS DUMERILII EXPRESSION ANALYSES

Platynereis dumerilii Culture Care and Husbandry

All worms were kept according to well-established regulations and protocols outlined previously (113) in the Marine Research Facility of the Max F. Perutz Laboratories, at a constant 18°C and provided with (unless specified otherwise) 16 hours light:8 hours darkness daily light cycles and 8 consecutive days per month of dim nocturnal light to establish communal circalunar timing. Different strain acronyms mentioned here, PIN, VIO, FL2 and Naples, are highly inbred populations of *P.du* kept separately to limit the effect that polymorphisms may have on comparative studies such as the chronobiological assays used here (Figures 10 and 13).

More specifically, the care and breeding *P.du* animals used in the shadow reflex assay, including incrossing of heterozygous Go-Opsin1+/- mutants to obtain siblings, was conducted as described in Ayers et al (35). These siblings, obtain by interbreeding local PIN strains with a homozygous mutant Go-Opsin1-/- line donated by the members of the Jekely Laboratory, underwent genotyping at least 7 days prior to the start of the shadow reflex assay to allow them to heal their clipped tails. Transgenic worms whose genomes contained stably inserted *r-Opsin1::eGFP-f2a-NTR* cassettes were generated previously and maintained in homozygous colonies to facilitate their use (66). Colonies of animals exposed to unnatural light conditions, namely those residing under purely 500nm light sources to assess circalunar maturation patterns, did so in a light tight box kept constantly at 17°C and were fed and underwent regular seawater changing as usual.

Genotyping

Animals of unknown genotype were tail-clipped under anaesthesia by submersion in 7.5% w/v $MgCl_2$. This involved the removal of the posterior-most segment of the animal along with its anal cirri. Anaesthetised worms were then returned to artificial seawater (ASW) and the removed tail segment incubated in 10% ProteinaseK for 2 hours at 55°C before inactivating the enzyme by incubation for 20 minutes at 95 degrees. This genomic DNA extracted was then used as a template for standard Polymerase Chain Reactions (PCR) with OneTaq Polymerase Mastermix with standard buffer (NEB) and oligonucleotide primers (Microsynth). The sequences of primers used to genotype Go-Opsin1 worms for the shadow reflex and chronobiological assays are listed in the supplementary materials of Ayers et al (35). The sequences of the primers used to generate an amplicon and allow us to assess the mutagenic efficiency of our two pairs of TALENs (Figure 16) on the integrity of exon1 of *pdu*-c-Opsin2 are listed below:

Sequence Name	Nucleotide Sequence
c-Opsin2_exon1_forward	GGATGACCTGGGATTTTTGGG
c-Opsin2_exon1_reverse	CTCCTAAAAAAGTGATGAATCC

After DNA amplicons were generated of the genes of interest, they were run on an agarose gel containing SYBRSafe DNA gel staining solution (Thermofisher) alongside a standard 50bp ladder (Thermofisher) to ascertain their sizes. The significance of c-Opsin2 amplicon sizes when cut with two different restriction enzymes, HaeIII and HpyCH4v, is explained in this results section, as it implies whether or not either TALEN pair has successfully generated mutation in its corresponding spacer region within the c-Opsin2 gene.

Immunostaining

Heads from immature *P.du* were collected in 2ml Eppendorf tubes and washed three times in fresh artificial seawater before undergoing fixation for two hours in Bouin' Fixative (proportional solution containing 15 parts Saturated Picric Acid, 5 parts 40% formaldehyde and 1 part acetic acid) at 4°C with shaking. This was then washed 5 times for 10 minutes in PBT (Phosphate Buffer Solution with 1% Triton-X100) and stored at 4°C overnight. Samples were then permeabilised at -20°C in 1ml acetone for 30 minutes before being washed 4 times for 5 minutes in PBT. Heads then underwent digestion with 0.04% ProteinaseK in PBT for 6 minutes without shaking and were washed afterwards with 2mg/ml glycine. 5 washes in PBT for 1, 2, 5, 10 then 20 minutes were conducted before the samples were blocked in 10% Sheep Serum in PBT for 2 hours at room temperature with shaking. The staining step involved removal of the blocking solution and incubation of the initial antibody, anti-*pdu-c-Opsin2* (raised in rabbit), for 3 days at 4°C shaking at 400rpm. This was removed and washed 3 times for 30 minutes and 3 times for 1 hour with PBT before the secondary antibody, anti-rabbit-conjugated Cy3, was placed onto the heads and incubates for another 3 days at 4°C, shaking at 400rpm and covered in aluminium foil to stop samples being photobleached. After another 6 washing steps, and kept in darkness from this point, a third antibody, anti-acetylated tubulin (raised in mouse), was incubated with the samples followed by incubation with anti-mouse-conjugated Alexa488 for another 3 days at 4°C each with washing steps in between each new solution. After this and a final washing step, samples were incubated with 0.4mg/ml DAPI (#D9524, Sigma-Aldrich) in PBT staining solution for 2 hours at 4°C before one final 3x30min+3x1hr washing step.

Stained samples were preserved in darkness in 2.5% DABCO Glycerol with 0.5% Vectashield Antifade Mounting Medium (Fisherlabs) and stored at 4°C before being mounted on cover slides and imaged dorsally using a Axiovert 100M Inverted confocal microscope (Zeiss) using Zenbase 2.5 software (Zeiss). Settings for confocal image acquisition were calibrated with sufficient laser power to avoid

background illumination with a pinhole size of 1 airy, detector gain of 420 and magnified with 40x water-immersion and 63x oil-immersion objectives. Images of reflected fluorescence were captured in three separate channels enforced by dichroic mirror long pass filters designed for the detection of Cy3 (548/563nm excitation/emission), Alexa 488 (488/509nm excitation/emission), and DAPI (360/460nm excitation emission) fluorescence to image c-Opsin2, acetylated tubulin and cell nuclei respectively (Figure 15).

Cloning

To generate plasmids capable of generating single stranded RNA probes to act as labels for Whole Mount *in situ* Hybridisation (WMISH) of Go-Opsin1 in adult *P.du*, we first conducted polymerase chain reaction with Phusion high-fidelity DNA polymerase (NEB) with primers flanking the Go-Opsin1 gene (Sequences available in Ayers et al (35)) on genomic DNA extracted from wild type adult worms (PIN strain). The resultant DNA was gel purified and blunt-end ligated into the pJet1.2/Blunt vector with the CloneJet PCR Cloning Kit (Fermentas) and transformed into chemically competent E.coli cells (Invitrogen) by heat shock. Following selection for transformants via incubation on Ampicillin-coated agar plates, 2 colonies were selected and miniprepped with inserts aligned in two different directions to obtain both sense and antisense probe-generating plasmids. The correct sequences and orientations of inserts were confirmed by Sanger sequencing performed by Microsynth AG provided with standard pJet forward and reverse primers which flank the insert site of our plasmids.

To generate the labelled RNA probes, both sense and antisense plasmids were linearised by digestion with XbaI and the cut products were purified on a gel. These products were then used as templates for *in vitro* transcription using the mMESSAGE mMACHINE T7 Ultra kit with DIG-RNA labelling mix (NTP/Digoxgenin-UTP Mix, Sigma-Aldrich) combined with ordinary NTPs in the reaction. After this, DNAse I treatment was used to remove excess template RNA was purified to acceptable standards with the RNeasy RNA cleanup kit, eluted in 50µl RNAse-free ddH_2O and stored in 75µl of Hybridisation Buffer (#11717472001, Roche) at -20°C.

Whole Mount *In Situ* Hybridisation

Whole heads and tails consisting of at least 15 intact segments were cut from immature *P.du* and washed three times with artificial seawater before being fixed in 4% Paraformaldehyde in 2xPTW (2x phosphate buffer solution with 0.1% Tween). All steps involving cutting, washing, eluting, transferring and shaking of *P.du* heads and tails were conducted with the utmost care to ensure that all cirri, both peristomal and anal were kept intact throughout the entire procedure. RNA sense and anti-sense probes were generated by reverse transcription with a mMESSAGE mMACHINE T7 transcription kit (Invitrogen) from individual pJet1.2 vectors as described in the Cloning section.

Following washing with titrated concentrations of methanol, embryos were transferred to 100% methanol and stored for WMISH at -20°C for 2 weeks to optimise permeabilisation of the tissue.

From here, the WMISH protocol was conducted as described in Ayers et al., 2018 (35), which utilised a commonly used protocol for performing whole mount in situ hybridisation in *Platynereis* (114). Minor optimisations were made to ensure that no disintegration of the delicate cirral structures occurred. These were a reduction of the ProteinaseK digestion time from 5 to 3 minutes for heads and from 10 to 7 minutes for tails. After staining, images were acquired by Differential Interference Contrast (DIC) imaging with a Zeiss Z2 upright Axioimager light microscope with a white light halogen lamp and recorded using an inbuilt Coolsnap HQ2 Firewire full colour camera (Zeiss) with Zen 2.5 (Zeiss) software. Following image acquisition, extracted tiff images of WMISH-stained heads and cirri were collated using Adobe Illustrator software (Figure 7).

SHADOW REFLEX ASSAY

Light Condition Measurements and Calibration

Controlled light conditions were established for three different experiments. Firstly, the shadow reflex assay took place in a behavioural chamber designed to be light-tight and vibration proof (placed on a rubber mat), suspended within which were six separate arrays of LEDs ranging from white light to monochromatic light between 400nm and 590nm. These individual monochromatic LEDs (Winger Electronics GmbH & Co.KG) were wired in series and calibrated according to measurements made by a ILT950 spectrometer (International Light Technologies Inc.) with its photodetector placed where the animal subjects would prospectively be placed (0.6m from the light source). The brightness for each wavelength of light was converted from Irradiance (μW/cm^2/s) to Absolute Photon Flux (photons/cm^2/s) with the following formula:

$$Absolute\ Photon\ Flux\ = Irradiance \times 5.03x10^{17} \times \lambda$$

Where λ represents the wavelength of the light component in metres.

Further explanation of the calibration of light conditions for the shadow reflex assay is available in Ayers et al (35).

Secondly, for the analysis of circalunar maturation rhythms in Go-Opsin1 +/+, +/- and -/- *P.du*, solar and lunar light stimuli were calibrated to be comparable in relative intensity to natural lunar and solar light sources. Moonlight spectra are almost uniformally 1000 times as dim as their equivalent sunlight spectra (97), and so our total photon flux for 500nm monochromatic lunar light was calibrated to deliver 10^3 less photons/cm^2/s than our solar stimulus (Figure 11). These stimuli were once again measured with the same spectrophotometer apparatus with its detector placed at the

presumptive location of the worm cultures, which in this case was 20cm from the nearest light sources (Figure 11).

Analysis of circadian locomotor behaviour took place in the same light-tight enclosure as our shadow reflex, and so the light conditions and conditions in general differed very little to those specified above. Notable differences were the specific light regimes (Figure 13) and the fact that we only used white light, 470nm and 500nm light in the circadian locomotor assays. Light intensity levels here were established for white light in Zantke et al (14), and the peak intensity of 470 and 500nm light conditions were calibrated to match their constituent wavelength maxima within the white light condition (Figure 12).

Shadow Reflex Behavioural Paradigm

The Shadow Reflex Assay protocol, its preparation and hardware acquisition was described at length in Ayers et al (35), and the motivation and optimisation of this assay is described in the first results section of this thesis. Four days before assay onset, immature *P.du* worms of approximately 20mm in length were isolated in individual enclosures (Six-well Dishes, Greiner Bio One International GmbH) and deprived of food until the assay was completed. 2 days before assay onset, these worms were loaded into individual divots (35mm diameter and 15mm depth) of a custom-made opaque plastic tray and kept separated at normal culture conditions to encourage them to create new home tubes. At ZT5, 5 hours after light normal circadian light onset, of the day of the assay, each animals well was refilled with new artificial seawater and 15 minutes before assay onset, 50µl of seawater which had been infused with fresh spinach was dropped into each well to encourage the animals to search for food. Each of the 6 light conditions were presented to all animals in a random order for each cohort of animals. For each single light condition, the light was switched ON for 60 minutes before the first shadow onset and new spinach-infused seawater was added 15 minutes before the first shadow onset. Each shadow stimulus was two seconds of abrupt darkness caused by removal of power from the respective LED array, and after this 60 more seconds of light ON to avoid sensitisation. Each light condition was comprised of 12 shadow stimuli and all movements during the assay were illuminated by an infrared (990nm) LED array (Roschwege GmbH) and video recorded at 15 frames per second using a camera with an aperture fitted with an infrared filter (990nm) as established in Zantke et al (14).

Shadow Reflex Assay Behaviour Quantification

Shadow reflex behaviour was quantified binarily as a success rate calculated by the number of successful shadow reflex reactions out of the 12 total shadow stimuli presented per light condition. Since each worm was awarded a score for each stimulus of only 0 or 1, success rates obtained from the assay takes on a finite number of possible values and appear stratified. Statistical analyses were

adjusted to work with stratified data of 12 distinct values accordingly, which with over 10 potential values can be approximated as continuous data (115). The precise equation and methodology used is explained in detail in Ayers et al (35). Recorded infrared videos were played back at 10 frames per second and each worm was analysed by eye and assessed for whether it reacted to each light OFF stimulus with a shadow reflex. The shadow reflex for the purposes of this assay was defined by a sudden shortening of the total length of the worm by either a retraction of the head or tail.

Shadow Reflex Assay Statistical Analysis

Statistical Analyses for all data pertaining to the shadow reflex assay were conducted as described in Ayers et al., 2018 (35), using the statistical packages included in the Graphpad Prism Version 7 Software (116). Attention was paid to statistical conventions which dictate that confirmation of a lack of significance (as in the comparison of wild type and r-Opsin1-expressing cell specific ablated worms (Figure 9)) was calculated using 95% confidence intervals with the Hodges-Lehmann non-parametric estimator to ascertain whether the similarity of given medians are by chance. This is as opposed to the more classical demonstrations of significant difference by Mann-Whitney U tests for all other shadow reflex success rate comparisons. Where appropriate, corrections for multiple testing were made using the Benjamini-Hochberg modifier.

Cirri Removal Surgery

Wild type (PIN strain) immature *P.du* of between 1.5 and 2mm in length were selected and anaesthetised in 50:50 75%w/v $MgCl_2$:artificial seawater. Half underwent cirri removal surgery and the other half acted as a negative control. Cirri removal surgery proceeded as described in Ayers et al (35), removing all anal and peristomal cirri with scalpel blades and tungsten needles, whilst avoiding damage to the rest of the prostomium, (particularly the eyes, antennae and palps). Animals were left to recover for 2 days prior to the start of the shadow reflex assay in seawater treated with 1:1000 Penicillin/Streptomycin to deter infections (Figure 8).

r-Opsin1+ Cell-Specific Ablation

Prior to ablation, immature *P.du* animals with potential to have a transgenic *r-Opsin1::eGFP-F2A-NTR* genotype were screened for strong GFP expression in the r-Opsin1-positive cells of the adult eyes with a Zeiss axioplan imager under full illumination with 488nm light produced by a LUMAR halogen UV light source with a FITC set of band-pass filters. These animals are kept in homozygous transgenic colonies, but still require screening in case of impromptu silencing of the transgenic *r-opsin1::eGFP-F2A-NTR* locus. Once confirmed for strong GFP expression, all worms, both GFP-positive and comparably sized wild types (PIN strain background) underwent 5 days of 12mM metronidazole treatment as described in Ayers et al (35). These worms were allowed to recover for 2 days in fresh artificial seawater before being introduced to the shadow reflex assay, and transgenic worms were

confirmed at this point to have undergone full cellular ablation by the demonstrated loss of ocular GFP fluorescence with a second screening using the aforementioned equipment (Figure 9).

BIOLOGICAL CLOCK ASSAYS

Circadian Locomotor Activity Monitoring

Animals were habituated to their wells as described previously in Shadow Reflex Assay Methods section. From 2 days prior to recording onset, immature *P.du* of around 20mm in size were placed in the same custom-made opaque glass tray containing 36 hemispherical wells cpable of housing one animal each. Animals were fed as normal during this time and had their water replaced with fresh artificial seawater prior to recording and being placed into the light-tight behavioural recording chamber. Behaviour was recorded by an infrared-limited (990nm) video camera at a constant 15 frames per second under an infrared light source as described in the shadow reflex assay. Light regimes for circadian analysis (Figure 12A) all begin with a single recorded 24 hour cycle of 16:8 hours light:dark, which was then perturbed using single wavelength monochromatic lighting to assess how the circalunar rhythms of the recorded worms overcame a time shift. After establishing a normal circadian rhythm of nocturnal activity in the subjects, the light regime was shifted by 12 hours using only monochromatic light of either 470 or 500nm, so that day and night cycles were inverted as shown in our schematic (Figure 12A). The 8 hour period where the next presumed night would have been without the phase shift was therefore suddenly in the middle of bright illumination by monochromatic light, and is dubbed the “subjective night”. The 16 hour period of “daylight” during the initial normal light-dark period is taken as a control for the baseline inactivity of each worm, and is hereafter referred to as the “LD Day”.

To analyse the video recordings, and unlike the binary scoring system used in Zantke et al (14), which graded animals as either active or inactive at a single timepoint each 10 minutes based on a series of behavioural criteria, the quantification of locomotor behaviour in this assay was conducted by specially designed tracking software (PlatynereisTracker, loopbio GmbH). Once the limits of each well were defined, this software logged the total distance travelled in millimetres of the centrepoint of each worm per timepoint, allowing us to plot individual locomotor activity traces for each worm. Following quantification, we grouped the distance travelled of each worm into bins of 60 seconds, equating to 1440 data points per 24 hour day. From this, we calculated the average distance travelled per hour during the 8 hour subjective night phase for each worm. To normalise the subjective night data, we subtracted from it the average distance travelled per hour during the normal LD Day period and plotted the normalised data of all worms. Each graph contains the normalised subjective night data pooled from at least two separate cohorts.

Circalunar Maturation Timing Monitoring

Colonies of *P.du* of all three genotypes (Go-Opsin1+/+, Go-Opsin1+/-, Go-Opsin1-/-) were placed in the light-tight containment shelf (Figure 11) from one month of age following genotype confirmation and kept at a constant 17 degrees Celsius. Light sources of lunar and solar intensity were maintained 30cm away from subjects, with the solar stimulus cycling through 16hrs ON to 8hrs OFF and the lunar stimulus being switched ON for 7 days and OFF for 21 days each lunar cycle. Daily, all animals were checked for signs of maturation, and upon undergoing their metamorphosis and colour change, were logged as "mature" and removed. All feeding, water changing and assessment of maturation over the course of 12 months was conducted in darkness during solar ON time to avoid light contamination of the purely 500nm light stimulated shelf.

Chronobiological Statistical Analyses

Reassessment of the circalunar maturation data of Go-Opsin1 mutant and wildtype animals was conducted on data extracted from a paper which had already made qualitative conclusions on the significance of the data (39). After replotting as described in our results, we normalised all data to the total number of matured individuals of each given genotype and plotted all maturation days as a function of where they fall within each given lunar month (Figure 10). From here, we conducted unpaired non-parametric Mann-Whitney U tests on the datasets to assess whether they were differently distributed. The same tests were performed on our own circalunar maturation data conducted on sibling animals. Significant differences between the normalised subjective night locomotor activity levels of animals undergoing 12 hour circadian phase shifting by monochromatic light were tested by Mann-Whitney U tests for differences in distribution (Figures 12 and 13). All statistical tests were performed in the Graphpad Prism Software version 7.03 (116).

PLATYNEREIS DUMERILII GENETIC ANALYSIS AND IMAGING

Phylogenetic Analysis

The phylogenetic tree containing *pdu*-c-Opsin2 was constructed using CLC Main Workbench (Version 7.7.1) and contained sequences obtained from NCBI's Genbank database. *P.du*-specific sequences were obtained from the 4dx PlatyBLAST database. This cross section of known opsin sequences were chosen to both adequately represent the ciliary-type opsin subset and to give sufficient comparisons from rhabdomeric and RGR opsins from varied animal groups. All accession numbers and source organisms of protein sequences used in this dataset are publicly available (35). Within CLC Workbench, the following settings were used: gap extension costs – 1, gap open costs – 10, end gap costs – as any other, very accurate alignment, setting tree – method UPGMA, protein distance measure – Kimura protein, bootstraps – 1000. Following this, non-ciliary-opsin outgroup nodes were collapsed and bootstrap values of less than 70 or not pertaining directly to pdu-c-Opsin2 were

omitted from the final figure using Adobe Illustrator (Figure 14). We generated a new genbank ID (MG182639) to hereafter document the correct *pdu*-c-Opsin2 coding sequence.

Transcriptional Activator-Like Effector Nuclease (TALEN) Generation

Two TALEN pairs for *pdu*-c-Opsin2 were designed and generated using a protocol established and optimised in Bannister et al. (94), which outlines the details of the protocol specific to this model organism. Two sites were isolated within exon 1 of the c-Opsin2 gene of between 15 and 20bp in length containing unique or semi-unique restriction enzyme cutting sites (HaeIII and HpyCH4V), and four TALEN recognition sites (between 15 and 18bp in length) were identified flanking each of these two spacer regions (Figure 15). Assembly of the TALEN expression vectors was conducted according to an established protocol (117). Constructed TALEN recognition sequences were ligated into the pCS2+_TAL3-WT expression vectors and confirmed for correct sequence and RVD order by Sanger sequencing. Capped TALEN mRNA of both pairs of c-Opsin2 TALENs was transcribed from its constituent plasmids in the same manner as RNA probes used for WMISH, the only differences being that linearization of the plasmid was achieved by the Not1 enzyme, UTPs were not labelled with DIG, and *in vitro* transcription was conducted using the Sp6 mMESSAGE mMACHINE kit (#AM1340, Life Technologies). This mRNA was then injected into *P.du* zygotes as described below. The mutational efficiency of the TALEN mRNA was assessed by PCR and restriction digest screening assays of genomic DNA harvested from injected larvae. Nucleotide sequences for the exonic primers used to generate an amplicon of the c-Opsin2 gene (Figure 16) and recognition sequences for the two TALEN pairs used here are provided in the table below:

Sequence Name	Nucleotide Sequence
Pdu-c-opsin2 exon 1 forward primer	GGATGACCTGGGATTTTTGGG
Pdu-c-opsin2 exon 1 reverse primer	CCTCCTAAAAAAGTGATGAATCC
Pdu-c-Opsin2 TALEN pair 1 forward RVD	TTTGTTGAGGATCCTC
Pdu-c-Opsin2 TALEN pair 1 reverse RVD	GGCAGTTATCACATAGGA
Pdu-c-Opsin2 TALEN pair 2 forward RVD	GTTCCAGTTCGGGCTG
Pdu-c-Opsin2 TALEN pair 2 reverse RVD	TCCAGGGCTCATGTA

Platynereis dumerilii zygote Microinjection

Microinjection of TALEN mRNA into *P.du* embryos was conducted according to an established embryo preparation and microinjection protocol detailed in Backfisch et al., 2013 (66). Following stimulation of fertilisation by induced spawning of a mature male and female *P.du*, zygotes were removed and rinsed with fresh natural seawater to wash away excess sperm. These embryos were then incubated at 17°C for 45 minutes to allow the cortical reaction to take place. In this time, a

stage was cast out of 1.5% Agarose in natural seawater and set around premade plastic moulds which create a shallow trench within which many zygotes can sit and be processed. The injection mix consisted of 400ng/µl of each individual TALEN, which considering we coinjected both pairs of TALENs simultaneously, left the final concentration of TALEN mRNA in the injection solution at 1.6µg/µl. This was mixed with 1µl TRITC in 5µl RNase-free double distilled water. After removing the cortical jelly from the embryos by gentle filtration through a fine gauze, they were injected with the mRNA solution until red TRITC colouration was barely visible inside them. Embryos were taken to an enclosure with fresh natural seawater and were left to develop for one week before being digested to extract their genomic DNA.

Platynereis dumerilii Fluorescence monitoring

Immature wildtype animals were genotyped with standard genotyping primers for the presence of eGFP, in order to confirm a lack of any GCaMP6s or any eGFP-based transiently fluorescent protein. Following this, animals were anaesthetised in 7.5%w/v $MgCl_2$ seawater and submerged in an artificial seawater and 1.5% low-melting point agarose (#50302, Lonza) solution to hinder movement and fully immobilised on concave microscope slides under glass cover slips. These cover slips were spaced apart from the slides using 3-4 pieces of stacked tape and dessication was avoided by surrounding each pool of seawater containing immature *P.du* worms with light mineral oil (#MKBR6962V, Sigma-Aldrich).Endogenous transient fluorescence (Figure 18) imaging was recorded using a Coolsnap HQ2 Firewire full colour camera at an image acquisition rate of 2Hz using a Zeiss Axioimager Z2 light microscope (Zeiss) with a 20x air objective and 40x and 63x oil-immersion objectives. Monochromatic illumination was achieved by a Sola SE mercury arc lamp light source filtered by eGFP, RFP, Cy3 and Cy5 bandpass filters (Olympus Lifescience) controlled by Zen light microscopy imaging software 2.5 (Zeiss). Following image capture, fluorescence was quantified by selecting Regions of Interest (RoIs) with a basic ImageJ software package, differential fluorescence intensity levels (ΔF) in the RoI were calculated by subtracting from them the total background fluorescence of the entire image for each timepoint. These were then normalised by division by the total background fluorescence (ΔF/F0) before being plotted.

REFERENCES

1. Lamb TD, Collin SP, Pugh Jr EN. Evolution of the vertebrate eye: opsins, photoreceptors, retina and eye cup. Nat Rev Neurosci. Nature Publishing Group; 2007 Dec 1;8:960.

2. Cronin TW, Johnson S. Extraocular, Non-Visual, and Simple Photoreceptors: An Introduction to the Symposium. Integr Comp Biol. 2016;56(5):758–63.

3. Ramirez MD, Pairett AN, Pankey MS, Serb JM, Speiser DI, Swafford AJ, et al. The Last Common Ancestor of Most Bilaterian Animals Possessed at Least Nine Opsins. Genome Biol Evol. Oxford University Press; 2016 Dec 26;8(12):3640–52.

4. Kojima D, Fukada Y. Non-visual photoreception by a variety of vertebrate opsins. Novartis Found Symp. 1999 Jan;224:265-79-82.

5. Kokel D, Dunn TW, Ahrens MB, Alshut R, Cheung CYJ, Saint-Amant L, et al. Identification of non-visual photomotor response cells in the vertebrate hindbrain. J Neurosci. 2013 Feb 27;33(9):3834–43.

6. Provencio I. The role of Melanopsin and other Opsins in Circadian Clock Resetting. Holick MF, editor. Boston, MA: Springer US; 2002. 451-459 p.

7. Kargacin GJ, Detwiler PB. Light-evoked contraction of the photosensitive iris of the frog. J Neurosci. 1985;5:3081–7.

8. Cronly-Dillon JR. Spectral Sensitivity of the Scallop Pecten maximus. Science. 1966;151(708):346–7.

9. Nilsson DE. Eyes As Optical Alarm Systems in Fan Worms and Ark Clams. Philos Trans R Soc London Ser B-Biological Sci. 1994;346(1316):195–212.

10. Randel N, Jékely G. Phototaxis and the origin of visual eyes. Philos Trans R Soc B Biol Sci. The Royal Society; 2016 Jan 5;371(1685):20150042.

11. Van Gelder RN. Non-Visual Photoreception: Sensing Light without Sight. Curr Biol. Elsevier; 2008 Jan 8;18(1):R38–9.

12. Apte C V. Biological clocks: The coming of age. Int J Appl Basic Med Res. India: Medknow Publications & Media Pvt Ltd; 2012;2(1):1–2.

13. Nishida A, Nordi N, Alves R. Molluscs production associated to lunar-tide cycle: a case study in Paraiba State under ethnoecology viewpoint. J Ethnobiol Ethnomed. 2006;2(28).

14. Zantke J, Ishikawa-Fujiwara T, Arboleda E, Lohs C, Schipany K, Hallay N, et al. Circadian and circalunar clock interactions in a marine annelid. Cell Rep. 2013 Oct 17;5(1):99–113.

15. Hauenschild C. Ueber die lunarperiodische Schwaermen von Platynereis dumerilii in Laboratorienzuchten. Naturwissensch. Naturwissensch. 1955;(42):556–7.

16. Backfisch B, Kozin V V, Kirchmaier S, Tessmar-Raible K, Raible F. Tools for gene-regulatory analyses in the marine annelid Platynereis dumerilii. Korzh V, editor. PLoS One. Public Library of Science; 2014 Jan;9(4):e93076.

17. Arendt D, Tessmar-Raible K, Snyman H, Dorresteijn AW, Wittbrodt J. Ciliary photoreceptors with a vertebrate-type opsin in an invertebrate brain. Science. 2004 Oct 29;306(5697):869–71.

18. Bok MJ, Capa M, Nilsson DE. Here, There and Everywhere: The Radiolar Eyes of Fan Worms (Annelida, Sabellidae). Integr Comp Biol. 2016;56(5):784–95.

19. Morton B. The evolution of Eyes in Bivalvia: New Insights. Am Malacol Bull. 2008;26(1–2):35–45.

20. Partridge JC. Sensory ecology: Giant eyes for giant predators? Curr Biol. Elsevier Ltd; 2012;22(8):R268–70.

21. Kingston ACN, Wardill TJ, Hanlon RT, Cronin TW. An unexpected diversity of photoreceptor classes in the longfin squid, Doryteuthis pealeii. PLoS One. 2015;10(9):1–14.

22. Zantke J, Bannister S, Rajan VBV, Raible F, Tessmar-Raible K. Genetic and genomic tools for the marine annelid Platynereis dumerilii. Genetics. 2014 May 1;197(1):19–31.

23. Tessmar-Raible K, Arendt D. Emerging systems: between vertebrates and arthropods, the Lophotrochozoa. Curr Opin Genet Dev. 2003;13(4):331–40.

24. Raible F, Tessmar-Raible K, Osoegawa K, Wincker P, Jubin C, Balavoine G, et al. Vertebrate-type intron-rich genes in the marine annelid Platynereis dumerilii. Science. 2005 Nov 25;310(5752):1325–6.

25. Britten RJ. Rates of DNA sequence evolution differ between taxonomic groups. Science. 1986;231(4744):1393–8.

26. Arendt D. Genes and homology in nervous system evolution: comparing gene functions, expression patterns, and cell type molecular fingerprints. Theory Biosci. 2005;124:185–97.

27. Achim K, Eling N, Vergara HM, Bertucci PY, Musser J, Vopalensky P, et al. Whole-body single-cell sequencing reveals transcriptional domains in the annelid larval body. Mol Biol Evol. 2018;35(May):1047–62.

28. Gomperts BD, Kramer IM, Tatham PE. Signal Transduction. 2002. 51, 127-141 p.

29. Wang W, Geiger JH, Borhan B. The photochemical determinants of color vision: Revealing how opsins tune their chromophore's absorption wavelength. Bioessays. 2014 Jan 24;36(1):65–74.

30. Yau K, Hardie R. Phototransduction Motifs and Variations. Cell. 2009;139(2):246–64.

31. Porter ML, Blasic JR, Bok MJ, Cameron EG, Pringle T, Cronin TW, et al. Shedding new light on opsin evolution. Proc R Soc B Biol Sci. 2011;279(1726):3–14.

32. Eakin RM. Evolution of Photoreceptors. Evol Biol. 1968;2:194–242.

33. Koyanagi M, Terakita A. Gq-coupled rhodopsin subfamily composed of invertebrate visual pigment and melanopsin. Photochem Photobiol. 2008;84(4):1024–30.

34. Terakita A. The opsins. Genome Biol. 2005;6(213).

35. Ayers T, Tsukamoto H, Gühmann M, Veedin Rajan VB, Tessmar-Raible K. A Go-type opsin mediates the shadow reflex in the annelid Platynereis dumerilii. BMC Biol. 2018;16(41).

36. Battelle B, Ryan JF, Kempler KE, Saraf SR, Marten CE, Warren WC, et al. Opsin Repertoire and Expression Patterns in Horseshoe Crabs : Genome Biol Evol. 8(5):1571–89.

37. Shichida Y, Matsuyama T. Evolution of Opsins and Phototransduction. Philos Trans R Soc London Ser B-Biological Sci. 2009;364(1531):2881–95.

38. Passamaneck YJ, Furchheim N, Hejnol A, Martindale MQ, Lüter C. Ciliary photoreceptors in the cerebral eyes of a protostome larva. Evodevo. 2011 Jan;2:6.

39. Gühmann M, Jia H, Randel N, Veraszto C, Bezares-caldero LA, Michiels NK, et al. Spectral Tuning of Phototaxis by a Go-Opsin in the Rhabdomeric Eyes of Platynereis. Curr Biol. 2015;25:2265–71.

40. Arendt D. The enigmatic Xenopsins. Elife. 2017;6.

41. Feuda R, Hamilton SC, McInerney JO, Pisani D. Metazoan opsin evolution reveals a simple route to animal vision. Proc Natl Acad Sci. 2012 Nov 13;109(46):18868 LP-18872.

42. Kojima D, Terakita A, Ishikawa T, Tsukahara Y, Maeda A, Shichida Y. A Novel Go-mediated

Phototransduction Cascade in Scallop Visual Cells. J Biol Chem. 1997;272(37):22979–82.

43. McReynolds JS, Gorman ALF. Photoreceptor Potentials of Opposite Polarity in the Eye of the Scallop, Pecten irradians. J Gen Physiol. 1970;56:376–91.

44. D'Aniello S, Delroisse J, Valero-Gracia A, Lowe E, Byrne M, Cannon J, et al. Opsin evolution in the Ambulacraria. Mar Genomics. 2015;24(2):177–83.

45. Hering L, Mayer G. Analysis of the Opsin Repertoire in the Tardigrade Hypsibius dujardini Provides Insights into the Evolution of Opsin Genes in Panarthropoda . Genome Biol Evol. 2014 Sep 1;6(9):2380–91.

46. Koyanagi M, Terakita A, Kubokawa K, Shichida Y. Amphioxus homologs of Go-coupled rhodopsin and peropsin having 11-cis- and all-trans-retinals as their chromophores. FEBS Lett. Wiley-Blackwell; 2002 Oct 29;531(3):525–8.

47. Zhang Z, Fong HKW. Coexpression of nonvisual opsin, retinal G protein-coupled receptor, and visual pigments in human and bovine cone photoreceptors. Mol Vis. Molecular Vision; 2018 Jul 2;24:434–42.

48. Hauenschild C. Der hormonale einfluss des gehirns auf die sexuelle Entwicklung bei dem polychaeten Platynereis dumerilii. Gen Comp Endocrinol. 1966;6(1):26–73.

49. Yilmaz M, Meister M. Rapid innate defensive responses of mice to looming visual stimuli. Curr Biol. 2013;23(20):2011–5.

50. Gibson WT, Gonzalez CR, Fernandez CM, Ramasamy L, Tabachnik T, Du RR, et al. Behavioral responses to a repetitive shadow stimulus express a persistent state of defensive arousal in Drosophila. Curr Biol. 2015 Jun 1;25(11):1401–15.

51. Yoshizawa M, Jeffery WR. Shadow response in the blind cavefish Astyanax reveals conservation of a functional pineal eye. J Exp Biol. 2008;211(3):292–9.

52. Millott N, Yoshida M. Reactions to Shading in the Sea Urchin, Psammechinus miliaris (Gmelin). Nature. Nature Publishing Group; 1956 Dec 8;178:1300.

53. Clark RB. Habituation of the polychaete Nereis to sudden stimuli. 2 Biological significance of habituation. Anim Behav. 1960;8(1–2):92–103.

54. Evans SM. Habituation of the withdrawal response in Nereid Polychaetes. 2. Rates of habituation in intact and decerebrate worms. Biol Bull. 1969;137:105–17.

55. Kiørboe T, Visser A. Predator and prey perception in copepods due to hydromechanical signals. Mar Ecol Prog Ser. 1999;179:81–95.

56. Veedin-Rajan VB, Fischer RM, Raible F, Tessmar-Raible K. Conditional and Specific Cell Ablation in the Marine Annelid Platynereis dumerilii. PLoS One. 2013;8(9):1–11.

57. Akerboom J, Carreras Calderón N, Tian L, Wabnig S, Prigge M, Tolö J, et al. Genetically encoded calcium indicators for multi-color neural activity imaging and combination with optogenetics. Front Mol Neurosci. Frontiers; 2013 Jan 4;6:2.

58. Fischer A, Dorresteijn A. The polychaete Platynereis dumerilii (Annelida): a laboratory animal with spiralian cleavage, lifelong segment proliferation and a mixed benthic/pelagic life cycle. BioEssays. 2004;26(3):314–25.

59. Serrano A, Preciado I. Environmental factors structuring polychaete communities in shallow rocky habitats: role of physical stress versus habitat complexity. Helgol Mar Res. 2007;61(1):17–29.

60. Dekens MPS, Foulkes NS, Tessmar-Raible K. Instrument design and protocol for the study of light controlled processes in aquatic organisms, and its application to examine the effect of infrared light on zebrafish. PLoS One. 2017;12(2):1–15.

61. Zattara E. Transplants in annelids, nemerteans and planarians: a tool for embryology, immunology, endocrinology and regeneration research. Int Surg J. 2015;12:247–63.

62. Bok MJ, Porter ML, Ten Hove HA, Smith R, Nilsson D-E. Radiolar Eyes of Serpulid Worms (Annelida, Serpulidae): Structures, Function, and Phototransduction. Biol Bull. 2017;233(August):39–57.

63. Bok MJ, Porter ML, Nilsson D. Phototransduction in fan worm radiolar eyes. Curr Biol. Elsevier; 2017;27(14):R698–9.

64. Clark RB, Bonney DG. Influence of the supra-oesophageal ganglion on posterior regeneration in Nereis diversicolor. J Embryol Dev Morphol. 1960;8:112–8.

65. Clark RB, Evans SM. The Effect of Delayed Brain Extirpation and Replacement on Caudal Regeneration in Nereis Diversicolor. J Embryol Exp Morphol. 1961;9(1):97–105.

66. Backfisch B, Veedin-Rajan VB, Fischer RM, Lohs C, Arboleda E, Tessmar-Raible K, et al. Stable transgenesis in the marine annelid Platynereis dumerilii sheds new light on photoreceptor evolution. Proc Natl Acad Sci U S A. 2013 Jan 2;110(1):193–8.

67. Stowers JR, Hofbauer M, Bastien R, Griessner J, Higgins P, Farooqui S, et al. Virtual reality for freely moving animals. Nat Methods. Nature Publishing Group, a division of Macmillan Publishers Limited. All Rights Reserved.; 2017 Aug 21;14:995.

68. Cameron AT, Donoghue CHO. Retinal Reflexes of Narcotized Animals to Sudden Changes of Intensity of Illumination. Univ Chicago Press. 1922;42(5):217–33.

69. Evans SM. Habituation of the withdrawal response in Nereid polychaetes. 1. The habituation process in Nereis polychaetes. Biol Bull. 1969;137:95–104.

70. Watson G, M. Hamilton K, E. Tuffnail W. Chemical alarm signalling in the polychaete Nereis (Neanthes) virens (Sars) (Annelida: Polychaeta). Animal Behaviour - ANIM BEHAV. 2005. 1125-1132 p.

71. Pause B, Adolph D, Prehn-Kristensen A, Ferstl R. Startle response potentiation to chemosensory anxiety signals on socially anxious individuals. Int J Physchophysiology. 2009;74(2):88–92.

72. Reise K. Experiments on epibenthic predation in the Wadden Sea. Helgoländer Wissenschaftliche Meeresuntersuchungen. 1978;31:55–101.

73. Chartier TF, Deschamps J, Duerichen W, Jekely G, Arendt D. Whole-head recording of chemosensory activity in the marine annelid Platynereis dumerilii. bioRxiv. 2018 Jan 1;

74. Cram A, Evans SM. Stability and lability in the evolution of behaviour in nereid polychaetes. Anim Behav. 1980;28(2):483–90.

75. Simpson M. Reproduction of the Polychaete Glycera dibranchiata at Solomons, Maryland. Biol Bull. Marine Biological Laboratory; 1962;123(2):396–411.

76. Bezares-Calderon LA, Berger J, Jasek S, Veraszto C, Mendes S, Guehmann M, et al. Neural circuitry of a polycystin-mediated hydrodynamic startle response for predator avoidance. bioRxiv. 2018 Jan 1;

77. Hays GC, Doyle TK, Houghton JDR, Lilley MKS, Metcalfe JD, Righton D. Diving behaviour of jellyfish equipped with electronic tags. J Plankton Res. 2008 Mar 1;30(3):325–31.

78. Colwill RM, Creton R. Imaging escape and avoidance behavior in zebrafish larvae. Rev Neurosci. 2011 Feb 1;22(1):63–73.

79. Weigert A, Helm C, Meyer M, Nickel B, Arendt D, Hausdorf B, et al. Illuminating the base of

the annelid tree using transcriptomics. Mol Biol Evol. 2014;31(6):1391–401.

80. Orrhage L. On the structure and homologues of the anterior end of the polychaete families Sabellidae and Serpulidae. Zoomorphology. 1980;168(96):113–68.

81. Nilsson D-E. The evolution of eyes and visually guided behaviour. Philos Trans R Soc B Biol Sci. 2009 Oct 12;364(1531):2833 LP-2847.

82. Ullrich-Luter EM, Dupont S, Arboleda E, Hausen H, Arnone MI. Unique system of photoreceptors in sea urchin tube feet. Proc Natl Acad Sci. 2011;108(20):8367–72.

83. Keshelava A, Solis GP, Hersch M, Koval A, Kryuchkov M, Bergmann S, et al. High capacity in G protein-coupled receptor signaling. Nat Commun. Springer US; 2018;9(1):1–8.

84. Picciani N, Kerlin JR, Sierra N, Swafford AJM, Ramirez MD, Roberts NG, et al. Prolific Origination of Eyes in Cnidaria with Co-option of Non-visual Opsins. Curr Biol. 2018;28(15):2413–2419.e4.

85. Bonar D. Feeding and tube construction in chone mollis Bush (polychaeta, sabellidae). J Exp Mar Bio Ecol. 1972;9(1):1–18.

86. Tsukamoto H, Chen I, Kubo Y, Furutani Y. A ciliary opsin in the brain of a marine annelid zooplankton is UV- sensitive and the sensitivity is tuned by a single amino acid residue. J Biol Chem. 2017;292:12971–80.

87. Verasztó C, Gühmann M, Jia H, Rajan VBV, Bezares-Calderón LA, Piñeiro-Lopez C, et al. Ciliary and rhabdomeric photoreceptor-cell circuits form a spectral depth gauge in marine zooplankton. Sengupta P, editor. Elife. eLife Sciences Publications, Ltd; 2018;7:e36440.

88. Shichida Y, Matsuyama T. Evolution of opsins and phototransduction. Philos Trans R Soc Lond B Biol Sci. 2009 Oct 12;364(1531):2881–95.

89. Velarde RA, Sauer CD, Walden KKO, Fahrbach SE, M RH. Pteropsin: A vertebrate-like non-visual opsin expressed in the honey bee brain. Insect Biochem Mol Biol. 2005;35(12):1367–77.

90. Leutscher-Hazelhoff JT. Ciliary cells evolved for vision hyperpolarize - Why? Naturwissenschaften. 1984;71(4):213–4.

91. Purves D, Augustine G, D F. Phototransduction. Neuroscience 2nd Edition. 2nd ed. Sunderland. MA: Sinauer Associates; 2001.

92. Hagins W, Penn R, Yokishama S. Dark Current and Photocurrent in Retinal Rods. Biophys J.

1970;10(5):380–412.

93. Starunov V V, Voronezhskaya EE, Nezlin LP. Development of the nervous system in Platynereis dumerilii (Nereididae, Annelida). Front Zool. London: BioMed Central; 2017 May 25;14:27.

94. Bannister S, Antonova O, Polo A, Lohs C, Hallay N, Valinciute A, et al. TALENs mediate efficient and heritable mutation of endogenous genes in the marine annelid Platynereis dumerilii. Genetics. 2014 May;197(1):77–89.

95. Pattanayak V, Guilinger J, Lui D. Determining the specificities of TALENs, Cas9, and other genome editing enzymes. Methods Enzymol. 2014;546:47–78.

96. Kaiser TS, Neumann D, Heckel DG. Timing the tides: genetic control of diurnal and lunar emergence times is correlated in the marine midge Clunio marinus. BMC Genet. 2011 Jan;12(1):49.

97. Warrant EJ, Johnsen S. Vision and the light environment. Curr Biol. Elsevier; 2013;23(22):R990–4.

98. Hastings MH. Circadian clocks: Self-assembling oscillators? Curr Biol. 2003;13(17):681–2.

99. Vanin S, Bhutani S, Montelli S, Menegazzi P, Green EW, Pegoraro M, et al. Unexpected features of Drosophila circadian behavioural rhythms under natural conditions. Nature. Nature Publishing Group, a division of Macmillan Publishers Limited. All Rights Reserved.; 2012 Apr 4;484:371.

100. Conzelmann M, Offenburger S-L, Asadulina A, Keller T, Münch TA, Jékely G. Neuropeptides regulate swimming depth of Platynereis larvae. Proc Natl Acad Sci U S A. National Academy of Sciences; 2011 Nov 15;108(46):E1174–83.

101. Harvey EN. What substance is the source of light in fireflies? Science (80-). 1917;251:171–234.

102. D Rabasovic M, V Pantelic D, Jelenkovic B, Ćurčić S, Rabasovic M, Vrbica M, et al. Nonlinear microscopy of chitin and chitinous structures: A case study of two cave-dwelling insects. Journal of biomedical optics. 2015. 16010 p.

103. Shimomura O. Bioluminescence: Chemical Principles and Methods (Revised Edition). 2012. 225-255 p.

104. Ohtsuka H, Rudie N, Wampler J. Structural identification and synthesis of luciferin from the

bioluminescent earthworm, Diplocardia longa. Biochemistry. 1976;15:1001–4.

105. Nicolas M, Bassot J, Shimomura O. Polynoidin: a membrane photoprotein isolated from the bioluminescent of scaleworms. Photochem Photobiol. 1982;35:201–7.

106. Shimomura O, Johnson F. Partial purfication and properties of the chaetopterus luminescence system. Biolumin Prog. 1966;495–521.

107. Harvey E. Bioluminescence. Bioluminescence. University of Michigan: Academic Press; 1952. 12-86 p.

108. Schultz D, Kotlobay A, Ziganshin R, Bannikov A, Markina N, Chepurnyh T, et al. Luciferase of the Japanese syllid polychaete Odontosyllis undecimdonta. Biochem Biophys Res Commun. 2018;502(3):318–23.

109. Brugler MR, Aguado MT, Tessler M, Siddall ME. The transcriptome of the Bermuda fireworm Odontosyllis enopla (Annelida: Syllidae): A unique luciferase gene family and putative epitoky-related genes. PLoS One. Public Library of Science; 2018 Aug 8;13(8):e0200944.

110. Mehr S, Verdes A, DeSalle R, Sparks J, Pieribone V, Gruber DF. Transcriptome sequencing and annotation of the polychaete Hermodice carunculata (Annelida, Amphinomidae). BMC Genomics. London: BioMed Central; 2015 Jun 10;16(1):445.

111. Revilla-i-Domingo R, Smolka M, Farlik M, Veedin-Rajan VB, Tessmar-Raible K, Bock C, et al. Dissecting the nature of non-cephalic putative photoreceptors in the marine bristleworm Platynereis dumerilii. International Congress of Comparative Physiology and Biochemistry. 2015. p. 111.

112. Dana H, Mohar B, Sun Y, Narayan S, Gordus A, Hasseman JP, et al. Sensitive red protein calcium indicators for imaging neural activity. Elife. 2016;5(MARCH2016):1–24.

113. Hauenschild C, Fischer A. Platynereis dumerilii. Mikroskopische Anatomie. Großes Zool Prakt. 1969;10b:1–54.

114. Tessmar-Raible K, Steinmetz PRH, Snyman H, Hassel M, Arendt D. Fluorescent two-color whole mount in situ hybridization in Platynereis dumerilii (Polychaeta, Annelida), an emerging marine molecular model for evolution and development. Biotechniques. 2005 Oct;39(4):460–4.

115. Whitlock M, Schluter D. The analysis of biological data. Greenwood Village, Colorado: Roberts and Company Publishers; 2009. 20-59 p.

116. Graphpad Software Inc. Graphpad Prism version 7.00 for Windows. La Jolla California USA: Graphpad Software Inc.; 2017.

117. Cermak T, Doyle EL, Christian M, Wang L, Zhang Y, Schmidt C, et al. Efficient design and assembly of custom TALEN and other TAL effector-based constructs for DNA targeting. Nucleic Acids Res. Oxford University Press; 2011 Jul 14;39(12):e82–e82.

PUBLICATIONS

Ayers.T, Tsukamoto.H, Guhmann.M, Veedin Rajan.VB, Tessmar-Raible.K, A Go-type opsin mediates the shadow reflex in the annelid *Platynereis dumerilii*, 2018, Current Biology, 16:41 (https://doi.org/10.1186/s12915-018-0505-8)